

DESY 96-106
June 1996

B Decays, Flavour Mixings and CP Violation in the Standard Model *

A. Ali

Deutsches Elektronen Synchrotron DESY, Hamburg

Abstract

These lectures review the progress made in our present understanding of B decays. The emphasis here is on applications of QCD to B decays and the attendant perturbative and non-perturbative uncertainties, which limit present theoretical precision in some cases but the overall picture that emerges is consistent with the standard model (SM). This is illustrated by quantitatively analyzing some of the key measurements in B physics. These lectures are divided in five parts. In the first part, the Kobayashi-Maskawa generalization of the Cabibbo-GIM matrix for quark flavour mixing is discussed. In the second part, the bulk properties of B decays, such as the inclusive decay rates, semileptonic branching ratios, B -hadron lifetimes, and the so-called charm counting in B decays are taken up. The third part is devoted to theoretical studies of rare B decays, in particular the electromagnetic penguins involving the decays $B \rightarrow K^* + \gamma$ and $B \rightarrow X_s + \gamma$. The photon energy spectrum and the branching ratios in the SM are discussed and compared with data, enabling a determination of the CKM matrix element $|V_{ts}|$, the b -quark mass, and the kinetic energy of the b -quark in the B meson. The CKM-suppressed inclusive decay $B \rightarrow X_d + \gamma$, and the exclusive decays $B \rightarrow (\rho, \omega) + \gamma$, are discussed in the SM using QCD sum rules for the latter. The importance of these decays in determining the CKM parameters is emphasized. This part ends with a discussion of the decay rates and distributions in $B \rightarrow X_s \ell^+ \ell^-$, including the long-distance effects, and estimates of a large number of other rare B decays, including $B \rightarrow X \nu \bar{\nu}$, and the two-body decays $B^0 \rightarrow \ell^+ \ell^-$ and $B^0 \rightarrow \gamma \gamma$. The fourth part is devoted to reviewing the present estimates of the CKM matrix elements from B decays and $B^0 - \overline{B^0}$ mixings, which determine five of the nine elements in this matrix. This is combined with our present knowledge of the other four CKM matrix elements and a quantitative test of the unitarity of the CKM matrix is presented. This information is then combined with the constraints from the CP-violation parameter $|\epsilon|$ in order to provide a profile of the CKM unitarity triangle and CP-violating asymmetries in B decays. These aspects are discussed in the fifth part of these lectures.

*Lectures given at the XX International Nathiagali Summer College on Physics and Contemporary Needs, Bhurban, Pakistan, June 24 - July 13, 1995; to appear in the Proceedings (Nova Science Publishers, New York), Editors: Riazuddin, K.A. Shoib et al.

TABLE OF CONTENTS

1.	Weak-coupling Lagrangian for the b Quark and the CKM Matrix	2
1.1	Some popular representations of the CKM Matrix	8
1.2	The CKM unitarity triangles	10
2.	Dominant B Decays in the Standard Model	12
2.1	Inclusive semileptonic decay rates of the B hadrons	14
2.2	Inclusive non-leptonic decay rates of the B hadrons	15
2.3	Power corrections in $\Gamma_{SL}(B)$ and $\Gamma_{NL}(B)$	21
2.4	Numerical estimates of $\mathcal{B}_{SL}(B)$ and $\langle n_c \rangle$	23
2.5	B -Hadron Lifetimes in the Standard Model	25
2.6	Determination of $ V_{cb} $ and $ V_{ub} $	26
3.	Electromagnetic Penguins and Rare B Decays in the Standard Model	29
3.1	The effective Hamiltonian for $B \rightarrow X_s + \gamma$	30
3.2	Real and virtual $\mathcal{O}(\alpha_s)$ corrections for the matrix element	34
3.3	Estimates of long-distance effects in $B \rightarrow X_s + \gamma$	38
3.4	Estimates of $\mathcal{B}(B \rightarrow X_s + \gamma)$ in the Standard Model	39
3.5	Photon energy spectrum in $B \rightarrow X_s + \gamma$	41
3.6	Inclusive radiative decays $B \rightarrow X_d + \gamma$	43
3.7	Estimates of $\mathcal{B}(B \rightarrow V + \gamma)$ and constraints on the CKM parameters	46
3.8	Inclusive rare decays $B \rightarrow X_s \ell^+ \ell^-$ in the SM	52
3.9	Summary and overview of rare B decays	58
4.	An Update of the CKM Matrix	59
4.1	The present profile of the CKM matrix	62
4.2	x_s and the unitarity triangle	65
5.	CP Violation in the B System	67
5.1.	Summary of the CKM fits and CP asymmetries in B decays	71
6.	Acknowledgements	73
7.	References	74

1 Weak-coupling Lagrangian for the b Quark and the CKM Matrix

The Lagrangian density of the standard model for electroweak interactions (henceforth called SM) can be symbolically written as [1]:

$$\mathcal{L} = \mathcal{L}(f, W, B) + \mathcal{L}(f, \Phi) + \mathcal{L}(W, B, \Phi) - V(\Phi) \quad (1)$$

where the symbols f, W, B and Φ represent fermions (leptons and quarks), $SU(2)_L$ gauge bosons, W_μ^i , $U(1)_Y$ gauge boson, B_μ and the Higgs doublet field, respectively. The SM particle content together with the (weak) isospin properties of the basic quanta are given below, where we have assumed that there are three families of leptons and quarks.

Fermions

$$\text{Leptons: } \begin{pmatrix} \nu_e \\ e \end{pmatrix}_L, \begin{pmatrix} \nu_\mu \\ \mu \end{pmatrix}_L, \begin{pmatrix} \nu_\tau \\ \tau \end{pmatrix}_L; e_R, \mu_R, \tau_R$$

$$\text{Quarks: } \begin{pmatrix} u \\ d \end{pmatrix}_L, \begin{pmatrix} c \\ s \end{pmatrix}_L, \begin{pmatrix} t \\ b \end{pmatrix}_L; u_R, d_R, c_R, \dots$$

Gauge bosons

$$\begin{pmatrix} W_\mu^1 \\ W_\mu^2 \\ W_\mu^3 \end{pmatrix}; B_\mu$$

Scalars

$$\Phi = \begin{pmatrix} \phi^+ \\ \phi^0 \end{pmatrix}, \Phi^\dagger = (\phi^-, \bar{\phi}^0). \quad (2)$$

The various terms in the SM Lagrangian can be written by demanding $SU(2)_L \otimes U(1)$ gauge invariance, lepton-quark universality, and family-independence of the electroweak interactions. Since the SM Lagrangian is given in any standard textbook on electroweak interactions [2] we shall not reproduce it here. The main interest in B physics lies in the study of the first two terms in (1) involving fermions, gauge bosons and the Higgs fields, in particular flavour-changing transitions. In order to appreciate how flavour-changing transitions emerge in the SM, it is worth while to write the first two terms in (1) explicitly. The interaction between the fermions and gauge bosons has the form:

$$\mathcal{L}(f, W, B) = \sum_{j=1}^3 \{ \bar{l}_L^j \not{D} l_L^j + \bar{l}_R^j \not{D}' l_R^j + \bar{q}_L^j \not{D} q_L^j \} + \sum_{i=1}^6 \bar{q}_R^i \not{D}' q_R^i, \quad (3)$$

where j is the family index,

$$l_L^1 = \begin{pmatrix} \nu_e \\ e \end{pmatrix}_L, \quad l_R^1 = e_R, \quad q_L^1 = \begin{pmatrix} u \\ d \end{pmatrix}_L, \quad q_R^1 = u_R, \quad q_R^2 = d_R, \dots$$

and the two covariant derivatives are defined as

$$\begin{aligned} \not{D} &\equiv D_\mu \gamma^\mu, \quad \not{D}' \equiv D'_\mu \gamma^\mu, \\ D_\mu &= \partial_\mu - ig_2 \left(\vec{W}_\mu \cdot \frac{\vec{\sigma}}{2} \right) - ig_1 \frac{Y}{2} B_\mu, \\ D'_\mu &= \partial_\mu - ig_1 \frac{Y}{2} B_\mu, \end{aligned} \quad (4)$$

where g_1 and g_2 are, respectively, the $U(1)_Y$ and $SU(2)_L$ coupling constants, σ^a ($a = 1, 2, 3$) are the (weak) isospin Pauli matrices, and the Gell-Mann – Nishijima formula $Q = I_3 + Y$ defines the (weak) hypercharge of the quarks and leptons. The interaction term $\mathcal{L}(f, \phi)$ involving the fermions and the Higgs fields has the Yukawa form

$$\begin{aligned} \mathcal{L}(f, \Phi) &= \sum_{j=1}^3 \left\{ (h_l)_j \bar{l}_L^j \Phi \bar{l}_R^j \right\} \\ &+ \sum_{j,k=1}^3 \left\{ (h'_q)_{jk} \bar{q}_L^j \Phi u_R^k + (h_q)_{jk} \bar{q}_L^j \Phi^c d_R^k \right\}, \end{aligned} \quad (5)$$

where

$$\Phi^c = i\sigma_2 \phi^* = \begin{pmatrix} \phi^{0*} \\ -\phi^- \end{pmatrix},$$

with both Φ and Φ^c transforming as a (weak) isospin doublet. The hypercharge of the Higgs fields can be written by inspection. The Yukawa coupling constants $(h_l)_j$, $(h_q)_{jk}$ and $(h'_q)_{jk}$ are arbitrary complex numbers and each term in (5) is independently $SU(2)_L \otimes U(1)_Y$ invariant due to the fact that the $SU(2)_L$ acts only on \bar{l}_L and \bar{q}_L and on the Higgs doublet Φ and Φ^c , whose products are $SU(2)$ scalars.

After spontaneous symmetry breaking $SU(2)_L \otimes U(1)_Y \rightarrow U(1)_{EM}$, which preserves the symmetry under $U(1)$ electromagnetism, the gauge bosons, fermions and the neutral scalar field ϕ acquire non-zero masses through the Higgs mechanism

$$V(\phi) = \mu^2 |\phi|^2 + \lambda |\phi|^4; \quad \mu^2 < 0, \lambda > 0, \quad (6)$$

with $V(\phi)_{\min}$ at $|\phi| = v/\sqrt{2} = \sqrt{-\mu^2/2\lambda}$, where v is the neutral-Higgs vacuum expectation value. Making the Higgs transformation $\phi \rightarrow \phi + v$ in (5), one finds (ϕ is the physical Higgs scalar with $m_\phi^2 = 2\lambda v^2$):

$$\begin{aligned} \mathcal{L}(f, \phi)^{\text{SSB}} &= \sum_{j=1}^3 (m_j)_l \bar{l}_L^j l_R^j \left(1 + \frac{1}{v} \phi \right) \\ &- \sum_{j,k=1}^3 \left\{ (m_{jk})_U \bar{u}_L^j u_R^k + (m_{jk})_D \bar{d}_L^j d_R^k \right\} \left(1 + \frac{1}{v} \phi \right) + \text{h. c.}, \end{aligned} \quad (7)$$

where

$$\begin{aligned}
(m_j)_l &= (h_j)_l \frac{v}{\sqrt{2}}, \\
(m_{jk})_U &= -(h_q)_{jk} \frac{v}{\sqrt{2}}, \\
(m_{jk})_D &= -\left(h'_q\right)_{jk} \frac{v}{\sqrt{2}}.
\end{aligned} \tag{8}$$

Since in the SM there are no right-handed fields ν_R^i ($i = 1, 2, 3$), the neutrinos ν^i remain massless and the charged lepton mass matrix $(m_j)_l$ is diagonal. Hence, in the SM there are no family-changing leptonic interactions – an aspect that will soon come under experimental scrutiny from the ongoing and planned experiments dedicated to the neutrino mass and oscillation measurements. In (8), $(m_{jk})_U$ and $(m_{jk})_D$ are the (3×3) quark mass matrices for the up- and down-type quarks, respectively. In order to write the Lagrangian in terms of the quark mass eigenstates one has to diagonalize the mass matrices $(m_{jk})_U$ and $(m_{jk})_D$. This can be done with the help of two unitary matrices. It is customary to denote them by V_L^{up} and $V_R^{\text{up}\dagger}$ (likewise for the down type quarks):

$$\begin{aligned}
V_L^{\text{up}} m_U V_R^{\text{up}\dagger} &\equiv (m_{\text{diag.}})_U \equiv \text{Diag.}(m_u, m_c, m_t), \\
V_L^{\text{down}} m_D V_R^{\text{down}\dagger} &\equiv (m_{\text{diag.}})_D \equiv \text{Diag.}(m_d, m_s, m_b),
\end{aligned} \tag{9}$$

with $V_L^{\text{up}\dagger} V_L^{\text{up}} = 1$, etc. Concentrating on the up-type quarks in (7) one can do the following manipulation :

$$\begin{aligned}
\bar{u}_L m_U u_R &= \bar{u}_L V_L^{\text{up}\dagger} V_L^{\text{up}} m_U V_R^{\text{up}\dagger} V_R^{\text{up}} u_R \\
&= \frac{V_L^{\text{up}} u_L}{V_R^{\text{up}} u_R} (m_{\text{diag.}})_U (V_R^{\text{up}} u_R),
\end{aligned} \tag{10}$$

which shows that the physical quark fields (mass eigenstates) are:

$$\begin{aligned}
u_L^{i(\text{Phys})} &= (V_L^{\text{up}} u_L)^i, \\
d_L^{i(\text{Phys})} &= (V_L^{\text{down}} d_L)^i.
\end{aligned} \tag{11}$$

Likewise, $u_R^{i(\text{Phys})} = (V_R^{\text{up}} u_R)^i$, $d_R^{i(\text{Phys})} = (V_R^{\text{down}} d_R)^i$. One can now rewrite the term $\mathcal{L}(f, \Phi)$ in the SM Lagrangian in terms of $(u_L^i)^{\text{Phys}}$ and $(d_L^i)^{\text{Phys}}$, obtaining

$$\mathcal{L}(f, \Phi)^{\text{SSB}} = -\left(1 + \frac{\phi}{v}\right) \left\{ \sum_{i=1}^6 m_{q_i} \bar{q}_i q_i + \sum_{j=1}^3 m_{l_j} \bar{l}_j l_j \right\}, \tag{12}$$

where it is now understood that $q_1 = \frac{1}{2} (u_L^{1\text{Phys}} + u_R^{1\text{Phys}}) = u$ etc., and we have dropped the superscript on the quark fields. The identification of the parameters m_{l_i} , m_{q_i} with the lepton and quark masses is now evident. In addition, the SM Lagrangian has specified the Higgs-fermion ($\phi f \bar{f}$) Yukawa couplings and their Lorentz structure, as well as their C, P, and CP properties. All these symmetries are separately conserved in $\mathcal{L}(f, \phi)^{\text{SSB}}$ and the Higgs-fermion Yukawa couplings are manifestly diagonal in flavour space. It should

be emphasized that this is a consequence of the choice made in the SM of a single doublet Higgs field since, otherwise, flavour-changing neutral-current (FCNC) transitions in the Higgs sector would be allowed in general.

Finally, one can carry through the transformation (10) in the part of the SM Lagrangian describing the fermion-gauge boson couplings, $\mathcal{L}(f, W, B)$. Written in terms of the physical boson (W_μ^\pm , Z_μ^0 , A_μ) and fermion fields, it is easy to show that the neutral current (NC) part of $\mathcal{L}(f, W, B)$ is manifestly flavour-diagonal. Thus, all flavour-changing transitions in the SM are confined to the charged current (CC) sector. Denoting the quarks and leptons by f_i ($i = 1 \dots 6$), the neutral current in the SM is given by:

$$J_\mu^{NC} = \sum_i \bar{f}_i \left[\frac{e}{\sin \theta_W \cos \theta_W} Z_\mu \left(I_{3L} - Q \sin^2 \theta_W \right)_i + e A_\mu Q_i \right] f_i, \quad (13)$$

where $(I_3)_L = (1 - \gamma_5)/2(I_3)$ with $I_3 = +1/2$ for u_i and ν_i and $-1/2$ for d_i and Q_i is the electric charge of the fermion f_i in units of the electron charge, i.e., $Q_e = +1$. The electroweak mixing angle in J_μ^{NC} , denoted by θ_W , has its origin in the diagonalization of the gauge boson mass matrix, and it has the usual definition $\cos \theta_W = g_2/\sqrt{g_1^2 + g_2^2}$, with the electric charge defined as $e \equiv g_2 \sin \theta_W$. It is easy to check that the neutral current interaction induced by the Z exchange violates P and C but conserves CP. The electromagnetic interaction conserves, of course, all three C, P, and CP separately.

The neutral current couplings specified in J_μ^{NC} have been measured in e^+e^- annihilation experiments, in particular at LEP and SLC, and elsewhere. A comparison of these couplings with data can be seen in the Particle Data Group (PDG) review of particle properties [3]. The present situation can be summarized by the statement that the SM is consistent with the vast majority of these measurements. Quantitatively, this can be expressed in terms of the following values of the basic parameters of the SM, obtained by averaging the LEP, SLD, $p\bar{p}$ and νN data [3][†]:

$$\begin{aligned} m_Z \text{ (GeV)} &= 91.184 \pm 0.0022, \\ m_W \text{ (GeV)} &= 80.26 \pm 0.16 \\ \sin^2 \hat{\theta}_W(m_Z) &= 0.2315 \pm 0.0002 \pm 0.0003, \\ m_t \text{ (GeV)} &= 180 \pm 7^{+12}_{-13} \\ \alpha_s(m_Z) &= 0.123 \pm 0.004 \pm 0.002, \end{aligned} \quad (14)$$

where $\sin^2 \hat{\theta}_W(m_Z)$ is defined in the modified minimal subtraction scheme ($\overline{\text{MS}}$) at the scale m_Z , and the particular definition of $\sin^2 \hat{\theta}_W$ used in the analysis can be seen in Langacker's review in [3]. In addition, $N_\nu = 2.991 \pm 0.016$ [4], where N_ν is the number of light neutrini. The fitted value of m_t from the electroweak data is in excellent agreement with the direct measurements of the same at the Fermilab experiments CDF and DO [5], $m_t = 180 \pm 12$ GeV. However, precision measurements at the Z^0 also yield decay rates $\Gamma(Z \rightarrow b\bar{b})$ and (to a smaller extent) $\Gamma(Z \rightarrow c\bar{c})$, which are on their face value at variance with those predicted in the SM, taken together with the measurement of the top quark

[†]The numbers are taken from P. Langacker's 1995 updated review available through the World Wide Web.

mass. The experimental situation at the end of 1995 has been summarized in [3, 4]:

$$\begin{aligned} R_b \equiv \frac{\Gamma(Z^0 \rightarrow b\bar{b})}{\Gamma(Z^0 \rightarrow \text{hadrons})} &= 0.2219 \pm 0.0017 \quad [R_b(\text{SM}) = 0.2156], \\ R_c \equiv \frac{\Gamma(Z^0 \rightarrow c\bar{c})}{\Gamma(Z^0 \rightarrow \text{hadrons})} &= 0.1543 \pm 0.0074 \quad [R_c(\text{SM}) = 0.1724]. \end{aligned} \quad (15)$$

These measurements constitute a pull factor of 3.7 and -2.5 on the SM values of R_b and R_c , respectively [‡]. We refer the interested reader to [3, 4] for further details of the data and a recent comprehensive theoretical analysis of the same in [6], in which a number of non-SM Ansätze are put forward to explain the present experimental anomalies. In the meanwhile, the value of the top quark mass has come down marginally; the present world average $m_t = 175 \pm 9.0$ GeV [8] has slightly eased the situation for the SM.

At this particular junction of experiments and SM, it is a fair question to ask: Quo Vadis SM? In our view, it is perhaps still too premature to argue persuasively that the SM and experiments have parted with each other. This is a tenable point of view as the case against the SM is at best circumstantial and by no means impeccable. It should be stressed that a good fraction of the LEP data remains to be analyzed. Likewise, lot more data will be collected at the SLC collider. The experimental jury is, therefore, still out on R_b and R_c and the final verdict on the validity of the SM is yet to be spoken. Improved measurements of m_W at LEP200, projected to yield a precision of $\Delta m_W \leq 50$ MeV [7], and a projected precision of $\Delta m_t = \pm 4$ GeV on the top quark mass at the Tevatron collider [8], likewise, will also have a direct bearing on the issues being discussed.

We shall concentrate in these lectures on the physics of the charged current processes in B decays, which is not effected directly by the possible modifications of J_μ^{NC} . However, the additional NC couplings, if present, may lead to modifications of some FCNC rare B decay rates and distributions, such as in $B \rightarrow X\ell^+\ell^-$ and $B \rightarrow X\nu\bar{\nu}$, in which such couplings do play a role. Since, in absolute terms, the possible deviation of the experimental widths in question from their SM value is small, we do not expect that such possible modifications in J_μ^{NC} will significantly alter the SM-based profile of FCNC B decays. The implications of a modified J_μ^{NC} in B decays must be investigated quantitatively, in case Z^0 data force such a modification. In the CC sector itself, despite suggestions to the contrary [9], we shall argue in these lectures that there is no evidence for new physics so far, though this may change as data and theory of weak decays get precise and compelling.

We now proceed to discuss the charged current, J_μ^{CC} , which is to be derived from the $\mathcal{L}(f, W, B)$ part of the SM Lagrangian using the mass eigenstates. The CC couplings in the SM involve only the left-handed fermions q_L^i and l_L^i . Concentrating on the hadronic (quark) part of \mathcal{L}^{CC} , one can now do the following manipulations:

$$\begin{aligned} \mathcal{L}^{CC} &= \frac{e}{\sqrt{2} \sin \theta_W} \sum_{i=1}^3 \bar{u}_L^i \gamma^\mu W_\mu^+ d_L^i + \text{h.c.} \\ &= \frac{e}{\sqrt{2} \sin \theta_W} \sum_{i=1}^3 \bar{u}_L^i V_L^{\text{up}\dagger} V_L^{\text{up}} \gamma^\mu W_\mu^+ V_L^{\text{down}\dagger} V_L^{\text{down}} d_L^i + \text{h.c.} \end{aligned}$$

[‡]This is defined as $P = (O(\text{expt}) - O(\text{th})) / \sigma(O)(\text{exp})$.

$$= \frac{e}{\sqrt{2} \sin \theta_W} \sum_{i=1}^3 \left(\bar{u}_L^{\text{Phys}} \right)^i \gamma^\mu W_\mu^+ \left(V_L^{\text{up}} V_L^{\text{down} \dagger} \right)_{ij} \left(d_L^{\text{Phys}} \right)^j + \text{h.c.} \quad (16)$$

Thus, the charged current J_μ^{CC} , which couples to the W^\pm , is

$$J_\mu^{CC} = \frac{e}{\sqrt{2} \sin \theta_W} (\bar{u}, \bar{c}, \bar{t})_L \gamma_\mu V_{\text{CKM}} \begin{pmatrix} d \\ s \\ b \end{pmatrix}_L, \quad (17)$$

where we have again dropped the superscript and $V_{\text{CKM}} \equiv V_L^{\text{up}} V_L^{\text{down} \dagger}$ is a (3×3) unitary matrix in flavour space, first written down by Kobayashi and Maskawa in 1973 [10]. It is a generalization of the Cabibbo rotation [11] for the three-quark-flavour (u, d, s) case, invented to keep the universality of weak interactions, which took the form of a (2×2) matrix by the inclusion of c -quark with the GIM construction [12], and is called the Cabibbo-Kobayashi-Maskawa (CKM) matrix. The charged current Lagrangian has the property that it has a $(V - A)$ structure, hence it violates P and C maximally, conserves the electric charge and the lepton- and baryon-number separately, but otherwise there are no restrictions on it except that $V_{\text{CKM}}^\dagger V_{\text{CKM}} = 1$. In general, \mathcal{L}^{CC} violates CP due to the possibility of a non-trivial phase in V_{CKM} .

From this discussion it is clear that the flavour-changing transitions in the SM are confined to the CC sector. They emerge in the process of diagonalization of the quark mass matrices after spontaneous symmetry breaking, which in turn depend on the Higgs-fermion Yukawa couplings. As stated already, the Yukawa couplings in the standard model are arbitrary complex numbers. Their adhoc nature in the standard model is in all likelihood pointing to the physics beyond the SM, which may help in understanding the observed pattern of the fermion masses and mixing angles. How such extensions will look like is, however, neither obvious nor the subject of these lectures. Here, we have a restricted mandate, namely we will investigate the question if the SM, which comes together with these masses and mixings, is a consistent and complete description of data or not.

The matrix elements of V_{CKM} are determined by the charged current coupling to the W^\pm bosons. Symbolically this matrix can be written as:

$$V_{\text{CKM}} \equiv \begin{pmatrix} V_{ud} & V_{us} & V_{ub} \\ V_{cd} & V_{cs} & V_{cb} \\ V_{td} & V_{ts} & V_{tb} \end{pmatrix}. \quad (18)$$

Of the nine elements of V_{CKM} , the four involving the u, d, c, s quarks and present in the upper left 2×2 block, are studied in decays which are not our principal concern here. Their current values can be seen in the PDG review, where also references to the original literature can be found [3].

We shall concentrate here on the remaining five matrix elements in which quarks in the third family are involved. Two of the matrix elements involving the b quark, V_{ub} and V_{cb} , have been measured in direct decays of the B hadrons in experiments at the e^+e^- storage rings CESR, DORIS and LEP. The theory and phenomenology behind their determination

will be discussed at some length here. The remaining three elements V_{td} , V_{ts} and V_{tb} can, in principle, be directly measured in the decays of the top quark $t \rightarrow bW^+$, $t \rightarrow sW^+$ and $t \rightarrow dW^+$, respectively. First measurements of V_{tb} have been reported by the CDF collaboration [13], through the measurement of the ratio R_{tb} ,

$$R_{tb} \equiv \frac{\mathcal{B}(t \rightarrow bW)}{\sum_{q=d,s,b} \mathcal{B}(t \rightarrow qW)} = 0.87^{+0.13}_{-0.30} {}^{+0.13}_{-0.11}, \quad (19)$$

which is consistent with unity but within experimental errors also consistent with a value of V_{tb} which is considerably less than that. Apart from establishing the dominance of V_{tb} (over the other two matrix elements) by improved measurements of the ratio R_{tb} [§] it will be difficult in the foreseeable future to get quantitative information on V_{td} and V_{ts} from decays of top quarks, both due to the scarcity of data involving top quark production and, more importantly, the issues having to do with efficient tagging of light-quark jets.

Fortunately, the matrix elements V_{ti} are also accessible in B and K decays through virtual transitions involving the couplings $Wt\bar{b}$, $Wt\bar{s}$ and $Wt\bar{d}$. Examples of these transitions in the B system are the $|\Delta B| = 2$ processes, $B^0 - \bar{B}^0$ mixings, and $|\Delta B| = 1$ FCNC processes, such as rare B decays $b \rightarrow (s, d) + \gamma$ and $b \rightarrow (s, d) + l^+l^-$. We discuss the theory and phenomenology of these processes here. Precision experiments involving B decays and mixings will completely determine the matrix V_{CKM} , including the CP-violating phase, establishing either that the SM provides a consistent theoretical framework for describing flavour physics or else that the charged current J_μ^{cc} must be modified.

1.1 Some popular representations of the CKM Matrix

We discuss a couple of popular representations of the CKM matrix. The original parametrization due to Kobayashi and Maskawa [10] was constructed from the rotation matrices in the flavour space involving the angles θ_i ($i = 1, 2, 3$) and a phase δ ,

$$V_{\text{KM}} = R_{23}(\theta_3, \delta) R_{12}(\theta_1, 0) R_{23}(\theta_2, 0), \quad (20)$$

where $0 \leq \theta_i \leq \pi/2$, $0 \leq \delta \leq 2\pi$, and $R_{ij}(\theta, \phi)$ denotes a unitary rotation in the (i, j) plane by the angle θ and the phase ϕ . The resulting representation is:

$$V_{\text{KM}} = \begin{pmatrix} c_1 & -s_1 c_3 & -s_1 s_3 \\ s_1 c_2 & c_1 c_2 c_3 - s_2 s_3 e^{i\delta} & c_1 c_2 s_3 + s_2 c_3 e^{i\delta} \\ s_1 s_2 & c_1 s_2 c_3 + c_2 s_3 e^{i\delta} & c_1 s_2 s_3 - c_2 c_3 e^{i\delta} \end{pmatrix}, \quad (21)$$

with $c_i = \cos \theta_i$, $s_i = \sin \theta_i$. This reduces to the usual Cabibbo form for $\theta_2 = \theta_3 = 0$, with the angle θ_1 , identified (up to a sign) with the Cabibbo angle. In the PDG review [3], however, another parametrization is advocated which differs from V_{KM} in assigning the complex phases (dominantly) to the (1,3) and (3,1) matrix elements of V_{CKM} . We shall not write the PDG representation of the CKM matrix but give instead the simpler

[§]A precision of $|V_{tb}| = 1.0 \pm 12\%$ is, for example, projected at the Fermilab Tevatron with an integrated luminosity of $2(f\text{b})^{-1}$, expected to be collected at the turn of this century [8].

approximate form, which follows from the *a posteriori* realization that $c_{13} \simeq 1$ to a very high accuracy, due to the measurement of $|V_{ub}| = s_{13} \simeq 0.003\text{--}0.006$ (see below).

$$V_{\text{PDG}} \simeq \begin{pmatrix} c_{12}c_{13} & s_{12}c_{13} & s_{13}e^{-i\delta_{13}} \\ -s_{12}c_{23} & c_{12}c_{23} & s_{23}c_{13} \\ s_{12}s_{23} - c_{12}c_{23}s_{13}e^{i\delta_{13}} & -c_{12}s_{23} & c_{23}c_{13} \end{pmatrix}. \quad (22)$$

The three angles called θ_{ij} , $i \neq j$, can be chosen to lie in the range $0 \leq \theta_{ij} \leq \pi/2$, making all the sines and cosines c_{ij} and s_{ij} real and positive. The KM phase, called for obvious reasons δ_{13} , lies in the range $0 \leq \delta_{13} \leq 2\pi$. In the limit $\theta_{13} = \theta_{23} = 0$, the third generation decouples; identifying the Cabibbo angle with θ_{12} , one recovers the Cabibbo form. To an excellent accuracy, which we will discuss, one could set $c_{13} = 1$ and $c_{23} = 1$. In that case, for the PDG parametrization,

$$|V_{us}| = |s_{12}c_{13}| \simeq |s_{12}|; \quad |V_{ub}| = |s_{13}|; \quad |V_{cb}| = |s_{23}c_{13}| \simeq |s_{23}|. \quad (23)$$

These can then be taken as three independent parameters, measured directly in decays, together with the phase δ_{13} .

Another approximate but very useful form of the matrix V_{CKM} is due to Wolfenstein [14], who made the observation that (empirically) the following pattern for the V_{CKM} matrix elements is suggested by data:

$$\begin{aligned} |V_{ii}| &\simeq 1, \quad i = 1\ldots 3, \\ |V_{12}| &\simeq |V_{21}| \sim \lambda, \\ |V_{23}| &\simeq |V_{32}| \sim \lambda^2 \\ |V_{13}| &\sim \lambda^3, \quad |V_{23}| \sim \lambda^3, \end{aligned} \quad (24)$$

with $\lambda \equiv \sin \theta_c \simeq 0.221$. Thus, it is useful to write a perturbative form (in λ) for V_{CKM} . Denoting this by $V_{\text{Wolfenstein}}$,

$$V_{\text{Wolfenstein}} = \begin{pmatrix} 1 - \frac{1}{2}\lambda^2 & \lambda & A\lambda^3(\rho - i\eta) \\ -\lambda & 1 - \frac{1}{2}\lambda^2 & A\lambda^2 \\ A\lambda^3(1 - \rho - i\eta) & -A\lambda^2 & 1 \end{pmatrix}. \quad (25)$$

Like the previous representations, $V_{\text{Wolfenstein}}$ has also three real parameters called A , λ and ρ , and a phase η . Since we shall be making extensive use of this parametrization, we write some relations involving the matrix elements of interest in this representation:

$$\frac{|V_{ub}|}{|V_{cb}|} = \lambda \sqrt{\rho^2 + \eta^2}, \quad \frac{|V_{td}|}{|V_{cb}|} = \lambda \sqrt{(1 - \rho)^2 + \eta^2}, \quad (26)$$

$$\frac{|V_{td}|}{|V_{ub}|} = \sqrt{\frac{(1 - \rho)^2 + \eta^2}{\rho^2 + \eta^2}}, \quad \frac{|V_{ts}|}{|V_{cb}|} = 1, \quad (27)$$

and the dominant phases are:

$$\Im(V_{ub}) = \Im(V_{td}) = -A\lambda^3\eta. \quad (28)$$

It should be recalled that the Wolfenstein parameterization given in Eq. (25) is an approximation and in certain situations in the future it may become mandatory to specify the matrix by taking into account the dropped terms in $O(\lambda^4)$ in $V_{\text{Wolfenstein}}$. For the present experimental and theoretical accuracy, the representation (25) is entirely adequate and we shall restrict ourselves to this form. Further discussions on this point and suggestions on improved treatment to include higher order terms in λ can be seen in [15].

The four CKM parameters and the six quark masses together with the masses of the three charged leptons make thirteen of the nineteen parameters of the standard model; the remaining six can be taken as the three gauge coupling constants, the Higgs boson mass, the mass of the W boson, and the parameters $\theta_{\text{vac}}(QCD)$ and $\theta_{\text{vac}}(EW)$, which are related to the instanton sectors of QCD and the electroweak theory, respectively. Being fundamental constants of nature, it is utmost important to measure them as precisely as possible and the main goal of flavour physics is to pin down at least the first thirteen of them.

1.2 The CKM unitarity triangles

The CKM matrix elements obey unitarity constraints, which state that any pair of rows, or any pair of columns, of the CKM matrix are orthogonal. This leads to six orthogonality conditions. The three involving the orthogonality of columns are listed below, with the quark pair in the parenthesis (jk) representing the product of the j 'th and k 'th columns:

$$\begin{aligned} (ds) : \quad \sum_i V_{id} V_{is}^* &= 0, \\ (sb) : \quad \sum_i V_{is} V_{ib}^* &= 0, \\ (db) : \quad \sum_i V_{id} V_{ib}^* &= 0. \end{aligned} \tag{29}$$

Similarly, there are three more such orthogonality conditions on the rows:

$$\begin{aligned} (uc) : \quad \sum_j V_{uj} V_{cj}^* &= 0, \\ (ct) : \quad \sum_j V_{cj} V_{tj}^* &= 0, \\ (ut) : \quad \sum_j V_{uj} V_{tj}^* &= 0. \end{aligned} \tag{30}$$

The six orthogonality conditions can be depicted as six triangles in the complex plane of the CKM parameter space [16]. The FCNC transitions in which the pair of quarks depicted participate test these triangular constraints directly. Thus, the triangle labeled (ds) represents the unitarity constraints on the transition $s \rightarrow d$, which, for example, one encounters in the $K^0 - \bar{K}^0$ transition and in rare K decays such as $K_L \rightarrow \pi^0 \ell^+ \ell^-$. The two others in this group, namely (sb) and (db) , are encountered in the FCNC transitions in B decays, such as particle-antiparticle mixings $B_d^0 - \bar{B}_d^0$ and $B_s^0 - \bar{B}_s^0$ and rare B decays $B \rightarrow K^* + \gamma$ and $B \rightarrow \omega + \gamma$, respectively. The unitarity conditions on the rows will be

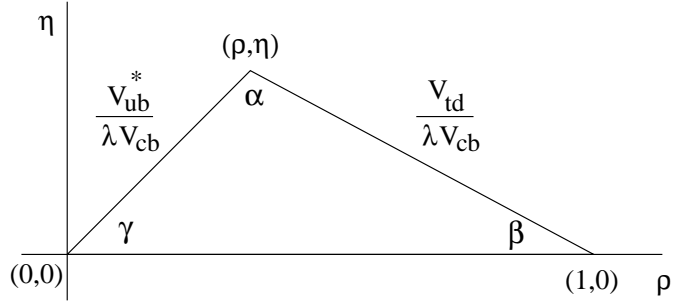


Figure 1: The unitarity triangle. The angles α , β and γ can be measured via CP violation in the B system and the sides from the CC- and FCNC-induced B decays.

difficult to test in FCNC transitions shown, as the rates of such transitions are enormously suppressed in the SM, and we shall not discuss this set in these lectures.

The constraint stemming from the orthogonality condition on the first and third row of V_{CKM} ,

$$V_{ud}V_{td}^* + V_{us}V_{ts}^* + V_{ub}V_{tb}^* = 0 \quad (31)$$

has received considerable attention. Since $V_{ud} \simeq V_{tb} \simeq 1$ and $V_{ts}^* \simeq -V_{cb}$, the unitarity relation (31) simplifies:

$$V_{ub} + V_{td}^* = V_{us}V_{cb}, \quad (32)$$

which can be conveniently depicted as a triangle relation in the complex plane, as shown in Fig. 1. Thus, knowing the sides of the CKM-unitarity triangle, the three angles of the triangle α , β and γ are determined. These angles are all related to the Kobayashi-Maskawa phase δ (equivalently the phase δ_{13} in V_{PDG} or the phase η in $V_{\text{Wolfenstein}}$), and they can, in principle, be independently measured in various CP-violating B decays. As we shall discuss below, the matrix elements V_{cb} and V_{ub} are already known from the CC B decays. With more data from B decays and an improved theory one would be able to determine them rather precisely. The matrix element V_{td} can, in principle, be determined from the rare decays $b \rightarrow d + \gamma$, $b \rightarrow d + l^+l^-$, $b \rightarrow d + \nu\bar{\nu}$ (and some selected exclusive decays), and $B_d^0 - B_d^0$ mixing, which already provides a first measurement of $|V_{td}|$ which is, however, not very precise. This set of experiments then provides another way of determining the triangle, namely by measuring its sides. The unitarity triangle represents an important testing ground for the SM flavour physics, in particular in B and K decays.

It has been pointed out by Jarlskog [17], that there exists a large number of different parametrizations of the CKM matrix. However, since the phases of the quark fields are unphysical quantities, the different parametrizations, emerging from specific choices of these phases, must all be equivalent. The parametrization independent quantities are the absolute values of the matrix elements $|V_{ij}|$ (hence also the angles of the unitarity triangles) and the area of the unitarity triangles, which is the same for all six triangles

and is an invariant measure of CP violation. This can be expressed as

$$\begin{aligned} \text{area}[\Delta(\text{CKM})] &= \frac{1}{2} s_{12} s_{23} s_{13} \sin \delta_{13} \quad [\text{PDG}], \\ &= \frac{1}{2} A \lambda^6 \eta \quad [\text{Wolfenstein}], \end{aligned} \quad (33)$$

for the PDG and Wolfenstein parametrizations of V_{CKM} . The Jarlskog invariant denoted by the symbol J [17] is twice this area, which in the standard model is typically of $O(10^{-5})$. It is being debated if the intrinsic smallness of J in the standard model is a serious problem in explaining the measured baryon asymmetry of the universe (BAU), whose quantitative measure is the ratio of the baryon number density to entropy density,

$$\Delta_B = \frac{\rho(B)}{s}, \quad (34)$$

and its present value is $\Delta_B = (4 - 6) \times 10^{-11}$ [3]. Electroweak baryogenesis is a subject of great theoretical interest and one which is not quite under quantitative control as it requires a deeper understanding of the dynamics of the electroweak theory at high energies and temperatures. We refer to a recent review on this subject by Rubakov and Shaposhnikov [18], where several of the key theoretical concepts and calculational strategies are discussed. There is one input to the electroweak baryogenesis issue that can possibly come from B decays, namely these decays will probe if nature admits more than one mechanism of CP violation. Along the same lines, new sources of CP violation, i.e., additional phases, such as are present in multi-Higgs models, may uncover themselves by inducing electric dipole moments for the neutron and the electron at a level just above their present upper bounds [3], which for sure will not be accommodated by the phase in the CKM matrix.

2 Dominant B Decays in the Standard Model

With this introduction, we now turn to study questions which are specific to B physics. We start by discussing the dominant decay rates which determine the lifetimes of the B hadrons, τ_B , their semileptonic branching ratios \mathcal{B}_{SL} and the charm quark multiplicity in B decays $\langle n_c \rangle$, a quantity which has become an important ingredient in understanding the semileptonic branching ratio in the standard model.

The effective lowest-order weak interaction Hamiltonian can be expressed in terms of J_μ^{CC} , introduced earlier,

$$\mathcal{H}_W = \frac{G_F}{2\sqrt{2}} \left(J_\mu^{CC} J^{\mu\dagger CC} + \text{h.c.} \right), \quad (35)$$

where G_F is the Fermi coupling constant. The calculational framework that will be used is QCD and we concentrate first on perturbative QCD improvements of the decay rates and distributions in B decays. The leading order (in α_s) perturbative QCD improvements using \mathcal{H}_W have been worked out in semileptonic processes in [19] - [25], which are modeled on the electromagnetic radiative corrections in the decay of the μ -lepton [26]. This

argument rests on the property of asymptotic freedom enabling one to use the parameter $\alpha_s(m_b)/\pi$ to do a perturbation expansion of the decay amplitudes. There still remains the question of how to relate the perturbative calculations to the actual decays of B hadrons. This involves some kind of parton-hadron duality that will be discussed later. For the non-leptonic decays, such perturbative corrections are calculated using the renormalization group techniques [27]–[30]. We shall discuss some of these techniques here. The underlying theoretical framework and its numerous applications in weak decays of the K and B mesons have been recently reviewed in a comprehensive paper by Buchalla, Buras and Lautenbacher [31], to which we refer for details.

The quantitative description of the physical decay processes, with hadrons in the initial and (in most cases of interest) also final states, requires the knowledge of the wave functions (using the quark-parton model language) or hadronic form factors and structure functions. The primary task of the theory therefore is to evaluate these non-perturbative functions which depend on the strong interaction dynamics. The methods that we shall be using here in studying weak decays are based on the lattice QCD framework, QCD sum rules, and the heavy quark limit of QCD which allows one to do a systematic expansion of decay amplitudes in $1/m_Q$, where $m_Q \gg \Lambda_{QCD}$, and Λ_{QCD} is the QCD scale parameter which is typically of $O(200 \text{ MeV})$ [3]. The lattice QCD framework aims at calculating Green's functions and their S-matrix elements from first principles, i.e. QCD. However, in practice, predictions are hampered by the limitations having to do with the computing power and/or appropriate lattice formulations. Unquenching lattice QCD is one of the foremost technical problems. In addition, simulating B systems directly on the lattice with present day technology introduces finite-size effects. In view of this, present lattice-QCD estimates in B systems are to be taken with some caution. For results on topics relevant for these lectures, we refer to recent reviews [32, 33, 34] from where we shall be drawing heavily. The approach, involving the QCD sum rules [35], allows one to make predictions about current correlation functions which are calculated using the operator product expansion (OPE). The results allow themselves to be expressed in terms of a limited number of non-perturbative parameters. To extract physical quantities, the notion of quark-hadron duality is invoked which enables one to compare suitably weighted quantities. While the method is theoretically well-founded, reliable calculations can only be made if the higher twist- and higher order QCD corrections have been calculated. This is not a limitation in principle but again in practice a trustworthy theoretical treatment is available only in a limited number of cases. For a recent review of the applications of the QCD sum rules in B decays and discussions of some of the inherent uncertainties, see, for example, the review by Braun [36].

Recently, remarkable progress has been made in the formulation of QCD as an effective theory in the heavy quark limit, in which the resulting theory shows symmetry properties not present in the original QCD Lagrangian. These symmetries enable one to make model-independent predictions for hadronic transition form factors involving some exclusive $B \rightarrow (D, D^*, \dots)$ decays at kinematic points where such symmetry relations hold. Some of the pioneering work in this direction can be seen in [37, 38]. In particular, these methods have enabled us to determine $|V_{cb}|$ with controlled theoretical errors and we shall discuss this application here. Along the same lines, equally interesting are the related techniques which involve a systematic expansion of the inclusive decay amplitudes in the inverse

heavy quark mass [39] - [43]. A very satisfying feature of this framework is that the parton model for heavy quark decays emerges as the leading term in a systematic expansion of the decay amplitudes. Power corrections to some of the inclusive and exclusive decay processes have been calculated in terms of a limited number of non-perturbative parameters. These methods, like the QCD sum rules, use operator product expansions which are well defined in Euclidean space. To make predictions in time-like regions, some notion of quark-hadron duality is again required. Theoretically, this aspect of the effective theories is not quite understood. We shall not enter into the technical details surrounding these developments and refer to the original literature and some excellent reviews on this subject [44] - [49]. However, we shall discuss several illustrative applications of this method in these lectures.

2.1 Inclusive semileptonic decay rates of the B hadrons

With this theoretical prelude, we start with the assumption that the inclusive decays of B hadrons can be modeled on the QCD-improved quark model decays. More specifically, while calculating rates, we shall be equating the partial and total decay rates of the B hadrons to the corresponding expressions obtained in the parton model, relying on the heavy quark expansion [39] - [41]:

$$\Gamma(B \rightarrow X) = \Gamma(b \rightarrow x) + O(1/m_b^2) , \quad (36)$$

For b quark semileptonic decays involving CC interactions, one has two partonic transitions:

$$\begin{aligned} b &\longrightarrow c\ell^-\bar{\nu}_\ell, \\ &\longrightarrow u\ell^-\bar{\nu}_\ell. \end{aligned} \quad (37)$$

There exists a close analogy between the b quark decays and μ decay, $\mu^- \rightarrow e^-\bar{\nu}_e\nu_\mu$, with the identification:

$$[b, (c, u), \bar{\nu}_\ell, \ell^-] \leftrightarrow [\mu^-, e^-, \bar{\nu}_e, \nu_\mu]. \quad (38)$$

This analogy holds in general; in particular, at the one loop level $O(\alpha)$ QED corrections to μ^- decay and $O(\alpha_s)$ QCD corrections to b semileptonic decays are related by simply replacing [19, 20, 21]

$$\alpha \longrightarrow \frac{1}{3}\alpha_s Tr \sum_{i=1}^8 \lambda_i \lambda_i = \frac{4}{3}\alpha_s, \quad (39)$$

where λ_i are the Gell-Mann $SU(3)$ matrices, and α_s is the lowest order QCD effective coupling constant,

$$\alpha_s = \frac{12\pi}{(33 - 2n_f) \ln(\frac{m_b^2}{\Lambda^2})} , \quad (40)$$

where n_f is the number of effective quarks. The semileptonic decay rates can then be read off the expression for the $O(\alpha)$ radiatively corrected μ -decay rate [26]. The rates for

$b \rightarrow (u, c)\ell\nu_\ell$ decays, setting $m_\ell = m_{\nu_\ell} = 0$, are given by the expression:

$$\Gamma_{SL}(b \rightarrow (u, c)\ell\nu_\ell) = \Gamma_0 f(r_i) \left[1 - \frac{2}{3} \frac{\alpha_s(m_b^2)}{\pi} g(r_i) \right], \quad (41)$$

with Γ_0 being the normalization factor in the lowest-order rate

$$\Gamma_0 = \frac{G_F^2}{192\pi^3} |V_{ib}|^2 m_b^5, \quad (42)$$

$r_i = m_i/m_b$ ($i = u, b$), and

$$f(r) = 1 - 8r^2 + 8r^6 - r^8 - 24r^4 \ln r. \quad (43)$$

The function $g(r)$ has the normalization $g(0) = \pi^2 - \frac{25}{4}$, and numerically $g(0.3) \simeq 2.51$, relevant for the $b \rightarrow u$ and $b \rightarrow c$ transitions, respectively [19, 20, 21]. With $\Lambda_{\text{QCD}} \simeq 200$ MeV and $n_f = 5$, this gives about (15)% corrections to the semileptonic decay widths involving $\ell = e, \mu$, reducing Γ_{SL} compared to the lowest order result $\Gamma_{SL}^{(0)} = \Gamma_0 f(r)$. The corresponding decrease in the decay width for the semileptonic decay $b \rightarrow c\tau\nu_\tau$ is obtained by an expression very similar to the above one in which the τ -mass effects are included in the phase space and in the QCD corrections.

$$\Gamma(b \rightarrow c\tau\nu_\tau) = \Gamma_0 P(x_c, x_\tau, 0) \left[1 + \frac{2\alpha_s(\mu)}{3\pi} g(x_c, x_\tau, 0) \right] \quad (44)$$

where $P(x_1, x_2, x_3)$ is the well known three-body phase space factor given for arbitrary masses $x_i = m_i/m_b$ by [50]:

$$P(x_1, x_2, x_3) = 12 \int_{(x_2+x_3)^2}^{(1-x_1)^2} \frac{ds}{s} (s - x_2^2 - x_3^2)(1 + x_1^2 - s) w(s, x_2^2, x_3^2) w(s, x_1^2, 1), \quad (45)$$

$$w(a, b, c) = (a^2 + b^2 + c^2 - 2ab - 2ac - 2bc)^{1/2} \quad (46)$$

The function $g(x_1, x_2, x_3)$ has been calculated for arbitrary arguments in [23] in terms of a one-dimensional integral. The functions $P(x_1, 0, 0)$ and $g(x_c, 0, 0)$ go over to the functions $f(r)$ and $(-g(r))$, respectively, given above for the massless lepton case. The numerical values for $g(x_c, x_\tau, 0)$ and $g(x_c, 0, 0)$ are tabulated in [51]. For the default value $x_c = 0.3$, one has $g(x_c, x_\tau, 0) = -2.08$, yielding about a 12 % decrease in $\Gamma(b \rightarrow c\tau\nu_\tau)$ compared to $\Gamma_{SL}^{(0)}(b \rightarrow c\tau\nu_\tau)$ as a result of the leading order QCD corrections [23]. For more modern calculations of the decay rate $\Gamma_{SL}(b \rightarrow c\tau\nu_\tau)$, see [24].

2.2 Inclusive non-leptonic decay rates of the B hadrons

The dominant CC-induced non-leptonic and semileptonic decays of B hadrons are governed by the effective Lagrangian,

$$\mathcal{L}_{eff} = -4 \frac{G_F}{\sqrt{2}} V_{ud}^* V_{cb} [C_1(\mu) \mathcal{O}_1(\mu) + C_2(\mu) \mathcal{O}_2(\mu)]$$

$$\begin{aligned}
& -4 \frac{G_F}{\sqrt{2}} V_{us}^* V_{cb} [C_1(\mu) \mathcal{O}'_1(\mu) + C_2(\mu) \mathcal{O}'_2(\mu)] \\
& -4 \frac{G_F}{\sqrt{2}} V_{cb} \left[\sum_{\ell=e,\mu,\tau} \bar{\ell}_L \gamma_\mu \nu_\ell \bar{c}_L \gamma^\mu b_L \right] + h.c. ,
\end{aligned} \tag{47}$$

and we have just discussed the $O(\alpha_s)$ renormalization effects to the matrix elements of the semileptonic piece in \mathcal{L} . Here \mathcal{O}_1 and \mathcal{O}_2 are the colour-octet and colour-singlet four-Fermi operators, respectively (here α and β are colour indices),

$$\begin{aligned}
\mathcal{O}_1 &= (\bar{d}_\alpha u_\beta)_L (\bar{c}_\beta b_\alpha)_L, \\
\mathcal{O}_2 &= (\bar{d}_\alpha u_\alpha)_L (\bar{c}_\beta b_\beta)_L,
\end{aligned} \tag{48}$$

and $q_L = 1/2(1 - \gamma_5)$ denotes a left-handed quark field. The operators \mathcal{O}'_i are related to the corresponding fields \mathcal{O}_i by the replacement $\bar{d} \rightarrow \bar{s}$. The octet-octet (\mathcal{O}_1) and singlet-singlet (\mathcal{O}_2) operators emerge due to a single gluon exchange between the weak current lines (quark fields) and follow from the colour charge matrix (T_{ij}^a) algebra:

$$T_{ik}^a T_{jl}^a = \frac{1}{2N_c} \delta_{ik} \delta_{jl} + \frac{1}{2} \delta_{il} \delta_{jk} . \tag{49}$$

Here, $N_c = 3$ for QCD. The Wilson coefficients $C_i(\mu)$ are calculated at the scale $\mu = m_W$ and then scaled down to the scale typical for B decays, $\mu = O(m_b)$, using the renormalization group equations, which brings to the fore the influence of strong interactions on the dynamics of weak non-leptonic decays. Without QCD corrections, the two Wilson coefficients have the values $C_1(m_W) = 0$, $C_2(m_W) = 1$. Since the operators \mathcal{O}_1 and \mathcal{O}_2 mix under QCD renormalization, it is convenient to introduce the operators $\mathcal{O}_\pm \equiv (\mathcal{O}_2 \pm \mathcal{O}_1)/2$ having the Wilson coefficients C_\pm which renormalize multiplicatively [27]. The results are now known to two-loop accuracy [30]:

$$C_\pm(\mu) = L_\pm(\mu) \left[1 + \frac{\alpha_s(m_W) - \alpha_s(\mu)}{4\pi} \frac{\gamma_\pm^{(0)}}{2\beta_0} \left(\frac{\gamma_\pm^{(1)}}{\gamma_\pm^{(0)}} - \frac{\beta_1}{\beta_0} \right) + \frac{\alpha_s(m_W)}{4\pi} B_\pm \right], \tag{50}$$

where the multiplicative factor in this expression represents the solution of the RG equations in the leading order QCD [27],

$$L_\pm(\mu) = \left[\frac{\alpha_s(M_W)}{\alpha_s(\mu)} \right]^{d_\pm}, \tag{51}$$

and the exponents have the values $d_+ = \gamma_+^{(0)}/(2\beta_0)$, $d_- = \gamma_-^{(0)}/(2\beta_0)$. The quantities $\gamma_\pm^{(i)}$ are the coefficients of the anomalous dimensions involving the operators \mathcal{O}_\pm (and \mathcal{O}'_\pm),

$$\gamma_\pm = \gamma_\pm^{(0)} \frac{\alpha_s}{4\pi} + \gamma_\pm^{(1)} \left(\frac{\alpha_s}{4\pi} \right)^2 + O(\alpha_s^3), \tag{52}$$

with

$$\gamma_+^{(0)} = 4, \quad \gamma_-^{(0)} = -8, \quad \gamma_+^{(1)} = -7 + \frac{4}{9} n_f, \quad \gamma_-^{(1)} = -14 - \frac{8}{9} n_f, \tag{53}$$

in the naive dimensional regularization (NDR) scheme, i.e., with anticommuting γ_5 . The β_i are the first two coefficients of the QCD β -function, and they have the values

$$\beta_0 = 11 - \frac{2}{3}n_f, \quad \beta_1 = 102 - \frac{38}{3}n_f. \quad (54)$$

Finally, the functions B_{\pm} are the matching conditions obtained by demanding the equality of the matrix elements of the effective Lagrangian calculated at the scale $\mu = m_W$ and in the full theory (i.e., SM) up to terms of $O(\alpha_s(m_W^2))$. They have the values:

$$B_{\pm} = \pm B \frac{N_c \mp 1}{2N_c}, \quad (55)$$

The constant B and the two-loop anomalous dimension $\gamma_{\pm}^{(1)}$ are both regularization-scheme dependent. In the NDR scheme one has $B = 11$. Following [30], we define a scheme-independent quantity R_{\pm} ,

$$R_{\pm} = B_{\pm} + \frac{\gamma_{\pm}^{(0)}}{2\beta_o} \left(\frac{\gamma_{\pm}^{(1)}}{\gamma_{\pm}^{(0)}} - \frac{\beta_1}{\beta_0} \right), \quad (56)$$

in terms of which the Wilson coefficients read

$$C_{\pm}(\mu) = L_{\pm}(\mu) \left[1 + \frac{\alpha_s(m_W) - \alpha_s(\mu)}{4\pi} R_{\pm} + \frac{\alpha_s(\mu)}{4\pi} B_{\pm} \right]. \quad (57)$$

In this form all the scheme-dependence resides in the coefficients B_{\pm} which is to be cancelled by the scheme-dependence of the matrix elements of the corresponding operators.

In addition to the decays $b \rightarrow c + \bar{u}d$, $b \rightarrow c + \bar{u}s$ and $b \rightarrow c + \ell\nu_{\ell}$, which are described by the effective Lagrangian (47), there are other decays involving the CC transitions $b \rightarrow uX$, $b \rightarrow (c, u) + \bar{c}s$ and $b \rightarrow (c, u) + \bar{c}d$, which are not included in this Lagrangian. In a systematic treatment involving QCD renormalization, one has to enlarge the operator basis to include these transitions and the so-called penguin operators. We shall return to a discussion of this part of the Lagrangian later in these lectures as we discuss rare B -decays, where the operator basis will be enlarged and the corresponding Wilson coefficients calculated in the leading logarithmic approximation.

We now discuss the semileptonic branching ratio \mathcal{B}_{SL} for the B mesons and to be specific will consider the case $\ell = e, \mu$. This branching ratio is to a large extent free of the CKM matrix element uncertainties but requires a QCD-improved calculation of the inclusive decay rates, Γ_{SL} , discussed above, and Γ_{tot} ,

$$\mathcal{B}_{\text{SL}} \equiv \frac{\Gamma(B \rightarrow X e \nu_e)}{\Gamma_{\text{tot}}(B)}, \quad (58)$$

with

$$\begin{aligned} \Gamma_{\text{tot}}(B) = & \sum_{\ell=e,\mu,\tau} \Gamma(B \rightarrow X \ell \nu_{\ell}) + \Gamma(B \rightarrow X_c X) + \Gamma(B \rightarrow X_{c\bar{c}} X) \\ & + \Gamma(B \rightarrow X_u X) + \Gamma(B)(\text{Penguins}) . \end{aligned} \quad (59)$$

In the spirit of the parton model, we shall equate $\Gamma(B \rightarrow X_c X) = \Gamma(b \rightarrow c\bar{u}d) + \Gamma(b \rightarrow c\bar{u}s)$, noting that the so-called W -annihilation and W -exchange two-body decays are expected to be small in inclusive B decays. This will be quantified later as we discuss the lifetime differences among B hadrons which arise from the matrix elements of the operators representing these contributions. The corrections for the decay widths $\Gamma(b \rightarrow c\bar{u}d)$ and $\Gamma(b \rightarrow c\bar{u}s)$ are identical neglecting m_u and m_s , and so their contributions can be described by similar functions. The resulting next-to-leading order QCD corrected sum can be expressed as:

$$\begin{aligned}
\Gamma(b \rightarrow c\bar{u}d) + \Gamma(b \rightarrow c\bar{u}s) &= \Gamma_0 P(x_c, 0, 0) \\
&\times \left[2L(\mu)_+^2 + L(\mu)_-^2 + \frac{\alpha_s(M_W) - \alpha_s(\mu)}{2\pi} (2L(\mu)_+^2 R_+ + L(\mu)_-^2 R_-) \right. \\
&+ \frac{2\alpha_s(\mu)}{3\pi} \left(\frac{3}{4} (L(\mu)_+ - L(\mu)_-)^2 c_{11}(x_c) + \frac{3}{4} (L(\mu)_+ + L(\mu)_-)^2 c_{22}(x_c) \right. \\
&\left. \left. + \frac{1}{2} (L(\mu)_+^2 - L(\mu)_-^2) (c_{12}(x_c, \mu) - 12 \ln \frac{\mu}{m_b}) \right) \right] \\
&\equiv 3\Gamma_0 \eta(\mu) J(x_c, \mu) ,
\end{aligned} \tag{60}$$

with $\eta(\mu)$ representing the leading order QCD corrections. The scheme independent R_{\pm} come from the NLO renormalization group evolution and are given by [30]

$$\begin{aligned}
R_+ &= \frac{10863 - 1278n_f + 80n_f^2}{6(33 - 2n_f)^2}, \\
R_- &= -\frac{15021 - 1530n_f + 80n_f^2}{3(33 - 2n_f)^2}
\end{aligned} \tag{61}$$

For $n_f = 5$, $R_+ = 6473/3174$, $R_- = -9371/1587$. Note that the leading dependence of $L(\mu)_{\pm}$ on the renormalization scale μ is canceled to $\mathcal{O}(\alpha_s)$ by the explicit μ -dependence in the α_s -correction terms. Virtual gluon and Bremsstrahlung corrections to the matrix elements of four fermion operators are contained in the mass dependent functions $c_{ij}(x)$. The analytic expressions for the functions $c_{11}(x)$, $c_{12}(x)$, $c_{22}(x)$ are given in [51] where also their numerical values are tabulated. For our default value $x_c = 0.3$, these coefficients have the values:

$$c_{11}(0.3) \simeq 2 \quad c_{12}(0.3, \mu = m_b) \simeq -10 \quad c_{22}(0.3) \simeq -1 . \tag{62}$$

Lumping together all the perturbative and finite charm quark corrections in a multiplicative factor $\Delta_c(m_b, x_c, \alpha_s(m_Z))$, the perturbatively corrected decay width can be expressed as:

$$\Gamma(b \rightarrow c\bar{u}d) + \Gamma(b \rightarrow c\bar{u}s) = 3\Gamma_0 P(x_c, 0, 0) [1 + \Delta_c(x_c, m_b, \alpha_s(m_Z))] . \tag{63}$$

For the central values of the parameters used here ($m_b = 4.8$ GeV, $x_c = 0.3$, $\mu = m_b$ and $\alpha_s(m_Z) = 0.117$), the QCD corrections lead to an enhancement [51]:

$$\Delta_c(m_b, x_c, \alpha_s(m_Z)) = 0.17 . \tag{64}$$

Out of this, the bulk is contributed by the leading log factor

$$\eta(\mu) - 1 = \frac{1}{3} (2L_+^2 + L_-^2) - 1 = 0.10 . \quad (65)$$

Next, we equate $\Gamma(B \rightarrow X_{c\bar{c}}) = \Gamma(b \rightarrow c\bar{c}s) + \Gamma(b \rightarrow c\bar{c}d)$ and discuss the perturbative QCD corrections to the decay width $\Gamma(b \rightarrow c\bar{c}s)$ and $\Gamma(b \rightarrow c\bar{c}d)$. Neglecting m_d and m_s , an assumption which has been found to be valid to a high accuracy in [52], the corrections in the two decay widths are identical and the result can be written in close analogy with the ones for the decay widths $\Gamma(b \rightarrow c\bar{u}s)$ discussed above.

$$\begin{aligned} \Gamma(b \rightarrow c\bar{c}s) + \Gamma(b \rightarrow c\bar{c}d) &= \Gamma_0 P(x_c, x_c, x_s) \\ &\times \left[2L(\mu)_+^2 + L(\mu)_-^2 + \frac{\alpha_s(M_W) - \alpha_s(\mu)}{2\pi} (2L(\mu)_+^2 R_+ + L(\mu)_-^2 R_-) \right. \\ &+ \frac{2\alpha_s(\mu)}{3\pi} \left(\frac{3}{4} (L(\mu)_+ - L(\mu)_-)^2 k_{11}(x_c, \mu) + \frac{3}{4} (L_+ + L_-)^2 k_{22}(x_c) \right. \\ &\left. \left. + \frac{1}{2} (L_+^2 - L_-^2) (k_{12}(x_c) - 12 \ln \frac{\mu}{m_b}) \right) \right]. \end{aligned} \quad (66)$$

The functions $k_{ij}(m_b, x_c, \alpha_s(m_Z))$ have been calculated and their numerical values are tabulated in [53]. For $m_b = 4.8$ GeV, $x_c = 0.3$ and $\alpha_s(m_Z) = 0.117$ and $\mu = m_b$, they have the values:

$$k_{11}(0.3) = 6.44 \quad k_{12}(0.3, \mu = m_b) = 0.82 \quad k_{22}(0.3) = 2.99 , \quad (67)$$

showing that these coefficients are rather sensitive functions of x_c . The corresponding numbers for k_{ij} for the choice $m_s/m_b = 0.04$ are given in [53]. Again, lumping together all the perturbative and finite charm quark corrections in a multiplicative factor $\Delta_{cc}(m_b, x_c, \alpha_s(m_Z))$, the perturbatively corrected decay width can be expressed as:

$$\Gamma(b \rightarrow c\bar{c}s) = 3\Gamma_0 P(x_c, x_c, x_s) [1 + \Delta_{cc}(x_c, m_b, \alpha_s(m_Z))] . \quad (68)$$

For the values of the parameters used here ($m_b = 4.8$ GeV, $x_c = 0.3$ and $\alpha_s(m_Z) = 0.117$), the QCD corrections lead to an enhancement [52, 53]:

$$\Delta_{cc}(m_b, x_c, \alpha_s(m_Z)) = 0.37 . \quad (69)$$

Out of this, the bulk is contributed by the next to leading order correction. This is by far the largest correction to the inclusive rates we have discussed so far. Using pole quark masses and the renormalization scale $\mu = m_b$, one gets [52]:

$$\frac{\Gamma(b \rightarrow c\bar{c}s)(NLO)}{\Gamma(b \rightarrow c\bar{c}s)(LO)} = 1.32 \pm 0.07 . \quad (70)$$

The NLO corrections go in the right direction in bringing theoretical estimates closer to the experimental value for the semileptonic branching ratio. However, this will also lead to enhanced charmed quark multiplicity $\langle n_c \rangle$ in B decays. We shall return to a quantitative analysis of $\mathcal{B}_{\text{SL}}(B)$ and $\langle n_c \rangle$ at the end of this section.

We now turn to a discussion of the CKM-suppressed and penguin transitions contributing at a smaller rate to $\Gamma_{\text{tot}}(B)$. They are of two kinds:

- $\Gamma(B \rightarrow X_u + X)$, which is suppressed due to the CKM matrix element $|V_{ub}|$, with the rate depending on $|V_{ub}|^2$, and
- $\Gamma(B)(\text{Penguin})$: The so-called penguin transitions $b \rightarrow s + X$, where $X = c\bar{c}$ and $X = g$ (QCD penguins), $X = \gamma$ (electromagnetic penguins), $X = \ell^+\ell^-, \nu\bar{\nu}$ (electroweak penguins).

There are even smaller transitions involving $b \rightarrow d + X$, as well as a host of other rare decays but we shall neglect them in estimating the total decay width for obvious reasons. We list below the numerical contributions where in all entries involving $b \rightarrow u + X$ transitions, we have set $|V_{ub}|/|V_{cb}| = 0.08$, corresponding to the present central value of this ratio [54]. The contribution of $b \rightarrow u\bar{u}d$ is calculated without penguins and the contribution to the $b \rightarrow c\bar{c}s$ rate given below is due to interference of the leading current-current type transitions with the penguin operators.

$$\Gamma(b \rightarrow u \sum_l l\nu) \approx 0.015\Gamma_0 \quad \Gamma(b \rightarrow u\bar{c}s) \approx 0.010\Gamma_0 \quad (71)$$

$$\Gamma(b \rightarrow u\bar{u}d) \approx 0.022\Gamma_0 \quad \Delta\Gamma_{\text{penguin}}(b \rightarrow c\bar{c}s) \approx -0.041\Gamma_0 \quad (72)$$

$$\Gamma(b \rightarrow sg) \approx 5.0 \times 10^{-3}\Gamma_0 \quad \Gamma(b \rightarrow s\gamma) \approx 8.0 \times 10^{-4}\Gamma_0 \quad (73)$$

$$\Gamma(b \rightarrow s\nu\bar{\nu}) \approx 1.2 \times 10^{-4}\Gamma_0 \quad \Gamma(b \rightarrow s\ell^+\ell^-) \approx 5.0 \times 10^{-5}\Gamma_0 \quad (74)$$

Note that the contribution due to the interference with the penguin transitions in $b \rightarrow c\bar{c}s$ is negative and it tends to cancel the other small contributions listed above in the total non-leptonic width. The sum of all these contributions add up to

$$\Gamma(B \rightarrow X_u + X) + \Gamma(B)(\text{Penguins}) \simeq 1.25 \times 10^{-2}\Gamma_0 , \quad (75)$$

and hence not of much consequence for the semileptonic branching ratio or the B hadron lifetime estimates. Rare B decays are either constrained by direct experimental searches or indirectly through the measurement of the branching ratio $\mathcal{B}(B \rightarrow X_s + \gamma)$ which excludes most of the allowed parameter space where these decay modes may have appreciably larger branching ratios. It may be parenthetically added here that the chromomagnetic QCD-penguin contribution $b \rightarrow s + g$ could be significantly large in some extensions of the SM, in particular the minimal supersymmetric standard model (MSSM) [55, 56]. This is sometime suggested as a possible source of enhanced non-leptonic decay width. There exist already an experimental bound on this decay branching ratio [54], obtained through the decay chain $b \rightarrow s + g \rightarrow X_s + \phi$ on the assumption that the ϕ -energy spectrum in inclusive B decays is rather hard, similar to the photon energy spectrum in electromagnetic penguin decays $B \rightarrow X_s + \gamma$. This quasi two-body E_ϕ -spectrum is suggested in [57]. However, in our opinion, such an assumed E_ϕ -spectrum is rather unrealistic as it is unlikely that the fragmentation of an $O(5 \text{ GeV})$ $s + g$ system will give rise to dominantly two-body or quasi-two body final states, hence the experimental bound so-obtained [54] is not very compelling.

2.3 Power corrections in $\Gamma_{SL}(B)$ and $\Gamma_{NL}(B)$

Before we discuss the numerical results for \mathcal{B}_{SL} , we include the $O(1/m_b^2)$ power corrections in the inclusive partonic decay widths, which have been calculated using the operator product expansion techniques [39]- [43] and they constitute the first non-trivial corrections to the parton model results. Taking the typical hadronic scale to be $O(1)$ GeV, one expects as a ball-park estimate $O(5)\%$ corrections in the inclusive rates. This is now discussed more quantitatively.

In HQET, the b -quark field is represented by a four-velocity-dependent field, denoted by $b_v(x)$. To first order in $1/m_b$, the b -quark field in QCD $b(x)$ and the HQET-field $b_v(x)$ are related through:

$$b(x) = e^{-im_b v \cdot x} \left[1 + i \frac{\not{D}}{2m_b} \right] b_v(x) \quad (76)$$

The QCD Lagrangian for the b quark in HQET in this order is:

$$\mathcal{L}^{\text{HQET}} = \bar{b}_v i v \cdot \not{D} b_v + \bar{b}_v \frac{i(\not{D})^2}{2m_b} b_v - Z_b \bar{b}_v \frac{g G_{\alpha\beta} \sigma^{\alpha\beta}}{4m_b} b_v + O\left[\frac{1}{m_b^2}\right], \quad (77)$$

where Z_b is a renormalization factor, with $Z_b(\mu = m_b) = 1$ and $\not{D} = D_\mu \gamma^\mu$, with D_μ being the covariant derivative. The operator $\bar{b}_v (i \not{D})^2 b_v / 2m_b$ is not renormalized due to the symmetries of HQET. (In technical jargon, this is termed as a consequence of the reparametrization invariance of $\mathcal{L}^{\text{HQET}}$.) With this Lagrangian, it has been shown in [39] - [40] that in the heavy quark expansion in order $(1/m_b^2)$, the hadronic corrections can be expressed in terms of two matrix elements

$$\langle B^{(*)} | \bar{b}_v (iD)^2 b_v | B^{(*)} \rangle = 2m_{B^{(*)}} \lambda_1, \quad (78)$$

$$\langle B^{(*)} | \bar{b}_v \frac{g}{2} \sigma_{\mu\nu} F^{\mu\nu} b_v | B^{(*)} \rangle = 2d_{B^{(*)}} m_{B^{(*)}} \lambda_2, \quad (79)$$

where $F^{\mu\nu}$ is the gluonic field strength tensor, and the constants $d_{B^{(*)}}$ have the value 3 and -1 for B and B^* , respectively. The constant λ_2 can be related to the hyperfine splitting in the B mesons, which gives:

$$\lambda_2 \simeq \frac{1}{4} (m_{B^*}^2 - m_B^2) = 0.12 \text{ GeV}^2. \quad (80)$$

The other quantity λ_1 is just the average kinetic energy of the b quark inside a B meson and has been estimated in the QCD sum rule approach [58] yielding $\lambda_1 = -(0.5 \pm 0.1)$ GeV 2 [59]. As we shall discuss later, this parameter influences the lepton- and photon-energy spectrum in the decays $B \rightarrow X \ell \nu_\ell$ and $B \rightarrow X_s + \gamma$, and has also been estimated using these spectra [60, 61]. Taking into account these corrections, the semileptonic and non-leptonic decay rates of a B meson $B \rightarrow X \ell \nu_\ell$ and $B \rightarrow X_c X$ can be written as [40, 41]:

$$\begin{aligned} \Gamma(B \rightarrow X_c \ell \nu_\ell) &= \Gamma^{(0)} f(r_c) \left[\left(1 - \frac{2}{3} \frac{\alpha_s(m_b^2)}{\pi} g(r_c) \right) \left(1 + \frac{\lambda_1}{2m_b^2} + \frac{3\lambda_2}{2m_b^2} - \frac{6(1-r_c)^4}{f(r_c)} \frac{\lambda_2}{m_b^2} \right) \right. \\ &\quad \left. + O(\alpha_s^2, \frac{\alpha_s}{m_b^2}, \frac{1}{m_b^3}) \right], \end{aligned} \quad (81)$$

and

$$\begin{aligned}\Gamma(B \longrightarrow X_c X) = 3\Gamma^{(0)} & \left[\eta(\mu) J(\mu) \left(1 + \frac{\lambda_1}{2m_b^2} + \frac{3\lambda_2}{2m_b^2} - \frac{6(1-r_c)^4}{f(r_c)} \frac{\lambda_2}{m_b^2} \right) \right. \\ & \left. - (L_+(\mu)^2 - L_-(\mu)^2) \frac{4(1-r_c)^3}{f(r_c)} \frac{\lambda_2}{m_b^2} + O(\alpha_s^2, \frac{\alpha_s}{m_b^2}, \frac{1}{m_b^3}) \right], \quad (82)\end{aligned}$$

where the product $\eta(\mu) J(\mu)$ denotes the NLO corrected result for the partonic decay discussed above in (60), to which Eq. (82) reduces in the limit $\lambda_1 = \lambda_2 = 0$.

The decay rates depend on the quark masses, which unlike lepton masses, do not appear as poles in the S -matrix nor do the quarks exist as asymptotic states. They are parameters of an interacting theory and hence subject to renormalization effects. Consequently, they require a regularization scheme, such as the \overline{MS} scheme, and a scale, where they are normalized, to become well-defined quantities. For example, the quark masses in the so-called \overline{MS} scheme and the pole masses (OS scheme) are related in the leading order [62],

$$\overline{m}_Q(m_Q) = m_Q \left[1 - 4 \frac{\alpha_s(m_Q)}{(3\pi)} + \dots \right]. \quad (83)$$

In HQET, quark masses can be expressed in terms of the heavy meson masses m_M and the parameters λ_1 , λ_2 and a quantity called $\bar{\Lambda}$, where

$$m_M = m_Q + \bar{\Lambda} - \frac{\lambda_1 + d_M \lambda_2}{2m_Q} + \dots \quad (84)$$

With this the decay rates then depend on the QCD-related parameters, Λ_{QCD} , λ_1 , λ_2 and $\bar{\Lambda}$. Since quark masses are scale- and (regularization) scheme-dependent quantities, this also holds for the parameter $\bar{\Lambda}$. As a consequence of this, the decay rates become scale- and scheme-dependent. This will reflect itself through increased theoretical dispersion on various physical quantities. More precise predictions for the decay rates and related quantities (such as \mathcal{B}_{SL} and $\langle n_c \rangle$) require knowledge of higher order corrections, which are unfortunately not known. In the context of the heavy quark expansion, one can relate the parameters λ_1 and λ_2 to the quark and hadron masses:

$$m_b - m_c = m_B - m_D + \frac{\lambda_1 + 3\lambda_2}{2} \left(\frac{1}{m_b} - \frac{1}{m_c} \right) + O\left(\frac{1}{m^2}\right), \quad (85)$$

and the quark mass differences can then be calculated knowing λ_1 and λ_2 , giving $(m_b - m_c) = (3.4 \pm 0.03 \pm 0.03)$ GeV [49]. This difference, which determines the inclusive rates and shape of the lepton energy spectrum in semileptonic decays, has also been determined from an analysis of the experimental lepton energy spectrum in B decays, yielding $(m_b - m_c) = 3.39 \pm 0.01$ GeV for the pole masses [61], in excellent agreement with the QCD sum rule based estimates. The quark masses themselves have considerable uncertainties. We shall not discuss them here. For a comprehensive discussion of the quark masses and their current values, we refer to the reviews by Leutwyler [63] and by Manohar in the PDG review of particle properties [3].

2.4 Numerical estimates of $\mathcal{B}_{SL}(B)$ and $\langle n_c \rangle$

The theoretical framework described in the previous section can now be used to predict two important quantities in B decays $\mathcal{B}_{SL}(B)$ and $\langle n_c \rangle$, which have been measured. Concerning $\mathcal{B}_{SL}(B)$, there is some discrepancy between the two set of experiments performed at the $\Upsilon(4S)$ and at the Z^0 resonance, although it must be stressed that these experiments measure a different mixture of B hadrons. The present measurements are reviewed recently in [54]:

$$\begin{aligned}\mathcal{B}_{SL}(B) &= (10.56 \pm 0.17 \pm 0.33)\% \quad \text{at } \Upsilon(4S) \\ \mathcal{B}_{SL}(B) &= (10.89 \pm 0.18 \pm 0.24)\% \quad \text{at } Z^0 \\ \langle n_c \rangle &< 1.16 \pm 0.05 \quad \text{at } \Upsilon(4S).\end{aligned}\quad (86)$$

The first error quoted for \mathcal{B}_{SL} is experimental and the second is an estimate of the model dependence. The number for $\langle n_c \rangle$ is obtained by summing over various bound and unbound charmed hadron states in B decays, and the inequality is to due to the present upper limit on the inclusive branching ratio $\mathcal{B}(B \rightarrow \eta_c X) < 0.018$.

The theoretical predictions for these quantities at present are somewhat fuzzy due to the uncertainties in the input parameters. We shall rely here on a recent theoretical update by Bagan et al. [52] [see also the recent analysis by Neubert and Sachrajda [64]], where the following ranges of parameters have been used:

$$m_b(\text{pole}) = 4.8 \pm 0.2 \text{ GeV}; \quad \alpha_s(m_Z) = 0.117 \pm 0.007, \quad m_b/2 < \mu < 2m_b, \quad (87)$$

$$\lambda_1 = -(0.5 \pm 0.1) \text{ GeV}^2; \quad \lambda_2 = 0.12 \text{ GeV}^2 \quad (88)$$

Their analysis leads to the following values [52]:

$$\mathcal{B}_{SL} = (12.0 \pm 0.7 \pm 0.5 \pm 0.2^{+0.9}_{-1.2})\%, \quad (89)$$

and

$$\overline{\mathcal{B}}_{SL} = (11.3 \pm 0.6 \pm 0.7 \pm 0.2^{+0.9}_{-1.7})\%, \quad (90)$$

using the pole (also called on shell OS) and \overline{MS} masses, respectively. The errors are from $\Delta(m_b)$, $\Delta\alpha_s(m_Z)$, $\Delta(\lambda_1)$, $\Delta(\Gamma(B \rightarrow X_{cc})$ and from the scale($= \mu$) variation, respectively. An estimate of the present theoretical uncertainty can be obtained by adding these errors in quadrature (a reasonable procedure since most errors given above are independent), yielding

$$\begin{aligned}\mathcal{B}_{SL} &= (12.0 \pm 1.4)\%, \\ \overline{\mathcal{B}}_{SL} &= (11.3 \pm 1.6)\%.\end{aligned}\quad (91)$$

This shows that this quantity has still significant theoretical spread:

$$\delta\mathcal{B}_{SL}(B) \simeq \pm 0.15\mathcal{B}_{SL}(B) \simeq \pm 0.018. \quad (92)$$

The corresponding estimates for $\langle n_c \rangle$ and $\langle \bar{n}_c \rangle$ in the OS and \overline{MS} schemes, respectively, are [52]:

$$\langle n_c \rangle = (1.24 \pm 0.05 \pm 0.01) \quad \text{and} \quad \langle \bar{n}_c \rangle = (1.30 \pm 0.03 \pm 0.04), \quad (93)$$

where the first error in both the schemes is due to Δm_b , and the second error combines the uncertainties in the rest of the parameters. The estimates (91) and (93) should be compared with the experimental measurements given in Eq. (86). A comparison of these theoretical estimates (eqs. (89), (90) and (93)) and data on $\langle n_c \rangle$ and \mathcal{B}_{SL} is shown in Fig. 2. It should be pointed out that in the analysis of Bagan et al. [52] for \mathcal{B}_{SL} and

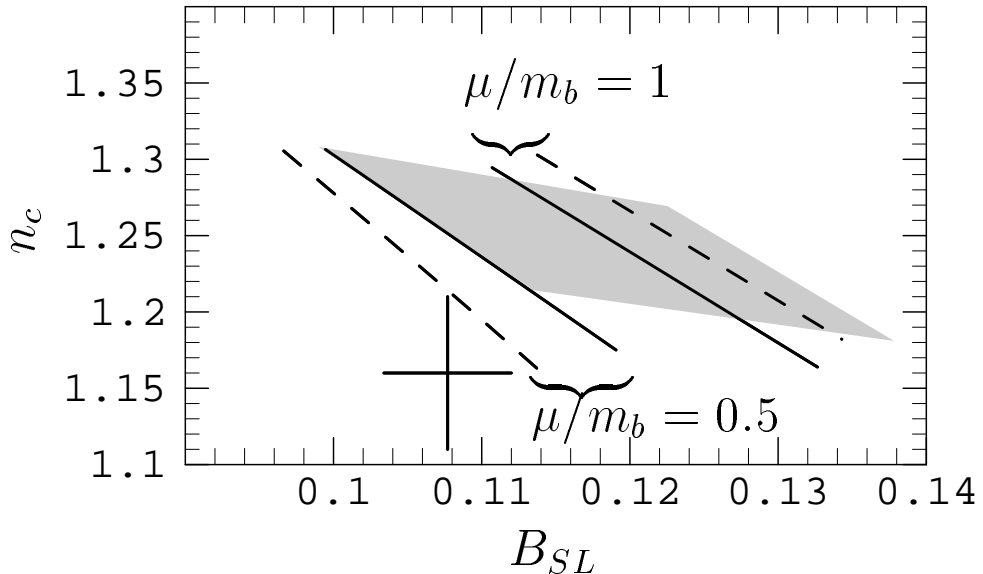


Figure 2: The charm content n_c vs. B_{SL} in B decays. Solid lines: theoretical predictions in the OS scheme for $0.23 < m_c/m_b < 0.33$; dashed lines: the same in the \overline{MS} scheme for $0.18 < \bar{m}_c(\bar{m}_c)/\bar{m}_b(\bar{m}_b) < 0.28$. Shaded area: theoretical predictions in the OS scheme by varying over the parameters as discussed in the text. The data point is from [54] (Figure taken from [52]).

$\langle n_c \rangle$, possible contributions from the so-called spectator effects (W -annihilation and W -exchange) have been neglected. Such effects depend on the wave-functions at the origin, using the quark model language, and are proportional to f_B^2 , which could lead to some $O(5)\%$ effects, well within the present theoretical noise $\delta(\mathcal{B}_{SL})$ discussed above. All in all, it is fair to conclude that within existing uncertainties, the current theoretical estimates for \mathcal{B}_{SL} and \overline{n}_c do not disagree significantly with the experimental values, though there is a tendency in these estimates to yield somewhat larger value for \overline{n}_c . More work is needed to make these comparisons precise. While still on the same subject, we note that the pattern of power corrections predicted by the short-distance expansion of the heavy quark effective theory in inclusive non-leptonic decays has been questioned in [65]. It is argued on phenomenological grounds that data on b - and c -decays are better accommodated if some account is taken of the linear ($1/m_Q$) corrections, which are absent in the HQET approach. Naive identification of the m_Q^5 factor in the inclusive decay widths with m_H^5 , with m_H being the heavy hadron mass, brings data and theoretical estimates in better agreement! The presence of $1/m_Q$ corrections could be related to the breakdown of local duality in non-leptonic decays. The real question is if one could derive this suggested pattern of power corrections in QCD.

While the suggestion of Altarelli et al. [65] is interesting and it raises new theoretical issues as to the reliability of Γ_{NL} calculated in the HQET approach, their arguments are purely phenomenological. It is fair to say that a big step in reducing the present theoretical uncertainties will be the completion of all the perturbative NLL corrections to the dominant decays discussed above. Parts of them, the so-called gluon bubble graphs having an arbitrary number of fermion loops, which take into account the effects of the running of α_s on \mathcal{B}_{SL} in all orders in perturbation theory, are available in the literature [66, 67]. This is related to the issue of defining a factorization scale, discussed earlier in a more general context by Brodsky et al. [68], which at present is a big uncertainty in this approach, as can be seen in Fig. 2.

2.5 *B*-Hadron Lifetimes in the Standard Model

A matter closely related to the semileptonic branching ratios is that of the individual *B* hadron lifetimes. The QCD-improved spectator model gives almost equal lifetimes. Power corrections will split the *B*-baryon lifetime from those of B_d , B^\pm and B_s . However, first estimates of these differences are at the few per cent level [40]. The experimental situation has been summarized as of summer 1995 in [69]:

$$\frac{\tau(B^-)}{\tau(B_d)} = 1.02 \pm 0.04; \quad \frac{\tau(B_s)}{\tau(B_d)} = 1.01 \pm 0.07; \quad \frac{\tau(\Lambda_b)}{\tau(B_d)} = 0.76 \pm 0.05. \quad (94)$$

Since then, a new result for the lifetime of the Λ_b baryon has been reported by the CDF collaboration, $\tau(\Lambda_b)/\tau(B_d) = 0.85 \pm 0.10 \pm 0.05$ [70], which is still less than the other two ratios involving the *B*-meson lifetimes but reduces the gap in the Λ_b and *B*-meson lifetimes.

This subject has received renewed theoretical attention lately [64, 71, 72], in which the possibly enhanced roles of the four-Fermion operators between baryonic states has been studied. We recall that such operators enter at $O(1/m_b^3)$ in the heavy quark expansion discussed above [40]. In this order, there are four such operators, which using the notation of [64], can be expressed as:

$$\begin{aligned} \mathcal{O}_{V-A}^q &= (\bar{b}_L \gamma_\mu q_L)(\bar{q}_L \gamma^\mu b_L), \\ \mathcal{O}_{S-P}^q &= (\bar{b}_R q_L)(\bar{q}_L b_R), \\ \mathcal{T}_{V-A}^q &= (\bar{b}_L \gamma_\mu t_a q_L)(\bar{q}_L \gamma^\mu t_a b_L), \\ \mathcal{T}_{S-P}^q &= (\bar{b}_R t_a q_L)(\bar{q}_L t_a b_R), \end{aligned} \quad (95)$$

where t_a are generators of colour $SU(3)$. The matrix elements of these operators between various *B*-meson and Λ_b -baryons are in general different and this contribution will thus split the decay widths of the various *B* hadrons. In general, the operators (95) introduce eight new parameters corresponding to the matrix elements of these operators. In the large- N_c limit, however, it has been argued in [64] that the *B*-mesonic matrix elements of the operators $\langle B_q | \mathcal{O}_{V-A}^q | B_q \rangle$ and $\langle B_q | \mathcal{O}_{S-P}^q | B_q \rangle$ are the dominant ones. While accurate numerical estimates require a precise knowledge of these matrix elements, one expects that they give rise typically to the spectator-type effects (using the parton model language):

$$\frac{\Gamma_{\text{spec}}}{\Gamma_{\text{tot}}} \simeq \left(\frac{2\pi f_B}{m_B} \right)^2 \simeq 5\%, \quad (96)$$

with f_B of order 200 MeV. In the case of Λ_b baryons, one can use the heavy quark spin symmetry to derive two relations among the operators between the Λ_b states. The problem is then reduced to the estimate of two matrix elements which in [64] are taken to be the following:

$$\frac{1}{2m_{\Lambda_b}} \langle \Lambda_b | \mathcal{O}_{V-A}^q | \Lambda_b \rangle \equiv -\frac{f_B^2 m_B}{48} r\left(\frac{\Lambda_b}{B_q}\right), \quad (97)$$

and

$$\langle \Lambda_b | \tilde{\mathcal{O}}_{V-A}^q | \Lambda_b \rangle = -\tilde{B} \langle \Lambda_b | \mathcal{O}_{V-A}^q | \Lambda_b \rangle, \quad (98)$$

The operator $\tilde{\mathcal{O}}_{V-A}$ is a linear combination of the operators \mathcal{T}_{V-A} and \mathcal{O}_{V-A} introduced earlier, $\tilde{\mathcal{O}}_{V-A} = 2\mathcal{T}_{V-A} + 3\mathcal{O}_{V-A}$, following from colour matrix algebra [64], and $r(\Lambda_b/B_q)$ is the ratio of the squares of the wave functions which can be expressed in terms of the probability of finding a light quark at the location of a b quark inside Λ_b baryon and the B meson, i.e.

$$r\left(\frac{\Lambda_b}{B_q}\right) = \frac{|\Psi_{bq}^{\Lambda_b}|^2}{|\Psi_{bq}^B|^2}. \quad (99)$$

One expects $\tilde{B} = 1$ in the valence-quark approximation. However, the ratio $r(\Lambda_b/B_q)$ has a large uncertainty on it, ranging from $r(\Lambda_b/B_q) \simeq 0.5$ in the non-relativistic quark model [73] to $r(\Lambda_b/B_q) = 1.8 \pm 0.5$ if one uses the ratio of the spin splittings between Σ_b and Σ_b^* baryons and B and B^* mesons, as advocated by Rosner [72] and using the preliminary data from DELPHI, $m(\Sigma_b^*) - m(\Sigma_b) = (56 \pm 16)$ MeV [74].

Using the ball-park estimates that \tilde{B} and $r(\Lambda_b/B_q)$ are both of order unity yields for the lifetime ratio $\tau(\Lambda_b)/\tau(B_d) > 0.9$ [64], significantly larger than the present world average. Reliable estimates of these constants can be got, in principle, using lattice-QCD and QCD sum rules. Very recently, QCD sum rules have been used to estimate $\langle \Lambda_b | \tilde{\mathcal{O}}_{V-A}^q | \Lambda_b \rangle$ and \tilde{B} , yielding $\langle \Lambda_b | \tilde{\mathcal{O}}_{V-A}^q | \Lambda_b \rangle = (0.4 - 1.2) \times 10^{-3}$ GeV³ and $\tilde{B} = 1.0$ [75]. This corresponds to the parameter $r(\Lambda_b/B_q)$ having a value in the range $r(\Lambda_b/B_q) \simeq 0.1 - 0.3$, much too small to explain the observed lifetime difference. One must conclude that the lifetime ratio $\tau(\Lambda_b)/\tau(B_d)$ remains a puzzle. New and improved measurements are needed, which we trust will be forthcoming from HERA-B and Tevatron experiments in not-too-distant a future.

2.6 Determination of $|V_{cb}|$ and $|V_{ub}|$

The CKM matrix element V_{cb} can be obtained from semileptonic decays of B mesons. We shall restrict ourselves to the methods based on HQET to calculate the exclusive semileptonic decay rates and use the heavy quark expansion to estimate the inclusive rates. Concerning exclusive decays, we recall that in the heavy quark limit ($m_b \rightarrow \infty$), it has been observed that all hadronic form factors in the semileptonic decays $B \rightarrow (D, D^*)\ell\nu_\ell$ can be expressed in terms of a single function, the Isgur-Wise function [38]. It has been shown that the HQET-based method works best for $B \rightarrow D^*\ell\nu$ decays, since these are unaffected by $1/m_Q$ corrections [76, 77, 78]. Since the rate is zero at the kinematic point $\omega = 1$, one uses data for $\omega > 1$ and an extrapolation procedure (discussed below) to determine $\xi(1)|V_{cb}|$ and the slope of the Isgur-Wise function $\hat{\rho}^2$.

Using HQET, the differential decay rate in $B \rightarrow D^* \ell \bar{\nu}_\ell$ is

$$\begin{aligned} \frac{d\Gamma(B \rightarrow D^* \ell \bar{\nu})}{d\omega} &= \frac{G_F^2}{48\pi^3} (m_B - m_{D^*})^2 m_{D^*}^3 \eta_A^2 \sqrt{\omega^2 - 1} (\omega + 1)^2 \\ &\quad \times [1 + \frac{4\omega}{\omega + 1} \frac{1 - 2\omega r + r^2}{(1 - r)^2}] |V_{cb}|^2 \xi^2(\omega) , \end{aligned} \quad (100)$$

where $r = m_{D^*}/m_B$, $\omega = v \cdot v'$ (v and v' are the four-velocities of the B and D^* meson, respectively), and η_A is the short-distance correction to the axial vector form factor. In the leading logarithmic approximation, this was calculated by Shifman and Voloshin some time ago – the so-called hybrid anomalous dimension [79]. In the absence of any power corrections, $\xi(\omega = 1) = 1$. The size of the $O(1/m_b^2)$ and $O(1/m_c^2)$ corrections to the Isgur-Wise function, $\xi(\omega)$, and partial next-to-leading order corrections to η_A have received a great deal of theoretical attention, and the state of the art has been summarized by Neubert [80] and Shifman [47]. Following [80], we take:

$$\begin{aligned} \xi(1) &= 1 + \delta(1/m^2) = 0.945 \pm 0.025 , \\ \eta_A &= 0.965 \pm 0.020 . \end{aligned} \quad (101)$$

This gives the range [80]:

$$\mathcal{F}(1) = \xi \cdot \eta_A = 0.91 \pm 0.04 . \quad (102)$$

Recently, the quantity η_A , and its counterpart for the vector current matrix element renormalization, η_V , have been calculated in the complete next-to-leading order by Czarnecki [81], getting

$$\begin{aligned} \eta_A &= 0.960 \pm 0.007 , \\ \eta_V &= 1.022 \pm 0.004 . \end{aligned} \quad (103)$$

The NLO central value for η_A is in agreement with the estimate of the same given in eq. (101) but the error on it is now reduced by a factor of 3. So, the error on $\mathcal{F}(1)$ is now completely dominated by the power corrections in $\xi(1)$.

Since the range of accessible energies in the decay $B \rightarrow D^* \ell \bar{\nu}$ is rather small ($1 < \omega < 1.5$), the extrapolation to the symmetry point can be done using an expansion around $\omega = 1$,

$$\mathcal{F}(\omega) = \mathcal{F}(1) \left[1 - \hat{\rho}^2(\omega - 1) + \hat{c}(\omega - 1)^2 + \dots \right] . \quad (104)$$

It is usual to use a linear form for extrapolation with the slope $\hat{\rho}^2$ left as a free parameter, as the effect of a curvature term is small [82]. The present experimental input from the exclusive semileptonic channels is based on the data by CLEO, ALEPH, ARGUS, and DELPHI, which is summarized in [83] to which we refer for details and references to the experimental analysis. For the updated ARGUS numbers, see [84]. The statistically weighted average used in the analysis [83] is:

$$|V_{cb}| \cdot \mathcal{F}(1) = 0.0353 \pm 0.0018 . \quad (105)$$

This agrees with the numbers presented by Skwarnicki last summer [54],

$$\begin{aligned} |V_{cb}| \cdot \mathcal{F}(1) &= 0.0351 \pm 0.0017 , \\ \hat{\rho}^2 &= 0.87 \pm 0.10 . \end{aligned} \quad (106)$$

Using $\mathcal{F}(1)$ from Eq. (102), gives the following value:

$$|V_{cb}| = 0.0388 \pm 0.0019 \text{ (expt)} \pm 0.0017 \text{ (th).} \quad (107)$$

Combining the errors linearly gives $|V_{cb}| = 0.0388 \pm 0.0036$. This is in good agreement with the value $|V_{cb}| = 0.037^{+0.003}_{-0.002}$ obtained from the exclusive decay $B \rightarrow D^* \ell \nu_\ell$, using a dispersion relation approach [85].

The value of $|V_{cb}|$ obtained from the inclusive semileptonic B decays using heavy quark expansion is quite compatible with the above determination of the same. The inclusive analysis has the advantage of having very small statistical error. However, as discussed previously, there is about 2σ discrepancy between the semileptonic branching ratios at the $\Upsilon(4S)$ and in Z^0 decays. Using an averaged value for the semileptonic decay width from these two sets of measurements gives: $\Gamma(b \rightarrow c \ell \nu_\ell) = \mathcal{B}_{SL}/\langle \tau_B \rangle = (67.3 \pm 2.7) \text{ ns}^{(-1)}$ [54], where $\langle \tau_B \rangle = (\tau_{B^-} + \tau_{B^0})/2 = 1.60 \pm 0.03 \text{ ps}$ and $\langle \tau_B \rangle = 1.55 \pm 0.02 \text{ ps}$ have been used for the $\Upsilon(4S)$ and Z^0 decays, respectively, and the error has been inflated to take into account the disagreement mentioned. This leads to a value [54]:

$$|V_{cb}| = 0.0398 \pm 0.0008 \text{ (expt)} \pm 0.004 \text{ (th).} \quad (108)$$

where the theoretical error estimate ($\pm 10\%$) has been taken from Neubert [80]. While still on the same quantity, it should be noted that Vainshtein has quoted a much smaller theoretical error, [48]:

$$|V_{cb}| = 0.0408 \left[\frac{\mathcal{B}(B \rightarrow X_c \ell \nu_\ell)}{0.105} \right]^{1/2} \left[\frac{1.6 \text{ ps}}{\tau_B} \right]^{1/2} (1.0 \pm 0.03(\text{th})). \quad (109)$$

For further discussion of these matters we refer to [47, 48, 80]. We shall use the following values for $|V_{cb}|$ and the Wolfenstein parameter A :

$$|V_{cb}| = 0.0388 \pm 0.0036 \implies A = 0.80 \pm 0.075. \quad (110)$$

Up to recently, $|V_{ub}/V_{cb}|$ was obtained by looking at the endpoint of the inclusive lepton spectrum in semileptonic B decays. Unfortunately, there still exists quite a bit of model dependence in the interpretation of the inclusive data by themselves yielding $|V_{ub}|/|V_{cb}| = 0.08 \pm 0.03$ [86, 84]. A recent new input to this quantity is provided by the measurements of the exclusive semileptonic decays $B \rightarrow (\pi, \rho) \ell \nu_\ell$ [87, 54]. The extracted branching ratios depend on the model used to correct for the experimental acceptance but they do provide some discrimination among the various models. In particular, models such as that of Isgur et al. [88], which give values well in excess of 3 for the ratio of the decay widths $\Gamma(B^0 \rightarrow \rho^- \ell^+ \nu)/\Gamma(B^0 \rightarrow \pi^- \ell^+ \nu)$, are disfavoured by the CLEO data which yield typically 1.7 ± 1.0 for the same quantity, with some marginal model dependence. The models with larger values for the ratio $\Gamma(B^0 \rightarrow \rho^- \ell^+ \nu)/\Gamma(B^0 \rightarrow \pi^- \ell^+ \nu)$ also lead to softer lepton energy spectrum in inclusive B decays, requiring larger values of $|V_{ub}|/|V_{cb}|$. A recent estimate of this ratio in the light-cone QCD sum rule approach gives 2.4 ± 0.8 [89], and yields a branching ratio $\mathcal{B}(B \rightarrow \rho \ell \nu_\ell) = (19 \pm 7)|V_{ub}|^2$, giving a value of $(1.95 \pm 0.72) \times 10^{-4}$, for $|V_{ub}| = 0.08$, in agreement with the experimental numbers, which, however, have significant errors. Excluding models which fail to reproduce the exclusive

data from further consideration, measurements in both the inclusive and exclusive modes are compatible with

$$\left| \frac{V_{ub}}{V_{cb}} \right| = 0.08 \pm 0.02 , \quad (111)$$

which is also the value adopted by the PDG Review [3]. This gives a constraint on the Wolfenstein parameters ρ and η :

$$\sqrt{\rho^2 + \eta^2} = 0.36 \pm 0.08 . \quad (112)$$

With the measurements of the form factors in semileptonic decays $B \rightarrow (\pi, \rho, \omega)\ell\nu_\ell$, one should be able to further constrain the models, thereby reducing the present theoretical uncertainty on this quantity.

We summarize this section by observing that the bulk properties of B decays are largely accounted for in the standard model. On the theoretical front, parton model estimates of the earlier epoch have been replaced by theoretically better founded calculations with controlled errors, though this point of view has not found universal acceptance [65]! In particular, methods based on HQET and heavy quark expansion have led to a quantitative determination of $|V_{cb}|$ at $\pm 10\%$ accuracy, which makes it after $|V_{ud}|$ and $|V_{us}|$, the third best measured CKM matrix element. The matrix element $|V_{ub}|$ has still large uncertainties ($\pm 25\%$) and there is every need to reduce this, as it is one of the principal handicaps at present in testing the unitarity of the CKM matrix precisely (more on this later). The quantities \mathcal{B}_{SL} , $\langle n_c \rangle$, and the individual B -hadron lifetimes are not in perfect agreement with data but the present theoretical estimates have still large uncertainties to abandon the SM. A completely quantitative comparison requires the missing NLL corrections and in the case of lifetime differences better evaluations of the matrix elements of four-quark operators, which we hope will be forthcoming. Finally, we stress that it will be very helpful to measure the semileptonic branching ratios \mathcal{B}_{SL} for the Λ_b baryons. With the lifetimes of the B hadrons now well measured, such a measurement would allow to compare $\Gamma_{SL}(B_d)$, $\Gamma_{SL}(B^\pm)$ and $\Gamma_{SL}(\Lambda_b)$, to check the pattern of power corrections in semileptonic decays.

3 Electromagnetic Penguins and Rare B Decays in the Standard Model

The SM does not admit FCNC transitions in the Born approximation, which is obvious from the Lagrangian given at the very outset of these lectures. However, they are induced through the exchange of W^\pm bosons in loop diagrams. We shall discuss representative examples from several such transitions involving B decays, starting with the decay $B \rightarrow X_s + \gamma$, which has been measured by CLEO [90]. This was preceded by the measurement of the exclusive decay $B \rightarrow K^* + \gamma$ [91]:

$$\mathcal{B}(B \rightarrow X_s + \gamma) = (2.32 \pm 0.57 \pm 0.35) \times 10^{-4} , \quad (113)$$

$$\mathcal{B}(B \rightarrow K^* + \gamma) = (4.5 \pm 1.0 \pm 0.6) \times 10^{-5} , \quad (114)$$

yielding an exclusive-to-inclusive ratio:

$$R_{K^*} = \frac{\Gamma(B \rightarrow K^* + \gamma)}{\Gamma(B \rightarrow X_s + \gamma)} = (19 \pm 6 \pm 4)\% . \quad (115)$$

These decay rates test the SM and the models for decay form factors and we shall study them quantitatively.

The leading contribution to $b \rightarrow s + \gamma$ arises at one-loop from the so-called penguin diagrams and the matrix element in the lowest order can be written as:

$$\mathcal{M}(b \rightarrow s + \gamma) = \frac{G_F}{\sqrt{2}} \frac{e}{2\pi^2} \sum_i V_{ib} V_{is}^* F_2(x_i) q^\mu \epsilon^\nu \bar{s} \sigma_{\mu\nu} (m_b R + m_s L) b , \quad (116)$$

where $x_i = m_i^2/m_W^2$, q_μ and ϵ_μ are, respectively, the photon four-momentum and polarization vector, the sum is over the quarks, u , c , and t , and V_{ij} are the CKM matrix elements. The (modified) Inami-Lim function $F_2(x_i)$ derived from the (1-loop) penguin diagrams is given by [92]:

$$F_2(x) = \frac{x}{24(x-1)^4} \left[6x(3x-2) \log x - (x-1)(8x^2 + 5x - 7) \right] , \quad (117)$$

where in writing the expression for $F_2(x_i)$ above we have left out a constant from the function derived by Inami and Lim, since on using the unitarity constraint these sum to zero. It is instructive to write the unitarity constraint for the decays $B \rightarrow X_s + \gamma$ in full:

$$V_{tb} V_{ts}^* + V_{cb} V_{cs}^* + V_{ub} V_{us}^* = 0 . \quad (118)$$

Now, since the last term in this sum is completely negligible compared to the others (by direct experimental measurements), one could set it to zero enabling us to express the one-loop electromagnetic penguin amplitude as follows:

$$\mathcal{M}(b \rightarrow s + \gamma) = \frac{G_F}{\sqrt{2}} \frac{e}{2\pi^2} \lambda_t (F_2(x_t) - F_2(x_c)) q^\mu \epsilon^\nu \bar{s} \sigma_{\mu\nu} (m_b R + m_s L) b . \quad (119)$$

The GIM mechanism [12] is manifest in this amplitude and the CKM-matrix element dependence is factorized in $\lambda_t \equiv V_{tb} V_{ts}^*$. The measurement of the branching ratio for $B \rightarrow X_s + \gamma$ can then be readily interpreted in terms of the CKM-matrix element product $\lambda_t/|V_{cb}|$ or equivalently $|V_{ts}|/|V_{cb}|$. In the approximation we are using (i.e., setting $\lambda_u = 0$), this is equivalent to measuring $|V_{cs}|$. For a quantitative determination of $|V_{ts}|/|V_{cb}|$, however, QCD radiative corrections have to be computed and the contribution of the so-called long-distance effects estimated. We proceed to discuss them below.

3.1 The effective Hamiltonian for $B \rightarrow X_s \gamma$

The appropriate framework to incorporate QCD corrections is that of an effective theory obtained by integrating out the heavy degrees of freedom, which in the present context are the top quark and W^\pm bosons. This effective theory is an expansion in $1/m_W^2$ and involves a tower of increasing higher dimensional operators built from the quark fields (u, d, s, c, b),

photon, gluons and leptons. The presence of the top quark and of the W^\pm bosons is reflected through the effective coefficients of these operators which become functions of their masses. The operator basis depends on the underlying theory and in these lectures we shall concentrate on the standard model. The basis that we shall use is restricted to dimension-6 operators and it closes under QCD renormalization. The operators which vanish on using the equations of motion are not included. The effective Hamiltonian \mathcal{H}_{eff} given below covers not only the decay $b \rightarrow s + \gamma$, in which we are principally interested in this section, but also other processes such as $b \rightarrow s + g$ and $b \rightarrow s + q\bar{q}$.

It is to be expected in general that due to QCD corrections, which induce operator-mixing, additional contributions with different CKM pre-factors have to be included in the amplitudes. Thus, QCD effects alter the CKM-matrix element dependence of the decay rates for both $B \rightarrow X_s + \gamma$ and (more importantly) $B \rightarrow X_d + \gamma$. However, with the help of the unitarity condition given above, the CKM matrix dependence in the effective Hamiltonian incorporating the QCD corrections for the decays $B \rightarrow X_s + \gamma$ factorizes, and one can write this Hamiltonian as [¶]:

$$\mathcal{H}_{eff}(b \rightarrow s + \gamma) = -\frac{4G_F}{\sqrt{2}} V_{ts}^* V_{tb} \sum_{i=1}^8 C_i(\mu) \mathcal{O}_i(\mu), \quad (120)$$

where the operator basis is chosen to be (here μ and ν are Lorentz indices and α and β are colour indices)

$$\mathcal{O}_1 = (\bar{s}_{L\alpha} \gamma_\mu b_{L\alpha})(\bar{c}_{L\beta} \gamma^\mu c_{L\beta}), \quad (121)$$

$$\mathcal{O}_2 = (\bar{s}_{L\alpha} \gamma_\mu b_{L\beta})(\bar{c}_{L\beta} \gamma^\mu c_{L\alpha}), \quad (122)$$

$$\mathcal{O}_3 = (\bar{s}_{L\alpha} \gamma_\mu b_{L\alpha}) \sum_{q=u,d,s,c,b} (\bar{q}_{L\beta} \gamma^\mu q_{L\beta}), \quad (123)$$

$$\mathcal{O}_4 = (\bar{s}_{L\alpha} \gamma_\mu b_{L\beta}) \sum_{q=u,d,s,c,b} (\bar{q}_{L\beta} \gamma^\mu q_{L\alpha}), \quad (124)$$

$$\mathcal{O}_5 = (\bar{s}_{L\alpha} \gamma_\mu b_{L\alpha}) \sum_{q=u,d,s,c,b} (\bar{q}_{R\beta} \gamma^\mu q_{R\beta}), \quad (125)$$

$$\mathcal{O}_6 = (\bar{s}_{L\alpha} \gamma_\mu b_{L\beta}) \sum_{q=u,d,s,c,b} (\bar{q}_{R\beta} \gamma^\mu q_{R\alpha}), \quad (126)$$

$$\mathcal{O}_7 = \frac{e}{16\pi^2} m_b (\bar{s}_{L\alpha} \sigma_{\mu\nu} b_{R\alpha}) F^{\mu\nu}, \quad (127)$$

$$\mathcal{O}'_7 = \frac{e}{16\pi^2} m_s (\bar{s}_{R\alpha} \sigma_{\mu\nu} b_{L\alpha}) F^{\mu\nu}, \quad (128)$$

$$\mathcal{O}_8 = \frac{g}{16\pi^2} m_b (\bar{s}_{L\alpha} T_{\alpha\beta}^a \sigma_{\mu\nu} b_{R\beta}) G_{\mu\nu}^a, \quad (129)$$

$$\mathcal{O}'_8 = \frac{g}{16\pi^2} m_s (\bar{s}_{R\alpha} T_{\alpha\beta}^a \sigma_{\mu\nu} b_{L\beta}) G_{\mu\nu}^a, \quad (130)$$

where e and g_s are the electromagnetic and the strong coupling constants, and $F_{\mu\nu}$ and $G_{\mu\nu}^a$ denote the electromagnetic and the gluonic field strength tensors, respectively. We

[¶]Note that in addition to the penguins with the u -quark intermediate state there are also non-factorizing contributions due to the operators $(\bar{u}_{L\alpha} \gamma^\mu b_{L\alpha})(\bar{s}_{L\beta} \gamma_\mu u_{L\beta})$, which like the u -quark contribution to the 1-loop electromagnetic penguins are proportional to the CKM-factor $\lambda_u \equiv V_{us} V_{ub}^*$, and hence are consistently set to zero.

call attention to the explicit mass factors in $\mathcal{O}_7(\mathcal{O}'_7)$ and $\mathcal{O}_8(\mathcal{O}'_8)$, which will undergo renormalization just as the Wilson coefficients. The dominant contributions in the radiative decays $B \rightarrow X_s + \gamma$ arise from the operators \mathcal{O}_2 , \mathcal{O}_7 and \mathcal{O}_8 , whereas the operators $\mathcal{O}_3, \dots, \mathcal{O}_6$ get coefficients through operator mixing only, which numerically are negligible. Historically, the anomalous dimension matrix was calculated in a truncated basis [93] and this basis is still often used for the sake of ease in calculating the real and virtual corrections, though as we discuss below, now the complete anomalous dimension matrix is available [94].

The perturbative QCD corrections to the decay rate $\Gamma(B \rightarrow X_s + \gamma)$ have two distinct contributions:

- Corrections to the Wilson coefficients $C_i(\mu)$, calculated with the help of the renormalization group equation, whose solution requires the knowledge of the anomalous dimension matrix in a given order in α_s .
- Corrections to the matrix elements of the operators \mathcal{O}_i entering through the effective Hamiltonian at the scale $\mu = \mathcal{O}(m_b)$.

The anomalous dimension matrix is needed in order to use the renormalization group and sum up large logarithms, i.e., terms like $\alpha_s^n(m_W) \log^m(m_b/M)$, where $M = m_t$ or m_W and $m \leq n$ (with $n = 0, 1, 2, \dots$). At present only the leading logarithmic corrections ($m = n$) have been calculated systematically in the complete basis given above [94].

Next-to-leading order corrections to the matrix elements are now available completely. They are of two kinds:

- QCD Bremsstrahlung corrections $b \rightarrow s\gamma + g$, which are needed both to cancel the infrared divergences in the decay rate for $B \rightarrow X_s + \gamma$ and in obtaining a non-trivial QCD contribution to the photon energy spectrum in the inclusive decay $B \rightarrow X_s + \gamma$.
- Next-to-leading order virtual corrections to the matrix elements in the decay $b \rightarrow s + \gamma$.

The Bremsstrahlung corrections were calculated in [95] - [97] in the truncated basis and last year also in the complete operator basis [60], which have been checked recently in [98]^{||}. The higher order matching conditions, i.e., $C_i(m_W)$, are known up to the desired accuracy, i.e., up to $\mathcal{O}(\alpha_s(M_W))$ terms [99]. Very recently, the next-to-leading order virtual corrections have also been calculated [100]. What still remains to be done is the calculation of $\gamma^{(1)}$, the next-to-leading order anomalous dimension matrix, which is the hardest part of this computation. This is clearly needed to get theoretical estimates of the branching ratio $\mathcal{B}(B \rightarrow X_s + \gamma)$ in the complete next-to-leading order. We discuss the presently available pieces to estimate $\mathcal{B}(B \rightarrow X_s + \gamma)$.

We recall that the Wilson coefficients obey the renormalization group equation

$$\left[\mu \frac{\partial}{\partial \mu} + \beta(g) \frac{\partial}{\partial g} \right] C_i \left(\frac{M_W^2}{\mu^2}, g \right) = \hat{\gamma}_{ji}(g) C_j \left(\frac{M_W^2}{\mu^2}, g \right). \quad (131)$$

^{||}This paper as it stands has some errors which we expect to be rectified!

The QCD beta function $\beta(g)$ has been defined earlier and $\hat{\gamma}(g)$ is the anomalous dimension matrix, which, to leading logarithmic accuracy, is given by

$$\hat{\gamma}(g) = \gamma_0 \frac{g^2}{16\pi^2}. \quad (132)$$

Here γ_0 is a 8×8 matrix given by [94, 101]

$$\gamma_0 = \begin{bmatrix} & & & & & & & \\ -2 & 6 & 0 & 0 & 0 & 0 & 0 & 3 \\ 6 & -2 & -\frac{2}{9} & \frac{2}{3} & -\frac{2}{9} & \frac{2}{3} & \frac{464}{81} & \frac{76}{27} \\ 0 & 0 & -\frac{22}{9} & \frac{22}{3} & -\frac{4}{9} & \frac{4}{3} & -\frac{368}{81} & \frac{152}{27} + 3f \\ 0 & 0 & 6 - \frac{2}{9}f & -2 + \frac{2}{3}f & -\frac{2}{9}f & \frac{2}{3}f & \frac{464}{81}u - \frac{184}{81}d & 6 + \frac{76}{27}f \\ 0 & 0 & 0 & 0 & 2 & -6 & -\frac{80}{9} & \frac{8}{3} - 3f \\ 0 & 0 & -\frac{2}{9}f & \frac{2}{3}f & -\frac{2}{9}f & -16 + \frac{2}{3}f & -\frac{400}{81}u + \frac{248}{81}d - \frac{80}{3} & -4 - \frac{113}{27}f \\ 0 & 0 & 0 & 0 & 0 & 0 & \frac{32}{3} & 0 \\ 0 & 0 & 0 & 0 & 0 & 0 & -\frac{32}{9} & \frac{28}{3} \end{bmatrix}.$$

where f is the number of active flavours, and u (d) is the number of up (down) flavours in the effective theory. For the case at hand we have $u = 2$, $d = 3$ and $f = u + d = 5$. This matrix is given in the NDR dimensional regularization scheme which is also used in the calculations of the matrix elements of the operators discussed below. The difference between the NDR and the HV schemes lies in the seventh and eighth columns and the corresponding matrix in the HV scheme can be seen in [129].

The solution of the renormalization group flow is obtained as

$$\vec{C}(\mu) = T^{-1}D(\mu, m_W)T\vec{C}(m_W) \quad (133)$$

where T diagonalizes the anomalous dimension matrix and D is a diagonal matrix, which is given for the relevant case by

$$D = \text{Diag}[\eta^{0.1456}, \eta^{-0.8994}, \eta^{16/23}, \eta^{14/23}, \eta^{-12/23}, \eta^{-0.4230}, \eta^{0.4086}, \eta^{6/23}]$$

where

$$\eta = \frac{\alpha_s(M_W)}{\alpha_s(\mu)}.$$

The transformation of the anomalous dimension matrix into a diagonal form can then be performed. Assuming that the coefficients $C_3 \cdots C_6$ vanish at the matching scale $\mu = M_W$, the result for the coefficients at the scale μ reads

$$C_1(\mu) = \frac{1}{2}C_2(M_W) \left(\eta^{6/23} - \eta^{-12/23} \right), \quad (134)$$

$$C_2(\mu) = \frac{1}{2}C_2(M_W) \left(\eta^{6/23} + \eta^{-12/23} \right), \quad (135)$$

$$C_3(\mu) = C_2(M_W) \left(-0.0112\eta^{-0.8994} + \frac{1}{6}\eta^{-12/23} - 0.1403\eta^{-0.4230} + 0.0054\eta^{0.1456} \right) \quad (136)$$

$$\begin{aligned}
& - 0.0714\eta^{6/23} + 0.0509\eta^{0.4086} \Big) , \\
C_4(\mu) &= C_2(M_W) \left(0.0156\eta^{-0.8994} - \frac{1}{6}\eta^{-12/23} + 0.1214\eta^{-0.4230} + 0.0026\eta^{0.1456} \right. \\
& \quad \left. - 0.0714\eta^{6/23} + 0.0984\eta^{0.4086} \right) ,
\end{aligned} \tag{137}$$

$$C_5(\mu) = C_2(M_W) \left(-0.0025\eta^{-0.8994} + 0.0117\eta^{-0.4230} + 0.0304\eta^{0.1456} - 0.0397\eta^{0.4086} \right) , \tag{138}$$

$$C_6(\mu) = C_2(M_W) \left(-0.0462\eta^{-0.8994} + 0.0239\eta^{-0.4230} - 0.0112\eta^{0.1456} + 0.0335\eta^{0.4086} \right) , \tag{139}$$

$$\begin{aligned}
C_7(\mu) &= C_7(M_W)\eta^{16/23} + C_8(M_W)\frac{8}{3} \left(\eta^{14/23} - \eta^{16/23} \right) , \\
& + C_2(M_W) \left(-0.0185\eta^{-0.8994} - 0.0714\eta^{-12/23} - 0.0380\eta^{-0.4230} - 0.0057\eta^{0.1456} \right. \\
& \quad \left. - 0.4286\eta^{6/23} - 0.6494\eta^{0.4086} + 2.2996\eta^{14/23} - 1.0880\eta^{16/23} \right) ,
\end{aligned} \tag{140}$$

$$\begin{aligned}
C_8(\mu) &= C_8(M_W)\eta^{14/23} \\
& + C_2(M_W) \left(-0.0571\eta^{-0.8994} + 0.0873\eta^{-0.4230} + 0.0209\eta^{0.1456} \right. \\
& \quad \left. - 0.9135\eta^{0.4086} + 0.8623\eta^{14/23} \right) .
\end{aligned} \tag{141}$$

The non-zero initial conditions in the SM are given at the scale M_W and read [92]

$$C_2 = 1 \tag{142}$$

$$C_7(M_W) = -\frac{1}{2}x \left[\frac{2x^2/3 + 5x/12 - 7/12}{(x-1)^3} - \frac{3x^2/2 - x}{(x-1)^4} \ln x \right] , \tag{143}$$

$$C_8(M_W) = -\frac{1}{2}x \left[\frac{x^2/4 - 5x/4 - 1/2}{(x-1)^3} + \frac{3x/2}{(x-1)^4} \ln x \right] , \tag{144}$$

and $x = m_t^2/M_W^2$. The numerical values for the Wilson coefficients at the scale $\mu = M_W$ (“Matching Conditions”) and at three other scales $\mu = 10.0$ GeV, 5.0 GeV and 10.0 GeV are given in Table 6. Also, for subsequent discussion it is useful to define two effective Wilson coefficients $C_7^{\text{eff}}(\mu)$ and $C_8^{\text{eff}}(\mu)$ [101]:

$$\begin{aligned}
C_7^{\text{eff}} &\equiv C_7 - \frac{C_5}{3} - C_6 \quad , \\
C_8^{\text{eff}} &\equiv C_8 + C_5 \quad .
\end{aligned} \tag{145}$$

Their values are also given in Table 1.

3.2 Real and virtual $O(\alpha_s)$ corrections for the matrix element

Now, we discuss the real and virtual $O(\alpha_s)$ corrections to the matrix element for $b \rightarrow s + \gamma$ at the scale $\mu \approx m_b$, which by themselves form a well-defined gauge invariant albeit scheme-dependent set of corrections. This scheme dependence will be cancelled against the one in the anomalous dimension $\gamma^{(1)}$, as discussed in the context of the dominant

$C_i(\mu)$	$\mu = m_W$	$\mu = 10.0$ GeV	$\mu = 5.0$ GeV	$\mu = 2.5$ GeV
C_1	0.0	−0.158	−0.235	−0.338
C_2	1.0	1.063	1.100	1.156
C_3	0.0	0.007	0.011	0.016
C_4	0.0	−0.017	−0.024	−0.034
C_5	0.0	0.005	0.007	0.009
C_6	0.0	−0.019	−0.029	−0.044
C_7	−0.193	−0.290	−0.333	−0.388
C_8	−0.096	−0.138	−0.153	−0.171
C_7^{eff}	−0.193	−0.273	−0.306	−0.347
C_8^{eff}	−0.096	−0.132	−0.146	−0.162

Table 1: Wilson coefficients $C_i(\mu)$ at the scale $\mu = m_W = 80.33$ GeV (“matching conditions”) and at three other scales, $\mu = 10.0$ GeV, $\mu = 5.0$ GeV and $\mu = 2.5$ GeV, evaluated with two-loop β -function and the leading-order anomalous-dimension matrix. The entries correspond to the top quark mass $\overline{m}_t(m_t^{pole}) = 170$ GeV (equivalently, $m_t^{pole} = 180$ GeV) and the QCD coupling constant $\alpha_s(m_Z^2) = 0.117$, both in the \overline{MS} scheme.

contributions to the non-leptonic decays of the B hadron earlier. The results presented here correspond to the NDR scheme.

Recapitulating the essential steps, we recall that the Bremsstrahlung corrections in $b \rightarrow s\gamma + g$, calculated in [95] - [97] and [60], were aimed at getting a non-trivial photon energy spectrum at the partonic level. In these papers, the virtual corrections to $b \rightarrow s\gamma$ in $O(\alpha_s)$ were included only by taking into account those virtual diagrams which are needed to cancel the infrared singularities (and also the collinear ones in the limit $m_s \rightarrow 0$) generated by the Bremsstrahlung diagram. The emphasis was on deriving the photon energy spectrum in $B \rightarrow X_s + \gamma$ away from the end-point $x_\gamma \rightarrow 1$ and the Sudakov-improved photon energy spectrum in the region $x_\gamma \rightarrow 1$. Clearly, the left-out virtual diagrams shown in Fig. 3 do not contribute either to the Sudakov spectrum or to the region $x_\gamma \neq 1$ at the parton level. They, however, do contribute to the overall decay rate in $B \rightarrow X_s + \gamma$. Recently, these additional virtual correction have been evaluated in [100], neglecting the contributions of the small operators O_3 – O_6 . This additional contribution reduces substantially the scale dependence of the leading order (or partial next-to-leading order) decay width $\Gamma(B \rightarrow X_s + \gamma)$, which previously was found to be substantial and constituted a good fraction of the theoretical uncertainty in the inclusive decay rate [102, 101, 103, 60].

We shall follow closely the derivation of the virtual corrections given in [100]. Concentrating on the dominant operators O_2 , O_7 and O_8 , the contribution of the next-to-leading order correction to the matrix element part in $b \rightarrow s + \gamma$ can be expressed as follows:

$$\mathcal{M} = \mathcal{M}_2 + \mathcal{M}_7 + \mathcal{M}_8 \quad (146)$$

and the various terms (including appropriate counterterm contributions) can be summa-

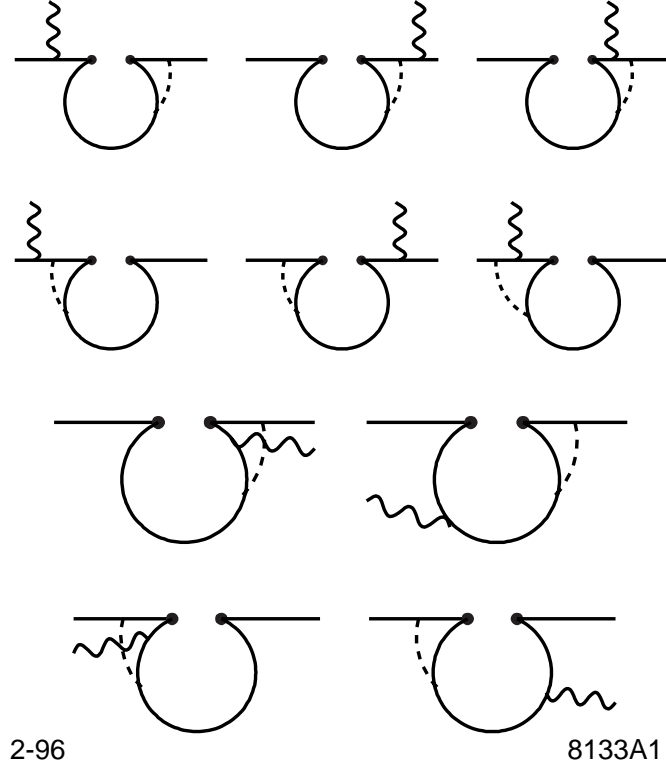


Figure 3: Non-vanishing two-loop diagrams associated with the operator O_2 calculated in [100]. The fermions (b , s and c quark) are represented by solid lines. The wavy (dashed) line represents the photon (gluon).

rized as [100]:

$$\mathcal{M}_2 = \langle s\gamma|O_7|b\rangle_{tree} \frac{\alpha_s}{4\pi} \left(\ell_2 \log \frac{m_b}{\mu} + r_2 \right) , \quad (147)$$

with

$$\ell_2 = \frac{416}{81} . \quad (148)$$

$$\begin{aligned} \Re r_2 = & \frac{2}{243} \left\{ -833 + 144\pi^2 z^{3/2} \right. \\ & + [1728 - 180\pi^2 - 1296\zeta(3) + (1296 - 324\pi^2)L + 108L^2 + 36L^3] z \\ & + [648 + 72\pi^2 + (432 - 216\pi^2)L + 36L^3] z^2 \\ & \left. + [-54 - 84\pi^2 + 1092L - 756L^2] z^3 \right\} \end{aligned} \quad (149)$$

$$\Im r_2 = \frac{16\pi}{81} \left\{ -5 + [45 - 3\pi^2 + 9L + 9L^2] z + [-3\pi^2 + 9L^2] z^2 + [28 - 12L] z^3 \right\} \quad (150)$$

Here, $\Re r_2$ and $\Im r_2$ denote the real and the imaginary part of r_2 , respectively, $z = (m_c/m_b)^2$ and $L = \log(z)$.

The real and virtual corrections associated with the operator O_7 , calculated in [95, 96, 60] can be combined into a modified matrix element for $b \rightarrow s\gamma$, in such a way that its square reproduces the result derived in these papers. This modified matrix element \mathcal{M}_7^{mod} reads [100]:

$$\mathcal{M}_7^{mod} = \langle s\gamma | O_7 | b \rangle_{tree} \left(1 + \frac{\alpha_s}{4\pi} \left(\ell_7 \log \frac{m_b}{\mu} + r_7 \right) \right) \quad (151)$$

with

$$\ell_7 = \frac{8}{3} \quad , \quad r_7 = \frac{8}{9} (4 - \pi^2) \quad . \quad (152)$$

Finally, the result for \mathcal{M}_8 is [100]:

$$\mathcal{M}_8 = \langle s\gamma | O_7 | b \rangle_{tree} \frac{\alpha_s}{4\pi} \left(\ell_8 \log \frac{m_b}{\mu} + r_8 \right) \quad , \quad (153)$$

with

$$\ell_8 = -\frac{32}{9} \quad , \quad r_8 = -\frac{4}{27} (-33 + 2\pi^2 - 6i\pi) \quad . \quad (154)$$

With the results given above, one can write down the amplitude $\mathcal{M}(b \rightarrow s\gamma)$ by summing the various contributions already mentioned. Since the relevant scale for a b quark decay is expected to be $\mu \sim m_b$, the matrix elements of the operators may be expanded around $\mu = m_b$ up to order $O(\alpha_s)$ and the next-to-leading order result can be written as:

$$\mathcal{M}(b \rightarrow s\gamma) = -\frac{4G_F\lambda_t}{\sqrt{2}} D \langle s\gamma | O_7(m_b) | b \rangle_{tree} \quad (155)$$

with

$$D = C_7^{eff}(\mu) + \frac{\alpha_s(m_b)}{4\pi} \left(C_i^{(0)eff}(\mu) \gamma_{i7}^{(0)eff} \log \frac{m_b}{\mu} + C_i^{(0)eff} r_i \right) \quad , \quad (156)$$

where the quantities $\gamma_{i7}^{(0)eff} = \ell_i + 8\delta_{i7}$ are the entries of the (effective) leading order anomalous dimension matrix and the quantities ℓ_i and r_i are given for $i = 2, 7, 8$ in eqs. (148,149), (152) and (154), respectively. The first term, $C_7^{eff}(\mu)$, on the r.h.s. of Eq. (156) has to be taken up to next-to-leading logarithmic precision in order to get the full next-to-leading logarithmic result, whereas it is sufficient to use the leading logarithmic values of the other Wilson coefficients in Eq. (156).

As pointed out by Buras et al. [101], the explicit logarithms of the form $\alpha_s(m_b) \log(m_b/\mu)$ in Eq. (156) are cancelled by the μ -dependence of $C_7^{(0)eff}(\mu)$. Therefore, the scale dependence is significantly reduced by including the virtual corrections completely to this order.

The decay width Γ^{virt} which follows from $\mathcal{M}(b \rightarrow s\gamma)$ in Eq. (155) reads

$$\Gamma^{virt} = \frac{m_{b,pole}^5 G_F^2 \lambda_t^2 \alpha_{em}}{32\pi^4} F |D|^2 \quad , \quad (157)$$

where the terms of $O(\alpha_s^2)$ in $|D|^2$ have been discarded. The factor F in Eq. (157) is

$$F = \left(\frac{m_b(\mu = m_b)}{m_{b,pole}} \right)^2 = 1 - \frac{8}{3} \frac{\alpha_s(m_b)}{\pi} \quad , \quad (158)$$

and its origin lies in the explicit presence of m_b in the operator \mathcal{O}_7 . To get the inclusive decay width for $b \rightarrow s\gamma(g)$, also the Bremsstrahlung corrections (except the part already absorbed above) must be added. The contribution of the operators \mathcal{O}_2 and \mathcal{O}_7 was calculated already in [95].

3.3 Estimating long-distance effects in $B \rightarrow X_s + \gamma$

In order to get the complete amplitude for $B \rightarrow X_s + \gamma$ one has to include also the effects of the long-distance contributions, which arise from the matrix elements of the four-quark operators in \mathcal{H}_{eff} , $\langle X_s \gamma | \mathcal{O}_i | B \rangle$. We shall discuss such contributions in the exclusive radiative decays $B \rightarrow (\rho, \omega) + \gamma$ subsequently, which have been calculated in a more robust theoretical framework using QCD sum rules. This framework (likewise lattice-QCD) is not applicable in inclusive decays in a straightforward manner. Lacking anything better, we discuss phenomenological models used in the literature in estimating the long-distance amplitude in radiative decays $B \rightarrow X_s + \gamma$.

In calculating the matrix elements of four-Fermion operators, it is usual to invoke the hypothesis of factorization. In the present context, factorization is combined with the additional assumption of vector meson dominance, involving the decays $B \rightarrow \sum_i V_i + X_s \rightarrow \gamma + X_s$, where $V_i = J/\psi, \psi', \dots$ [104] - [108]. It should be remarked that non-leptonic decays, such as $B \rightarrow (J/\psi, \psi' + X_s)$, by themselves are not under the quantitative control of the factorization-based framework due to the presence of significant non-factorizing pieces in the non-leptonic amplitudes - perhaps a sign of the breakdown of local quark-hadron duality (?). Phenomenologically, however, data on two-body and quasi two-body decays are well accounted for in terms of the Bauer-Stech-Wirbel effective parameters $a_1 \equiv c_1/N_c + c_2$ and $a_2 \equiv c_1 + c_2/N_c$ [109]. The details of this analysis and a host of other related decay modes can be seen in [110]. Concerning the use of vector meson dominance, one has to ensure that the resulting amplitude $\mathcal{M}(B \rightarrow X_s + \gamma)$ remains manifestly gauge invariant. In the present model this amounts to discarding the longitudinal polarization contribution in the non-leptonic decays $B \rightarrow (J/\psi, \psi', \dots) + X_s$, which in fact dominates the decay widths [110], and keeping only the smaller contribution from the transverse polarization of $J/\psi, \psi', \dots$. Following [106, 107], one can write the decay amplitude as:

$$\mathcal{M}(b \rightarrow sJ/\psi)_T = \frac{G_F}{\sqrt{2}} a_2 V_{cb} V_{cs}^* \frac{g_{J/\psi}(m_{J/\psi}^2)}{m_b} \bar{s} \sigma^{\mu\nu} (1 + \gamma_5) b q_\nu \epsilon_\mu^\dagger(q) , \quad (159)$$

where g_ψ is defined as $\langle \psi(q) | \bar{c} \gamma_\mu c | 0 \rangle = -i g_\psi(q^2) \epsilon_\mu^\dagger(q)$. For the decays under consideration one needs the value of a_2 , which has been found to be $|a_2| = 0.24 \pm 0.04$ [110]. One also needs to evaluate the coupling constant $g_V(q^2)$ at the point $q^2 = 0$. From leptonic decays of vector mesons, one gets, however, $g_V(q^2 = M_V^2)$. It has been remarked in literature, in particular in [106, 107], that using $g_V(q^2 = 0) = g_V(q^2 = M_V^2)$ would substantially overestimate the long-distance contribution due to the expected dynamical suppression of the effective coupling $g_V(q^2)$, as one extrapolates to the point $q^2 = 0$. Taking all this into account, an estimate of the long-distance amplitude from the intermediate J/ψ state is [106]:

$$\mathcal{M}_{LD}(b \rightarrow sJ/\psi \rightarrow s\gamma) = \frac{G_F}{2\sqrt{2}} a_2 V_{tb} V_{ts}^* \left(\frac{2}{3} e \frac{g_{J/\psi}^2(0)}{m_{J/\psi}^2 m_b} \right) \bar{s} \sigma^{\mu\nu} (1 + \gamma_5) b F_{\mu\nu} , \quad (160)$$

where use has been made of the ψ to γ conversion vertex,

$$\langle 0 | e J_{em}^\mu | \psi \rangle = (2e/3) \langle 0 | \bar{c} \gamma^\mu c | \psi \rangle = -(2e/3) i g_\psi(0) \epsilon_\mu , \quad (161)$$

and we must use the value $g_{J/\psi}(0)$ for the conversion coupling constant. Including all the ($c\bar{c}$) resonances and the short distance contribution \mathcal{M}_{SD} , the two-body decay amplitude ($b \rightarrow s\gamma$) can be written as

$$\mathcal{M}(b \rightarrow s\gamma) = -\frac{eG_F}{2\sqrt{2}} V_{tb} V_{ts}^* \left[\frac{1}{4\pi^2} m_b D(\mu) - a_2 \frac{2}{3} \sum_i \frac{g_{\psi_i}^2(0)}{m_{\psi_i}^2 m_b} \right] \bar{s} \sigma^{\mu\nu} (1 + \gamma_5) b F_{\mu\nu} , \quad (162)$$

where ψ_i represents the following vector $c\bar{c}$ resonant states: $\psi(1S)$, $\psi(2S)$, $\psi(3770)$, $\psi(4040)$, $\psi(4160)$, and $\psi(4415)$, and D is the function given earlier. Since in the LD-amplitude, gluon Bremsstrahlung is neglected, it is consistent to neglect this also in the SD-piece. Taking this estimate as giving the right order of magnitude for the long-distance contribution, Deshpande et al. [106] conclude that such long-distance effects can be as large as 10%. Other estimates, in particular by Golowich and Pakvasa [107], lead to an even smaller long-distance contribution. Clearly, one can not argue very conclusively if such estimates are completely quantitative due to the assumptions involved. In future, one could improve these estimates by using data from HERA on elastic J/ψ -, and ψ' -photoproduction to get $g_{J/\psi}$ and $g_{\psi'}(0)$ directly, reducing at least the extrapolation uncertainties involved in the presently adopted procedure of extracting these coupling constants from the leptonic decay widths of each state and extrapolating to the point $q^2 = 0$ using an Ansatz.

3.4 Estimates of $\mathcal{B}(B \rightarrow X_s + \gamma)$ in the Standard Model

In the quantitative estimates of the SM branching ratio $\mathcal{B}(B \rightarrow X_s + \gamma)$ given below we have neglected the LD-contributions. This is an assumption, which as we discussed above, we do not expect to work much better than $O(10\%)$. It is theoretically preferable to calculate this quantity in terms of the semileptonic decay branching ratio

$$\mathcal{B}(B \rightarrow X_s \gamma) = \left[\frac{\Gamma(B \rightarrow \gamma + X_s)}{\Gamma_{SL}} \right]^{th} \mathcal{B}(B \rightarrow X \ell \nu_\ell) , \quad (163)$$

where, the leading-order QCD corrected Γ_{SL} has been given earlier. The leading order power corrections in the heavy quark expansion, discussed in the context of the semileptonic decay rate, are identical in the inclusive decay rates for $B \rightarrow X_s + \gamma$ and $B \rightarrow X \ell \nu_\ell$, entering in the numerator and denominator in the square bracket, respectively, and hence drop out [39, 40].

The error on the branching ratio $\mathcal{B}(B \rightarrow X_s \gamma)$ comes from four different sources. We list them below:

1. Δm_t : The present value of m_t is $m_t = 175 \pm 9$ GeV [8], which is usually interpreted as the pole mass although this is not unambiguous. With this the running top quark mass in the \overline{MS} scheme is $\overline{m_t} = 166 \pm 9$ GeV. However, in Eq. (156), there is no distinction made between m_t^{pole} and $\overline{m_t}$. To take both the theoretical and experimental errors into account, we take $m_t = 170 \pm 15$ GeV. This leads to an error of $\pm 5\%$ in $\mathcal{B}(B \rightarrow X_s \gamma)$.

2. $\Delta\mu$: The scale dependence is now reduced thanks to the work done in [100]. It is usual to estimate the residual μ -dependence by taking a range $m_b/2 \leq \mu \leq 2m_b$. This is plotted in Fig. 4 (solid curves), which shows that it yields an error of $\pm 6\%$ on $\mathcal{B}(B \rightarrow X_s + \gamma)$.
3. Errors from the extrinsic parameters,
 - (i) $\Delta(m_b)$ (equivalently from $\Delta(m_c/m_b)$),
 - (ii) $\Delta(\alpha_s(m_Z))$ (equivalently $\Delta\Lambda_5$, the uncertainty on the QCD-scale parameter),
 - (iii) $\Delta(BR_{SL})$, the experimental uncertainty on the semileptonic branching ratio.
 Taking $m_c/m_b = 0.29 \pm 0.02$, $\mathcal{B}(B \rightarrow X\ell\nu_\ell) = (10.4 \pm 0.4)\%$, $\alpha_s(m_Z) = 0.117 \pm 0.006$ [3], an uncertainty of $\pm 12\%$ was estimated on $\mathcal{B}(B \rightarrow X_s + \gamma)$ in [60].
4. Last, but by no means least, there is at present an incalculable error due to the fact that C_7^{eff} is not yet available in the next-to-leading order.

In view of this missing piece, it is not possible to give a completely corrected NLL prediction for $\mathcal{B}(B \rightarrow X_s + \gamma)$ at present. In what follows, we shall replace C_7^{eff} by its leading log value, which yields the branching ratio [111]:

$$\mathcal{B}(B \rightarrow X_s + \gamma) = (3.20 \pm 0.30 \pm 0.38) \times 10^{-4} \quad (164)$$

where the first error comes from the combined error on Δm_t and $\Delta\mu$, as can be seen in Fig. 4, and the second from the extrinsic source. This estimate is subject to an additive renormalization due to the missing NLL anomalous dimension piece and the somewhat less tractable contribution of the LD-effect, discussed in the previous subsection but not included in the numerical estimates of the branching ratio (164). However, if the NLL anomalous dimensions of the four-quark operators $\mathcal{O}_1, \dots, \mathcal{O}_6$, which are known [30], are any useful guide for estimating C_7^{eff} , we do not expect a substantial change of this branching ratio in the complete NLL. Of course, the big challenge is to show that this indeed is the case. In view of this, we propose to add an additional theoretical uncertainty of order $\pm 10\%$ on $\mathcal{B}(B \rightarrow X_s + \gamma)$, yielding $\mathcal{B}(B \rightarrow X_s + \gamma) = (3.20 \pm 0.30 \pm 0.38 \pm 0.32) \times 10^{-4}$. Combining the theoretical errors in quadrature gives

$$\mathcal{B}(B \rightarrow X_s + \gamma) = (3.20 \pm 0.58) \times 10^{-4}, \quad (165)$$

which we consider is a fairly robust estimate of the SM branching ratio at present. This can be improved only after the two estimated pieces are replaced by the actual calculations. The SM branching ratio $\mathcal{B}(B \rightarrow X_s + \gamma)$ is compatible with the present measurement $\mathcal{B}(B \rightarrow X_s + \gamma) = (2.32 \pm 0.67) \times 10^{-4}$ [90]. Expressed in terms of the CKM matrix element ratio, one gets

$$\frac{|V_{ts}|}{|V_{cb}|} = 0.85 \pm 0.12(\text{expt}) \pm 0.10(\text{th}), \quad (166)$$

which is within errors consistent with unity, as expected from the unitarity of the CKM matrix.

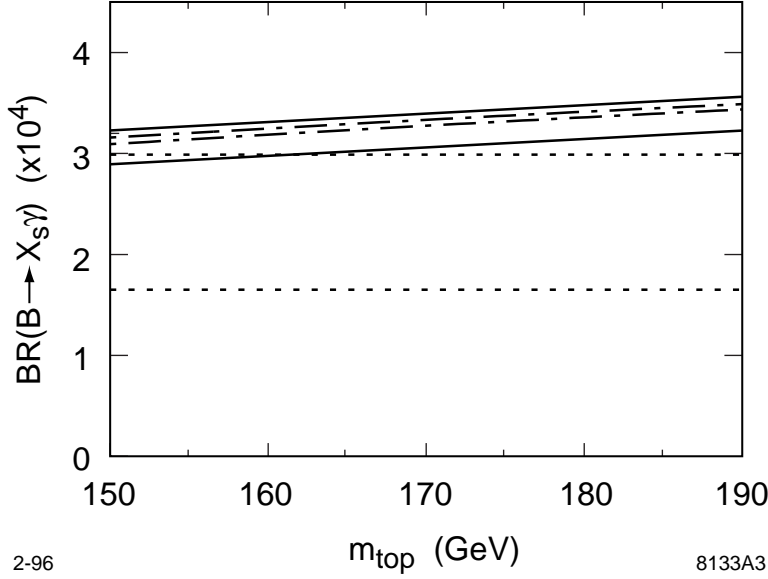


Figure 4: Branching ratio for $b \rightarrow s\gamma(g)$ calculated in [100] with the parameters $|V_{ts}|/|V_{cb}| = 1$, $|V_{tb}| = 1$, $m_b^{pole} = 4.8$ GeV and $m_c/m_b = 0.29$. The different curves are explained in the text.

3.5 Photon energy spectrum in $B \rightarrow X_s + \gamma$

The two-body partonic process $b \rightarrow s\gamma$ yields a photon energy spectrum $1/(\Gamma)d\Gamma(b \rightarrow s\gamma) = \delta(1-x)$, where the scaled photon energy x is defined as $E_\gamma = (m_b^2 - m_s^2)/(2 m_b) x$. Perturbative QCD corrections, such as $b \rightarrow s\gamma + g$, give a characteristic Bremsstrahlung spectrum in x in the interval $[0, 1]$ peaking near the end-points, $E_\gamma \rightarrow E_\gamma^{max}$ (or $x \rightarrow 1$) and $E_\gamma \rightarrow 0$ (or $x \rightarrow 0$), arising from the soft-gluon and soft-photon configurations, respectively. Near the end-points, one has to improve the spectrum obtained in fixed order perturbation theory. This is usually done in the region $x \rightarrow 1$ by isolating and exponentiating the leading behaviour in $\alpha_{em}\alpha_s(\mu)^m \log^{2n}(1-x)$ with $m \leq n$, where μ is a typical momentum in the decay $B \rightarrow X_s + \gamma$. The running of α_s is a non-leading effect, but as it is characteristic of QCD it modifies the Sudakov-improved end-point photon energy spectrum [112, 113] compared to its analogue in QED [114]. As long as the s -quark mass is non-zero, there is no collinear singularity in the spectrum. However, parts of the spectrum have large logarithms of the form $\alpha_s \log(m_b^2/m_s^2)$, which are important near the end-point $x \rightarrow 0$ but their influence persists also in the intermediate photon energy region and they have to be resummed [60, 115].

It has been observed in a number of papers [112, 116, 117], that the x -moments (scaled photon energy) in $B \rightarrow X_s + \gamma$ and those involving lepton energy in the decay $B \rightarrow X_u \ell \nu_\ell$ are related. Defining the moments as:

$$\begin{aligned} \mathcal{M}^{(n)}(B \rightarrow X_s + \gamma) &\equiv \frac{1}{\Gamma} \int_0^{M_B/m_b} dx x^{n-1} \frac{d\Gamma}{dx} \\ \mathcal{M}^{(n)}(B \rightarrow X_u \ell \nu_\ell) &\equiv - \int_0^{M_B/m_b} dx x^n \frac{d}{dx} \left(\frac{1}{\Gamma} \frac{d\Gamma_\ell}{dx} \right) \end{aligned} \quad (167)$$

$$= \frac{n}{\Gamma_\ell} \int_0^{M_B/m_b} dx x^{n-1} \frac{d\Gamma_\ell}{dx} ,$$

The moments $\mathcal{M}^{(n)}$ have been worked out in the leading non-trivial order in perturbation theory and the results can be expressed as:

$$\mathcal{M}^{(n)} \sim 1 + \frac{\alpha_s}{2\pi} C_F (A \log^2 n + B \log n + \text{const.}) \quad (168)$$

where $C_F = 4/3$, the leading coefficient is universal with $A = -1$ [114], and the non-leading coefficients are process dependent; $B = 7/2$ [95] and $B = 31/6$ [25], for $B \rightarrow X_s + \gamma$ and $B \rightarrow X_u \ell \nu_\ell$, respectively. Measurements of the moments could eventually be used to relate the CKM matrix element V_{ts} and V_{ub} .

How about calculating the photon energy spectrum in $B \rightarrow X_s + \gamma$ and the lepton energy spectrum in $B \rightarrow X_u \ell \nu_\ell$ completely in QCD? Concentrating on $B \rightarrow X_s + \gamma$, it is known that there is a gap between the end-points of the physical spectrum ($E_\gamma^{max} = (m_B^2 - m_X^2)/(2m_B)$), where $X = (m_K + m_\pi)$, and the partonic spectrum ($E_\gamma^{max} = (m_b^2 - m_s^2)/(2m_b)$), and hence in the parton-model description there is a window in E_γ which remains empty. This gap can only be filled up by non-perturbative effects, which in their simple form can be attributed to the b -quark motion in the B hadron. Phenomenological models were already proposed in the infancy of B physics which took into account non-perturbative smearing of the partonic spectra to fill this gap. The question is if this effect can be computed in QCD proper.

Attempts to calculate the photon and lepton energy spectra in the heavy quark expansion method lead to formal expressions which near the end-point are divergent [41], [117] - [118]. The point is that near the end-point, the energy release for the light quark system for the final state is not of $O(m_b)$ but of the order of the parameter $\bar{\Lambda} = M_B - m_b \sim O(\Lambda_{\text{QCD}})$. Thus, the expansion parameter is no longer $1/m_b^2$ and the operator product expansion - the backbone of the heavy quark expansion - breaks down. This divergent series in the effective theory has to be cleverly resummed and the distributions averaged over momentum bins [116] to smooth the increasing number of derivatives of the delta function, $\delta^n(1-x)$. This resummation allows to define an effective non-perturbative shape function [116, 113], which can not be calculated in the effective theory, but one could use this concept advantageously to relate the energy spectra in the semileptonic decays $B \rightarrow X_u \ell \nu_\ell$ and $B \rightarrow X_s + \gamma$. It has been further argued in [113] that a Gaussian distribution, such as the one used in the Fermi motion model in [21, 22], with an appropriate definition of the effective momentum-dependent b -quark mass, as prescribed by the heavy quark effective theory, is a good approximation to the shape function in $B \rightarrow X_u \ell \nu_\ell$ and $B \rightarrow X + \gamma$.

We shall confine ourselves to the discussion of the photon energy spectrum, which combines the perturbatively computed spectrum, discussed in the previous section, with a model of the quark motion which fills the mentioned energy gap in the end-point region. We will then show a comparison of this spectrum with the measured photon energy spectrum in $B \rightarrow X_s + \gamma$ [90]. In this model [21], which admittedly is simplistic but has received some theoretical support in the HQET approach subsequently [41, 117], the b quark in B hadron is assumed to have a Gaussian distributed Fermi motion determined

by a non-perturbative parameter, p_F ,

$$\phi(p) = \frac{4}{\sqrt{\pi} p_F^3} \exp\left(\frac{-p^2}{p_F^2}\right) \quad , \quad p = |\vec{p}| \quad (169)$$

with the wave function normalization $\int_0^\infty dp p^2 \phi(p) = 1$. The photon energy spectrum from the decay of the B -meson at rest is then given by

$$\frac{d\Gamma}{dE_\gamma} = \int_0^{p_{max}} dp p^2 \phi(p) \frac{d\Gamma_b}{dE_\gamma}(W, p, E_\gamma) \quad , \quad (170)$$

where p_{max} is the maximally allowed value of p and $\frac{d\Gamma_b}{dE_\gamma}$ is the photon energy spectrum from the decay of the b -quark in flight, having a momentum-dependent mass $W(p)$. This is calculated in perturbation theory taking into account the appropriate Sudakov behaviour in the E_γ end-point region at the partonic level.

An analysis of the CLEO photon energy spectrum has been undertaken in [60] to determine the non-perturbative parameters of this model, namely $m_b(pole)$ and p_F . The latter is related to the kinetic energy parameter λ_1 defined earlier in the HQET approach. The experimental errors are still large and the fits result in relatively small χ^2 values; the minimum, $\chi^2_{min} = 0.038$, is obtained for $p_F = 450$ MeV and $m_b(pole) = 4.77$ GeV, in good agreement with theoretical estimates of the same, namely $m_b(pole) = 4.8 \pm 0.15$ GeV [45, 119] and $p_F^2 = -\lambda_1/2 = 0.25 \pm 0.05$ GeV² obtained from the QCD sum rules [59]. The central value, $\lambda_1 = -0.4$ GeV², obtained from the photon energy spectrum in $B \rightarrow X_s + \gamma$ is also in good agreement with a recent determination of the same from the lepton energy spectrum in $B \rightarrow X \ell \nu_\ell$ in which partially integrated spectrum and its first moment are analyzed in terms of the HQET parameters $\bar{\Lambda}$ and λ_1 using CLEO data, getting $\lambda_1 = -0.35 \pm 0.05$ GeV² and $\bar{\Lambda} = 0.55 \pm 0.05$ GeV [61]. In Fig. 5 we have plotted the photon energy spectrum normalized to unit area in the interval between 1.95 GeV and 2.95 GeV for the parameters which correspond to the minimum χ^2 (solid curve) and for another set of parameters that lies near the χ^2 -boundary defined by $\chi^2 = \chi^2_{min} + 1$. (dashed curve). Data from CLEO [90] are also shown. Further details of this analysis can be seen in [60].

3.6 Inclusive radiative decays $B \rightarrow X_d + \gamma$

The theoretical interest in studying the (CKM-suppressed) inclusive radiative decays $B \rightarrow X_d + \gamma$ lies in the first place in the possibility of determining the CKM-Wolfenstein parameters ρ and η . The relevant region in the decays $B \rightarrow X_d + \gamma$ is the end-point photon energy spectrum, which has to be measured requiring that the hadronic system X_d recoiling against the photon does not contain strange hadrons to suppress the large- E_γ photons from the decay $B \rightarrow X_s + \gamma$. Assuming that this is feasible, one can determine from the ratio of the decay rates $\mathcal{B}(B \rightarrow X_d + \gamma)/\mathcal{B}(B \rightarrow X_s + \gamma)$ the CKM-Wolfenstein parameters. This measurement was proposed in [96], where the photon energy spectra were also worked out. In spirit, such an analysis is very similar to the already undertaken for the inclusive semileptonic decays in which the end-point lepton energy spectrum is solved for the ratio $|V_{ub}|/|V_{cb}|$. Now, the end-point spectra in $B \rightarrow X + \gamma$ will be analyzed

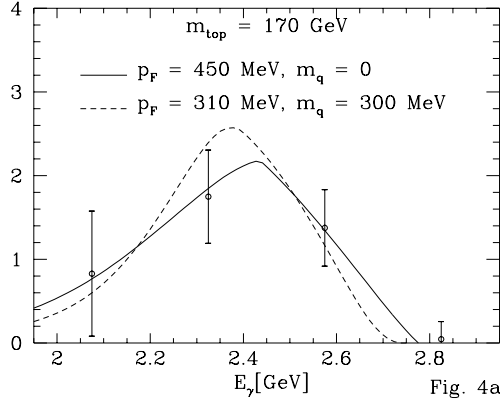


Figure 5: Comparison of the normalized photon energy distribution using the CLEO data [90] corrected for detector effects and theoretical distributions from [60], both normalized to unit area in the photon energy interval between 1.95 GeV and 2.95 GeV. The solid curve corresponds to the values with the minimum χ^2 , $(m_q, p_F) = (0, 450 \text{ MeV})$, and the dashed curve to the values $(m_q, p_F) = (300 \text{ MeV}, 310 \text{ MeV})$.

in terms of the ratio $|V_{td}|/|V_{ts}|$. Of course, the experimental issues involved in the two cases are quite different and measuring $B \rightarrow X_d + \gamma$ is lot more challenging than measuring $B \rightarrow X_u \ell \nu_\ell$.

In close analogy with the $B \rightarrow X_s + \gamma$ case discussed earlier, the complete set of dimension-6 operators relevant for the processes $b \rightarrow d\gamma$ and $b \rightarrow d\gamma g$ can be written as:

$$\mathcal{H}_{eff}(b \rightarrow d) = -\frac{4G_F}{\sqrt{2}} \xi_t \sum_{j=1}^8 C_j(\mu) \hat{O}_j(\mu), \quad (171)$$

where $\xi_j = V_{jb} V_{jd}^*$ for $j = t, c, u$. The operators \hat{O}_j , $j = 1, 2$, have implicit in them CKM factors. In the Wolfenstein parametrization [14], one can express these factors as :

$$\xi_u = A \lambda^3 (\rho - i\eta), \quad \xi_c = -A \lambda^3, \quad \xi_t = -\xi_u - \xi_c. \quad (172)$$

We note that all three CKM-angle-dependent quantities ξ_j are of the same order of magnitude, $O(\lambda^3)$, where $\lambda = \sin \theta_C \simeq 0.22$. This is an important difference as compared to the effective Hamiltonian $\mathcal{H}_{eff}(b \rightarrow s)$ written earlier, in which case the effective Hamiltonian factorizes into an overall CKM factor $\lambda_t = V_{tb} V_{ts}^*$. For calculational ease, this difference can be implemented by defining the operators \hat{O}_1 and \hat{O}_2 entering in $\mathcal{H}_{eff}(b \rightarrow d)$ as follows [96]:

$$\begin{aligned} \hat{O}_1 &= -\frac{\xi_c}{\xi_t} (\bar{c}_{L\beta} \gamma^\mu b_{L\alpha}) (\bar{d}_{L\alpha} \gamma_\mu c_{L\beta}) - \frac{\xi_u}{\xi_t} (\bar{u}_{L\beta} \gamma^\mu b_{L\alpha}) (\bar{d}_{L\alpha} \gamma_\mu u_{L\beta}), \\ \hat{O}_2 &= -\frac{\xi_c}{\xi_t} (\bar{c}_{L\alpha} \gamma^\mu b_{L\alpha}) (\bar{d}_{L\beta} \gamma_\mu c_{L\beta}) - \frac{\xi_u}{\xi_t} (\bar{u}_{L\alpha} \gamma^\mu b_{L\alpha}) (\bar{d}_{L\beta} \gamma_\mu u_{L\beta}), \end{aligned} \quad (173)$$

and the rest of the operators (\hat{O}_j ; $j = 3 \dots 8$) are defined like their counterparts O_j in $\mathcal{H}_{eff}(b \rightarrow s)$, with the obvious replacement $s \rightarrow d$. With this definition, the matching

conditions $C_j(m_W)$ and the solutions of the RG equations yielding $C_j(\mu)$ become identical for the two operator bases O_j and \hat{O}_j .

It has been explicitly checked in the $O(\alpha_s)$ calculations of the decay rate and photon energy spectrum involving $b \rightarrow d\gamma$ and $b \rightarrow dg\gamma$ transitions that the limit $m_u \rightarrow 0$ for the decay rate $\Gamma(B \rightarrow X_d + \gamma)$ exists [96]. This implies that the rates and E_γ -spectrum are free of mass singularities. In a recent paper by Greub, Hurth and Wyler [100], the finiteness proof has been extended to the NLL order, in which the virtual corrections to the matrix elements are calculated completely. From this it follows that there are no logarithms of the type $\alpha_{em}\alpha_s \log(m_u^2/m_c^2)$ [108, 100]. Some papers, estimating LD-contributions in radiative B decays, seem to contradict this by assuming light-quark contributions which have such spurious log-dependence. There is no calculational basis for this assumption. On the other hand, as far as the dependence of the decay rate and spectra on the external light quark masses is concerned, one encounters logarithms of the type $\alpha_{em}\alpha_s[(1+(1-x)^2)/x] \log(m_b^2/m_s^2)$ (for $b \rightarrow sg\gamma$) and $\alpha_{em}\alpha_s[(1+(1-x)^2)/x] \log(m_b^2/m_d^2)$ (for $b \rightarrow dg\gamma$), which are important near the soft-photon ($x \rightarrow 0$) region [60] and must also be exponentiated [115].

The essential difference between $\Gamma(B \rightarrow X_s + \gamma)$ and $\Gamma(B \rightarrow X_d + \gamma)$ lies in the matrix elements of the first two operators O_1 and O_2 (in $H_{eff}(b \rightarrow s)$) and \hat{O}_1 and \hat{O}_2 (in $H_{eff}(b \rightarrow d)$). The derivation of the inclusive decay rate and the final-state distributions in $B \rightarrow X_d + \gamma$ otherwise goes along very similar lines as for the decays $B \rightarrow X_s + \gamma$. The branching ratio $\mathcal{B}(B \rightarrow X_d + \gamma)$ in the SM can be written as:

$$\begin{aligned} \mathcal{B}(B \rightarrow X_d + \gamma) &= D_1 |\xi_t|^2 \\ &\{1 - \frac{1-\rho}{(1-\rho)^2 + \eta^2} D_2 - \frac{\eta}{(1-\rho)^2 + \eta^2} D_3 + \frac{D_4}{(1-\rho)^2 + \eta^2}\}, \end{aligned} \quad (174)$$

where the functions D_i depend on the parameters m_t, m_b, m_c, μ , as well as the others we discussed in the context of $\mathcal{B}(B \rightarrow X_s + \gamma)$ in the previous section. For the central values of these parameters, one gets $D_1 = 0.21$, $D_2 = 0.17$, $D_3 = 0.03$, $D_4 = 0.10$ [96]. This analysis has to be updated taking into account the complete NLL virtual calculations in [100], and so the numbers being quoted for D_i are subject to some change. To get the inclusive branching ratio the CKM parameters ρ and η have to be constrained from the unitarity fits. Taking the parameters from a recent fit, one gets $5.0 \times 10^{-3} \leq |\xi_t| \leq 1.4 \times 10^{-2}$ (at 95% C.L.) [120], yielding an order of magnitude uncertainty in $\mathcal{B}(B \rightarrow X_d + \gamma)$ - hence the interest in measuring this branching ratio. Taking the central values of the fitted CKM parameters discussed later in these lectures $A = 0.8$, $\lambda = 0.2205$, $\eta = 0.34$ and $\rho = -0.07$ [120], one gets

$$\mathcal{B}(B \rightarrow X_d + \gamma) = (1.7 \pm 0.85) \times 10^{-5}, \quad (175)$$

which is approximately a factor 10 – 20 smaller than the CKM-allowed branching ratio $\mathcal{B}(B \rightarrow X_s + \gamma)$, measured by CLEO [90].

3.7 Estimates of $\mathcal{B}(B \rightarrow V + \gamma)$ and constraints on the CKM parameters

Exclusive radiative B decays $B \rightarrow V + \gamma$, with $V = K^*, \rho, \omega$, are also potentially very interesting from the point of view of determining the CKM parameters [121]. The extraction of these parameters would, however, involve a trustworthy estimate of the SD- and LD-contributions in the decay amplitudes.

The SD-contribution in the exclusive decays $(B_u, B_d) \rightarrow (K^*, \rho) + \gamma$, $B_d \rightarrow \omega + \gamma$ and the corresponding B_s decays, $B_s \rightarrow (\phi, K^*) + \gamma$, involve the magnetic moment operator \mathcal{O}_7 and the related one obtained by the obvious change $s \rightarrow d$, $\hat{\mathcal{O}}_7$. The transition form factors governing the radiative B decays $B \rightarrow V + \gamma$ can be generically defined as:

$$\langle V, \lambda | \frac{1}{2} \bar{\psi} \sigma_{\mu\nu} q^\nu b | B \rangle = i \epsilon_{\mu\nu\rho\sigma} e_\nu^{(\lambda)} p_B^\rho p_V^\sigma F_S^{B \rightarrow V}(0). \quad (176)$$

Here V is a vector meson with the polarization vector $e^{(\lambda)}$, $V = \rho, \omega, K^*$ or ϕ ; B is a generic B -meson B_u, B_d or B_s , and ψ stands for the field of a light u, d or s quark. The vectors p_B , p_V and $q = p_B - p_V$ correspond to the 4-momenta of the initial B -meson and the outgoing vector meson and photon, respectively. In (176) the QCD renormalization of the $\bar{\psi} \sigma_{\mu\nu} q^\nu b$ operator is implied. Keeping only the SD-contribution leads to obvious relations among the exclusive decay rates, exemplified here by the decay rates for $(B_u, B_d) \rightarrow \rho + \gamma$ and $(B_u, B_d) \rightarrow K^* + \gamma$:

$$\frac{\Gamma((B_u, B_d) \rightarrow \rho + \gamma)}{\Gamma((B_u, B_d) \rightarrow K^* + \gamma)} = \frac{|\xi_t|^2}{|\lambda_t|^2} \frac{|F_S^{B \rightarrow \rho}(0)|^2}{|F_S^{B \rightarrow K^*}(0)|^2} \Phi_{u,d} \simeq \kappa_{u,d} \left[\frac{|V_{td}|}{|V_{ts}|} \right]^2, \quad (177)$$

where $\Phi_{u,d}$ is a phase-space factor which in all cases is close to 1 and

$$\kappa_i \equiv \left[\frac{F_S^{B_i \rightarrow \rho\gamma}}{F_S^{B_i \rightarrow K^*\gamma}} \right]^2 \quad (178)$$

is the ratio of the (SD) form factors squared. The transition form factors F_S are model dependent, and since the exclusive-to-inclusive ratio R_{K^*} has been measured, one could use data to distinguish among models. This aside, the ratios of the form factors, i.e. κ_i , should be more reliably calculable as they depend essentially only on the SU(3)-breaking effects. If the SD-amplitudes were the only contributions, the measurements of the CKM-suppressed radiative decays $(B_u, B_d) \rightarrow \rho + \gamma$, $B_d \rightarrow \omega + \gamma$ and $B_s \rightarrow K^* + \gamma$ could be used in conjunction with the decays $(B_u, B_d) \rightarrow K^* + \gamma$ to determine the CKM parameters. The present experimental upper limits on the CKM ratio $|V_{td}|/|V_{ts}|$ from radiative B decays are indeed based on this assumption, yielding at 90% C.L.[54]:

$$\left| \frac{V_{td}}{V_{ts}} \right| \leq 0.64 - 0.76, \quad (179)$$

depending on the models used for the $SU(3)$ breaking effects in the form factors [121, 122].

The possibility of significant LD-contributions in radiative B decays from the light quark intermediate states has been raised in a number of papers [104] – [108]. Their

amplitudes necessarily involve other CKM matrix elements and hence the simple factorization of the decay rates in terms of the CKM factors involving $|V_{td}|$ and $|V_{ts}|$ no longer holds thereby invalidating the relationships given above. The discussion about the LD-contribution that we presented in the context of the inclusive decays $B \rightarrow X_s + \gamma$ applies in its essence also for the exclusive decays, such as $B \rightarrow K^* + \gamma$, with appropriate modifications. In line with this discussion, we shall assume that the LD-contributions are small also in exclusive decays $B \rightarrow K^* + \gamma$. In what follows, we discuss some charged and neutral exclusive B -decays, $B^\pm \rightarrow \rho^\pm \gamma$ and B -decays $B \rightarrow (\rho^0, \omega) \gamma$, involving the CKM-suppressed transitions and estimate the SD- and LD-contributions.

The LD-contributions in $B \rightarrow V + \gamma$ are induced by the matrix elements of the four-Fermion operators \hat{O}_1 and \hat{O}_2 (likewise O_1 and O_2). Estimates of these contributions require non-perturbative methods. This problem has been investigated recently in [123, 124] using a technique [125] which treats the photon emission from the light quarks in a theoretically consistent and model-independent way. This has been combined with the light-cone QCD sum rule approach to calculate both the SD and LD — parity conserving and parity violating — amplitudes in the decays $B_{u,d} \rightarrow \rho(\omega) + \gamma$. To illustrate this, we concentrate on the B_u^\pm decays, $B_u^\pm \rightarrow \rho^\pm + \gamma$ and take up the neutral B decays $B_d \rightarrow \rho(\omega) + \gamma$ at the end. The LD-amplitude of the four-Fermion operators \hat{O}_1 , \hat{O}_2 is dominated by the contribution of the weak annihilation of valence quarks in the B meson. It is color-allowed for the decays of charged B^\pm mesons, as shown in Fig. 6, where also the tadpole diagram is shown, which, however, contributes only in the presence of gluonic corrections, and hence neglected. In the factorization approximation, one may write the dominant contribution in the operator \hat{O}_2 (here O'_2 is the part of \hat{O}_2 with the CKM factor ξ_u/ξ_t in Eq. (173)

$$\langle \rho \gamma | O'_2 | B \rangle = \langle \rho | \bar{d} \Gamma_\mu u | 0 \rangle \langle \gamma | \bar{u} \Gamma^\mu b | B \rangle + \langle \rho \gamma | \bar{d} \Gamma_\mu u | 0 \rangle \langle 0 | \bar{u} \Gamma^\mu b | B \rangle , \quad (180)$$

and make use of the definitions of the decay constants

$$\begin{aligned} \langle 0 | \bar{u} \Gamma_\mu b | B \rangle &= i p_\mu f_B, \\ \langle \rho | \bar{d} \Gamma_\mu u | 0 \rangle &= \varepsilon_\mu^{(\rho)} m_\rho f_\rho, \end{aligned} \quad (181)$$

to reduce the problem at hand to the calculation of simpler form factors induced by vector and axial-vector currents.

The factorization approximation assumed in [123, 124] has not been tested experimentally in radiative B decays. From a theoretical point of view, non-factorizable contributions belong to either the $O(\alpha_s)$ (and higher order) radiative corrections or to contributions of higher-twist operators to the sum rules. Their inclusion should not change the conclusions substantially.

The LD-amplitude in the decay $B_u \rightarrow \rho^\pm + \gamma$ can be written in terms of the form factors F_1^L and F_2^L ,

$$\begin{aligned} \mathcal{A}_{long} &= -\frac{e G_F}{\sqrt{2}} V_{ub} V_{ud}^* \left(C_2 + \frac{1}{N_c} C_1 \right) m_\rho \varepsilon_\mu^{(\gamma)} \varepsilon_\nu^{(\rho)} \\ &\times \left\{ -i [g^{\mu\nu} (q \cdot p) - p^\mu q^\nu] \cdot 2F_1^L(q^2) + \epsilon^{\mu\nu\alpha\beta} p_\alpha q_\beta \cdot 2F_2^L(q^2) \right\}. \end{aligned} \quad (182)$$

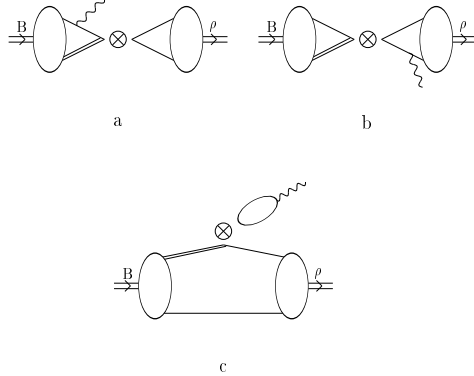


Figure 6: Weak annihilation contributions in $B_u \rightarrow \rho\gamma$ involving the operators O'_1 and O'_2 denoted by \otimes with the photon emission from a) the loop containing the b quark, b) the loop containing the light quark, and c) the tadpole which contributes only with additional gluonic corrections.

Again, one has to invoke a model to calculate the form factors. Estimates from the light-cone QCD sum rules give [124]:

$$F_1^L/F_S = 0.0125 \pm 0.0010, \quad F_2^L/F_S = 0.0155 \pm 0.0010, \quad (183)$$

where the errors correspond to the variation of the Borel parameter in the QCD sum rules. Including other possible uncertainties, one expects an accuracy of the ratios in (183) of order 20%. Estimates of F_S in the normalization of Eq. (176) range between $F_S(B \rightarrow K^*\gamma) = 0.31$ (Narison in [122]) to $F_S(B \rightarrow K^*\gamma) = 0.37$ (Ball in [122]), with a typical error of $\pm 15\%$, and hence are all consistent with each other. This, for example, gives $R_{K^*} = 0.16 \pm 0.05$, using the result from [121], which is in good agreement with data.

Returning to the discussion of the LD-contribution, we note that the parity-conserving and parity-violating amplitudes turn out to be numerically close to each other, $F_1^L \simeq F_2^L \equiv F_L$, hence the ratio of the LD- and the SD- contributions reduces to a number [124]

$$\mathcal{A}_{long}/\mathcal{A}_{short} = R_{L/S}^{B_u \rightarrow \rho\gamma} \cdot \frac{V_{ub}V_{ud}^*}{V_{tb}V_{td}^*}. \quad (184)$$

Using $C_2 = 1.10$, $C_1 = -0.235$, $C_7^{eff} = -0.306$ from Table 6 (corresponding to the scale $\mu = 5$ GeV) [60] gives:

$$R_{L/S}^{B_u \rightarrow \rho\gamma} \equiv \frac{4\pi^2 m_\rho (C_2 + C_1/N_c)}{m_b C_7^{eff}} \cdot \frac{F_L^{B_u \rightarrow \rho\gamma}}{F_S^{B_u \rightarrow \rho\gamma}} = -0.30 \pm 0.07, \quad (185)$$

which is not negligible. To get a ball-park estimate of the ratio $\mathcal{A}_{long}/\mathcal{A}_{short}$, we take the central values of the CKM matrix elements, $V_{ud} = 0.9744 \pm 0.0010$ [3], $|V_{td}| = (1.0 \pm 0.2) \times 10^{-2}$, $|V_{cb}| = 0.039 \pm 0.004$ and $|V_{ub}/V_{cb}| = 0.08 \pm 0.02$ [83], yielding,

$$|\mathcal{A}_{long}/\mathcal{A}_{short}|^{B_u \rightarrow \rho\gamma} = |R_{L/S}^{B_u \rightarrow \rho\gamma}| \frac{|V_{ub}V_{ud}|}{|V_{td}V_{bt}|} \simeq 10\%. \quad (186)$$

Thus, the CKM factors suppress the LD-contributions.

The analogous LD-contributions to the neutral B decays $B_d \rightarrow \rho\gamma$ and $B_d \rightarrow \omega\gamma$ are expected to be much smaller, a point that has also been noted in the context of the VMD and quark model based estimates [104]. In the present approach, the corresponding form factors for the decays $B_d \rightarrow \rho^0(\omega)\gamma$ are obtained from the ones for the decay $B_u \rightarrow \rho^\pm\gamma$ discussed above by the replacement of the light quark charges $e_u \rightarrow e_d$, which gives the factor $-1/2$; in addition, and more importantly, the LD-contribution to the neutral B decays is colour-suppressed, which reflects itself through the replacement of the factor a_1 by a_2 . This yields for the ratio

$$\frac{R_{L/S}^{B_d \rightarrow \rho\gamma}}{R_{L/S}^{B_u \rightarrow \rho\gamma}} = \frac{e_d a_2}{e_u a_1} \simeq -0.13 \pm 0.05, \quad (187)$$

where the numbers are based on using $a_2/a_1 = 0.27 \pm 0.10$ [110]. This would then yield at most $R_{L/S}^{B_d \rightarrow \rho\gamma} \simeq R_{L/S}^{B_d \rightarrow \omega\gamma} = 0.05$, which in turn gives

$$\frac{\mathcal{A}_{\text{long}}^{B_d \rightarrow \rho\gamma}}{\mathcal{A}_{\text{short}}^{B_d \rightarrow \rho\gamma}} \leq 0.02. \quad (188)$$

Even if this underestimates the LD-contribution by a factor 2, due to the approximations made in [123, 124], we conclude that it is quite safe to neglect the LD-contribution in the neutral B -meson radiative decays.

Restricting to the colour-allowed LD-contributions, the relations, which obtains ignoring such contributions (and isospin invariance),

$$\Gamma(B_u \rightarrow \rho^+\gamma) = 2 \Gamma(B_d \rightarrow \rho^0\gamma) = 2 \Gamma(B_d \rightarrow \omega\gamma), \quad (189)$$

get modified to

$$\begin{aligned} \frac{\Gamma(B_u \rightarrow \rho\gamma)}{2\Gamma(B_d \rightarrow \rho\gamma)} &= \frac{\Gamma(B_u \rightarrow \rho\gamma)}{2\Gamma(B_d \rightarrow \omega\gamma)} = \left| 1 + R_{L/S}^{B_u \rightarrow \rho\gamma} \frac{V_{ub} V_{ud}^*}{V_{tb} V_{td}^*} \right|^2 = \\ &= 1 + 2 \cdot R_{L/S} V_{ud} \frac{\rho(1-\rho) - \eta^2}{(1-\rho)^2 + \eta^2} + (R_{L/S})^2 V_{ud}^2 \frac{\rho^2 + \eta^2}{(1-\rho)^2 + \eta^2}. \end{aligned} \quad (190)$$

where $R_{L/S} \equiv R_{L/S}^{B_u \rightarrow \rho\gamma}$. The ratio $\Gamma(B_u \rightarrow \rho\gamma)/2\Gamma(B_d \rightarrow \rho\gamma)$ ($= \Gamma(B_u \rightarrow \rho\gamma)/2\Gamma(B_d \rightarrow \omega\gamma)$) is shown in Fig. 7 as a function of the parameter ρ , with $\eta = 0.2, 0.3$ and 0.4 . This suggests that a measurement of this ratio would constrain the Wolfenstein parameters (ρ, η) , with the dependence on ρ more marked than on η . In particular, a negative value of ρ leads to a constructive interference in $B_u \rightarrow \rho\gamma$ decays, while large positive values of ρ give a destructive interference. This behaviour is in qualitative agreement with what has been also pointed out in [105].

The ratio of the CKM-suppressed and CKM-allowed decay rates for charged B mesons gets modified due to the LD contributions. Following [107], we ignore the LD-contributions in $\Gamma(B \rightarrow K^*\gamma)$. The ratio of the decay rates in question can therefore be written as:

$$\begin{aligned} \frac{\Gamma(B_u \rightarrow \rho\gamma)}{\Gamma(B_u \rightarrow K^*\gamma)} &= \kappa_u \lambda^2 [(1-\rho)^2 + \eta^2] \\ &\times \left\{ 1 + 2 \cdot R_{L/S} V_{ud} \frac{\rho(1-\rho) - \eta^2}{(1-\rho)^2 + \eta^2} + (R_{L/S})^2 V_{ud}^2 \frac{\rho^2 + \eta^2}{(1-\rho)^2 + \eta^2} \right\}, \end{aligned} \quad (191)$$

Using the central value from the estimates of the ratio of the form factors squared $\kappa_u = 0.59 \pm 0.08$ [121], we show the ratio (191) in Fig. 8 as a function of ρ for $\eta = 0.2, 0.3$, and 0.4 . It is seen that the dependence of this ratio is rather weak on η but it depends on ρ rather sensitively. The effect of the LD-contributions is modest but not negligible, introducing an uncertainty comparable to the $\sim 15\%$ uncertainty in the overall normalization due to the $SU(3)$ -breaking effects in the quantity κ_u .

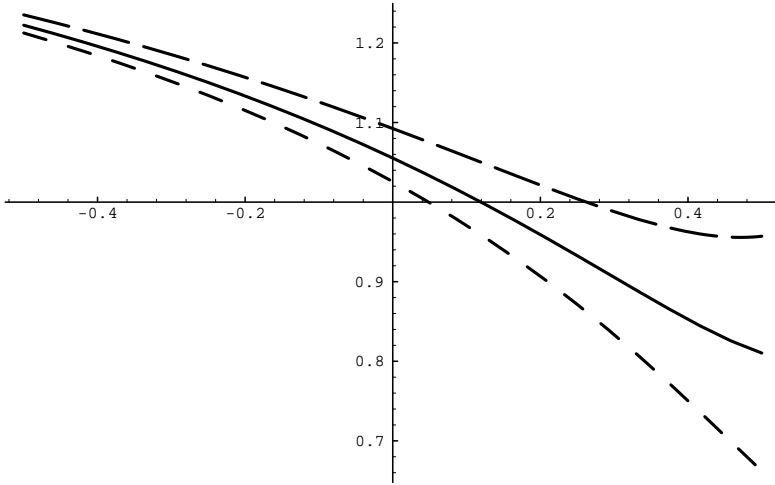


Figure 7: Ratio of the neutral and charged B -decay rates $\Gamma(B_u \rightarrow \rho\gamma)/2\Gamma(B_d \rightarrow \rho\gamma)$ as a function of the Wolfenstein parameter ρ , with $\eta = 0.2$ (short-dashed curve), $\eta = 0.3$ (solid curve), and $\eta = 0.4$ (long-dashed curve). (Figure taken from [124].)

Neutral B -meson radiative decays are less-prone to the LD-effects, as argued above, and hence one expects that to a good approximation the ratio of the decay rates for neutral B meson obtained in the approximation of SD-dominance remains valid [121]:

$$\frac{\Gamma(B_d \rightarrow \rho\gamma, \omega\gamma)}{\Gamma(B \rightarrow K^*\gamma)} = \kappa_d \lambda^2 [(1 - \rho)^2 + \eta^2], \quad (192)$$

where this relation holds for each of the two decay modes separately. It is a realistic hope that this relation is theoretically (almost) on the same footing in the standard model as the one for the ratio of the B^0 - \bar{B}^0 mixing-induced mass differences, which satisfies the relation [120]:

$$\frac{\Delta M_s}{\Delta M_d} = \kappa_{sd} \left| \frac{V_{ts}}{V_{td}} \right|^2 = \kappa_{sd} \frac{1}{\lambda^2 [(1 - \rho)^2 + \eta^2]} . \quad (193)$$

The hadronic uncertainty in this ratio is in the $SU(3)$ -breaking factor $\kappa_{sd} \equiv (f_{B_s}^2 \hat{B}_{B_s} / f_{B_d}^2 \hat{B}_{B_d})$, which involves the pseudoscalar coupling constants and the so-called bag constants. This

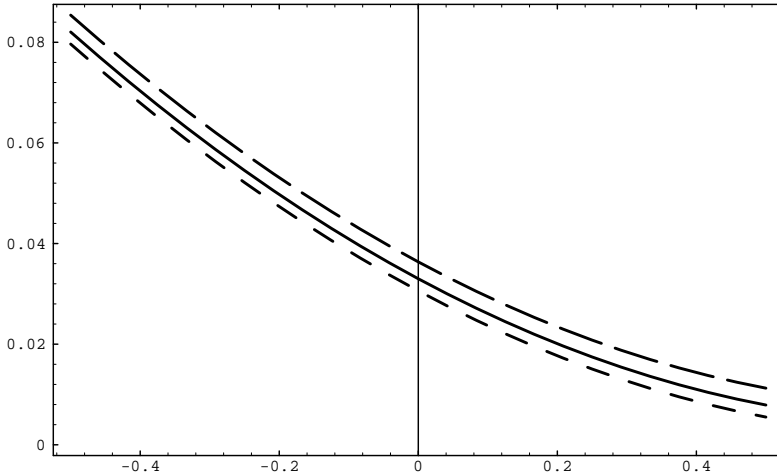


Figure 8: Ratio of the CKM-suppressed and CKM-allowed radiative B -decay rates $\Gamma(B_u \rightarrow \rho\gamma)/\Gamma(B \rightarrow K^*\gamma)$ (with $B = B_u$ or B_d) as a function of the Wolfenstein parameter ρ , a) with $\eta = 0.2$ (short-dashed curve), $\eta = 0.3$ (solid curve), and $\eta = 0.4$ (long-dashed curve). (Figure taken from [124].)

quantity is estimated as $\kappa_{sd} = 1.35 \pm 0.25$ in the QCD sum rules and lattice QCD approaches. (For details and references, see [120]). The present upper limit for the mass-difference ratio $\Delta M_s/\Delta M_d > 12.3$ at 95 % C.L. from the ALEPH data [126] provides a better constraint on the CKM parameters, yielding $|V_{td}|/|V_{ts}| < 0.35$, than the corresponding constraints from the rare radiative decays $B \rightarrow (\rho, \omega) + \gamma$, which give an upper limit of 0.75 for the same CKM-ratio. We expect experimental sensitivity to increase in both measurements, reaching the level predicted for this ratio in the standard model, $|V_{td}|/|V_{ts}| = 0.24 \pm 0.05$ [120], in the next several years in the ongoing experiments at CLEO, SLC and Tevatron, and the forthcoming ones at the B factories, HERA-B and LHC.

Finally, combining the estimates for the LD- and SD-form factors in [124] and [121], respectively, and restricting the Wolfenstein parameters in the range $-0.4 \leq \rho \leq 0.4$ and $0.2 \leq \eta \leq 0.4$, as suggested by the CKM-fits [120], we give the following ranges for the absolute branching ratios:

$$\begin{aligned} \mathcal{B}(B_u \rightarrow \rho\gamma) &= (1.9 \pm 1.6) \times 10^{-6}, \\ \mathcal{B}(B_d \rightarrow \rho\gamma) &\simeq \mathcal{B}(B_d \rightarrow \omega\gamma) = (0.85 \pm 0.65) \times 10^{-6}, \end{aligned} \quad (194)$$

where we have used the experimental value for the branching ratio $\mathcal{B}(B \rightarrow K^* + \gamma)$ [91], adding the errors in quadrature. The large error reflects the poor knowledge of the CKM

matrix elements and hence experimental determination of these branching ratios will put rather stringent constraints on the Wolfenstein parameter ρ .

Summarizing the effect of the LD-contributions in radiative B decays, we note that they are dominantly given by the annihilation diagrams. QCD sum-rule-based estimates are encouraging in that they strengthen the hope that such contributions are modest in exclusive radiative B decays, in particular in the neutral B -decays $B^0 \rightarrow (\rho^0, \omega) + \gamma$, with $B^\pm \rightarrow \rho^\pm \gamma$ modified by $O(20)\%$ from its SD-rate. This should be checked in other theoretically sound frameworks. Of course, forthcoming data on charged and neutral B -meson decays will be able to determine the LD-contribution directly. Presently available data in general suggest that the contribution of annihilation diagrams in B decays is not significant, as seen through the near equality of the lifetimes for the B^\pm , B_d^0 and B_s^0 mesons and the near equality of the observed B^\pm and B^0 radiative decay rates. In terms of the operator product expansion, they all involve the four-Fermi operators, sandwiched between various inclusive and exclusive states. The matrix elements are process-dependent and have to be estimated as well as possible. Some illustrative examples were given here.

3.8 Inclusive rare decays $B \rightarrow X_s \ell^+ \ell^-$ in the SM

The decays $B \rightarrow X_s \ell^+ \ell^-$, with $\ell = e, \mu, \tau$, provide a more sensitive search strategy for finding new physics in rare B decays than for example the decay $B \rightarrow X_s \gamma$, which constrains only the magnitude of C_7^{eff} . This experimental constraint has triggered a lot of theoretical investigations on beyond-the-SM frameworks, as can be judged from the incomplete list of papers in [127, 128]. The sign of C_7^{eff} , which depends on the underlying physics, is not determined by the measurement of $\mathcal{B}(B \rightarrow X_s + \gamma)$. This sign in our convention is negative in the SM (see Table 6). However, it is known (see for example [129]) that in supersymmetric models, both the negative and positive signs are allowed as one scans over the allowed parameter space of this model. The determination of the sign of C_7^{eff} is an important matter as this will impose further constraints on the parameters of many models. It will also test the prediction of the SM, by the same token.

Continuing this discussion, we recall that a part of the amplitude for $B \rightarrow X_s \ell^+ \ell^-$ involving the coupling of the virtual photon to the charged lepton pair depends on the effective Wilson coefficient C_7^{eff} encountered in the electromagnetic penguin decays $B \rightarrow X_s + \gamma$. For low dilepton masses, the differential decay rate for $B \rightarrow X_s \ell^+ \ell^-$ is dominated by this contribution. However, as we shall see below, the $B \rightarrow X_s \ell^+ \ell^-$ amplitude in the standard model has two additional terms, arising from the two FCNC four-Fermi operators, ** which are not constrained by the $B \rightarrow X_s + \gamma$ data. Calling their coefficients C_9 and C_{10} , it has been argued in [129] that the signs and magnitudes of all three coefficients C_7^{eff} , C_9 and C_{10} can, in principle, be determined from the decays $B \rightarrow X_s + \gamma$ and $B \rightarrow X_s \ell^+ \ell^-$. The coefficient C_8 , which governs the strength of the chromomagnetic moment transition, can, in principle, also be determined by measuring the photon energy spectrum in $B \rightarrow X_s + \gamma$ in low-to-intermediate photon energy region.

The SM-based rates for the decay $b \rightarrow s \ell^+ \ell^-$, calculated in the free quark decay

**This also holds for a large class of models such as MSSM and two-Higgs doublet models but not for all. In LR symmetric models, for example, there are additional FCNC four-Fermi operators involved [134].

approximation, have been known in the LO approximation for some time [93]. The LO calculations have the unpleasant feature that the decay distributions and rates are scheme-dependent. The required NLO calculation is in the meanwhile available, which reduces the scheme-dependence of the LO effects in these decays [130, 131]. In addition, long-distance (LD) effects, which are expected to be very important in the decay $B \rightarrow X_s \ell^+ \ell^-$ [132], have also been estimated from data on the assumption that they arise dominantly due to the charmonium resonances J/ψ and ψ' through the decay chains $B \rightarrow X_s J/\psi(\psi', \dots) \rightarrow X_s \ell^+ \ell^-$. The effect of these resonances persists even far away from the resonant masses deforming the short-distance based distributions appreciably [132]. Likewise, the leading ($1/m_b^2$) power corrections to the partonic decay rate and the dilepton invariant mass distribution have been calculated with the help of the operator product expansion in the effective heavy quark theory [133]. A theoretically complete description including the improved perturbative treatment of the decay $B \rightarrow X_s \ell^+ \ell^-$, the LD-effects and power corrections mentioned above, to the best of our knowledge, is still lacking. In what follows, we shall not take into account the power corrections but include the rest to get estimates for the decay rates and distributions in $B \rightarrow X_s \ell^+ \ell^-$.

The amplitude for $B \rightarrow X_s \ell^+ \ell^-$ is calculated in the effective theory approach, which we have discussed earlier, by extending the operator basis of the effective Hamiltonian introduced in Eq. (120):

$$\mathcal{H}_{eff}(b \rightarrow s + \gamma; b \rightarrow s + \ell^+ \ell^-) = \mathcal{H}_{eff}(b \rightarrow s + \gamma) - \frac{4G_F}{\sqrt{2}} V_{ts}^* V_{tb} [C_9 \mathcal{O}_9 + C_{10} \mathcal{O}_{10}], \quad (195)$$

where the two additional operators are:

$$\begin{aligned} \mathcal{O}_9 &= \frac{\alpha}{4\pi} \bar{s}_\alpha \gamma^\mu P_L b_\alpha \bar{\ell} \gamma_\mu \ell, \\ \mathcal{O}_{10} &= \frac{\alpha}{4\pi} \bar{s}_\alpha \gamma^\mu P_L b_\alpha \bar{\ell} \gamma_\mu \gamma_5 \ell. \end{aligned} \quad (196)$$

The analytic expressions for $C_9(m_W)$ and $C_{10}(m_W)$ can be seen in [31, 129] and will not be given here. We recall that the coefficient C_9 in LO is scheme-dependent. However, this is compensated by an additional scheme-dependent part in the (one loop) matrix element of \mathcal{O}_9 . We call the sum C_9^{eff} , which is scheme-independent and enters in the physical decay amplitude given below,

$$\begin{aligned} \mathcal{M}(b \rightarrow s + \ell^+ \ell^-) &= \frac{4G_F}{\sqrt{2}} V_{ts}^* V_{tb} \frac{\alpha}{\pi} \\ &\left[C_9^{eff} \bar{s} \gamma^\mu P_L b \bar{\ell} \gamma_\mu \ell + C_{10} \bar{s} \gamma^\mu P_L b \bar{\ell} \gamma_\mu \gamma_5 \ell - 2C_7^{eff} \bar{s} i \sigma_{\mu\nu} \frac{q^\nu}{q^2} (m_b P_R + m_s P_L) b \bar{\ell} \gamma^\mu \ell \right], \end{aligned} \quad (197)$$

with

$$C_9^{eff}(\hat{s}) \equiv C_9 \eta(\hat{s}) + Y(\hat{s}). \quad (198)$$

The function $Y(\hat{s})$ is the one-loop matrix element of \mathcal{O}_9 and is defined as:

$$Y(\hat{s}) = g(m_c, \hat{s}) (3C_1 + C_2 + 3C_3 + C_4 + 3C_5 + C_6)$$

$$\begin{aligned}
& -\frac{1}{2}g(1, \hat{s})(4C_3 + 4C_4 + 3C_5 + C_6) \\
& -\frac{1}{2}g(0, \hat{s})(C_3 + 3C_4) \\
& +\frac{2}{9}(3C_3 + C_4 + 3C_5 + C_6) \\
& -\xi \frac{4}{9}(3C_1 + C_2 - C_3 - 3C_4), \tag{199}
\end{aligned}$$

$$\eta(\hat{s}) = 1 + \frac{\alpha_s(\mu)}{\pi} \omega(\hat{s}) . \tag{200}$$

Here $\hat{s} \equiv (\hat{p}_+ + \hat{p}_-)^2/m_b^2$ is the scaled dilepton mass, with $p_\pm = (E_\pm, \mathbf{p}_\pm)$ denoting four-momenta of ℓ^\pm , \hat{m}_i are the scaled quark masses, $\hat{m}_i = m_i/m_b$, and the function $\omega(\hat{s})$ represents the $O(\alpha_s)$ correction from one-gluon exchange in the matrix element of \mathcal{O}_9 , the analogue of which we have discussed in the context of the semileptonic B decays earlier, derived in [25]:

$$\begin{aligned}
\omega(\hat{s}) = & -\frac{2}{9}\pi^2 - \frac{4}{3}\text{Li}_2(s) - \frac{2}{3}\ln\hat{s}\ln(1-\hat{s}) - \frac{5+4\hat{s}}{3(1+2\hat{s})}\ln(1-\hat{s}) \\
& - \frac{2\hat{s}(1+\hat{s})(1-2\hat{s})}{3(1-\hat{s})^2(1+2\hat{s})}\ln\hat{s} + \frac{5+9\hat{s}-6\hat{s}^2}{6(1-\hat{s})(1+2\hat{s})}. \tag{201}
\end{aligned}$$

The function $g(z, \hat{s})$ includes the charm quark-antiquark pair contribution [130, 131]:

$$\begin{aligned}
g(z, \hat{s}) = & -\frac{8}{9}\ln\left(\frac{m_b}{\mu}\right) - \frac{8}{9}\ln z + \frac{8}{27} + \frac{4}{9}y - \frac{2}{9}(2+y)\sqrt{|1-y|} \\
& \times \left[\Theta(1-y)\left(\ln\frac{1+\sqrt{1-y}}{1-\sqrt{1-y}} - i\pi\right) + \Theta(y-1)2\arctan\frac{1}{\sqrt{y-1}} \right], \tag{202}
\end{aligned}$$

$$g(0, \hat{s}) = \frac{8}{27} - \frac{8}{9}\ln\left(\frac{m_b}{\mu}\right) - \frac{4}{9}\ln\hat{s} + \frac{4}{9}i\pi, \tag{203}$$

where $y = 4z^2/\hat{s}$. We recall from the discussion in [130, 131] that ξ is dependent on the dimensional regularization scheme, with,

$$\xi = \begin{cases} 0 & (\text{NDR}) \\ -1 & (\text{HV}). \end{cases} \tag{204}$$

For numerical estimates, the Wilson coefficients C_1, \dots, C_6 and C_7^{eff} are given in Table 6 and we give here the value for C_9 (in the NDR-scheme) and C_{10} for the central values of the parameters used in Table 6 ($\overline{m_t} = 170$ GeV and $\Lambda_{QCD} = 0.195$ GeV):

$$\begin{aligned}
C_9^{\text{NDR}}(\mu = 5.0_{-2.5}^{+5.0} \text{ GeV}) & = 4.09_{-0.41}^{+0.27}, \\
C_{10}(m_W) & = -4.32. \tag{205}
\end{aligned}$$

Note that the coefficient $C_{10}(m_W)$ does not get renormalized by QCD corrections.

Following refs. [129] and [135], the differential decay rates in $B \rightarrow X_s \ell^+ \ell^-$ (ignoring lepton masses) are,

$$\frac{d\mathcal{B}(\hat{s})}{d\hat{s}} = \mathcal{B}_{sl} \frac{\alpha^2}{4\pi^2} \frac{\lambda_t^2}{|V_{cb}|^2} \frac{1}{f(\hat{m}_c)\kappa(\hat{m}_c)} u(\hat{s}) \left[\left(|C_9^{eff}(\hat{s})|^2 + C_{10}^2 \right) \alpha_1(\hat{s}, \hat{m}_s) + \frac{4}{\hat{s}} (C_7^{eff})^2 \alpha_2(\hat{s}, \hat{m}_s) + 12\alpha_3(\hat{s}, \hat{m}_s) C_7^{eff} \Re(C_9^{eff}(\hat{s})) \right], \quad (206)$$

with $u(\hat{s}) = \sqrt{[\hat{s} - (1 + \hat{m}_s)^2][\hat{s} - (1 - \hat{m}_s)^2]}$, $f(z)$ has been defined earlier as we discussed Γ_{SL} , $\kappa(z) = 1 - 2\alpha_s(\mu)/3\pi [(\pi^2 - 31/4)(1 - z)^2 + 3/2]$, and

$$\alpha_1(\hat{s}, \hat{m}_s) = -2\hat{s}^2 + \hat{s}(1 + \hat{m}_s^2) + (1 - \hat{m}_s^2)^2, \quad (207)$$

$$\alpha_2(\hat{s}, \hat{m}_s) = -(1 + \hat{m}_s^2)\hat{s}^2 - (1 + 14\hat{m}_s^2 + \hat{m}_s^4)\hat{s} + 2(1 + \hat{m}_s^2)(1 - \hat{m}_s^2)^2, \quad (208)$$

$$\alpha_3(\hat{s}, \hat{m}_s) = (1 - \hat{m}_s^2)^2 - (1 + \hat{m}_s^2)\hat{s}. \quad (209)$$

Here $\Re(C_7^{eff})$ represents the real part of C_7^{eff} . A useful quantity is the differential FB asymmetry in the c.m.s. of the dilepton defined in refs. [135]:

$$\frac{d\mathcal{A}(\hat{s})}{d\hat{s}} = \int_0^1 \frac{d\mathcal{B}}{dz} - \int_0^{-1} \frac{d\mathcal{B}}{dz}, \quad (210)$$

where $z = \cos \theta$, which can be expressed as:

$$\frac{d\mathcal{A}(\hat{s})}{d\hat{s}} = -\mathcal{B}_{sl} \frac{3\alpha^2}{4\pi^2} \frac{1}{f(\hat{m}_c)} u^2(\hat{s}) C_{10} \left[\hat{s} \Re(C_9^{eff}(\hat{s})) + 2C_7^{eff}(1 + \hat{m}_s^2) \right]. \quad (211)$$

The Wilson coefficients C_7^{eff} , C_9^{eff} and C_{10} appearing in the above equations can be determined from data by solving the partial branching ratio $\mathcal{B}(\Delta\hat{s})$ and partial FB asymmetry $\mathcal{A}(\Delta\hat{s})$, where $\Delta\hat{s}$ defines an interval in the dilepton invariant mass [129].

There are other quantities which one can measure in the decays $B \rightarrow X_s \ell^+ \ell^-$ to disentangle the underlying dynamics. We mention here the longitudinal polarization of the lepton in $B \rightarrow X_s \ell^+ \ell^-$, in particular in $B \rightarrow X_s \tau^+ \tau^-$, proposed by Hewett [136]. In a recent paper, Krüger and Sehgal [137] have stressed that complementary information is contained in the two orthogonal components of polarization (P_T , the component in the decay plane, and P_N , the component normal to the decay plane), both of which are proportional to m_ℓ/m_b , and therefore significant for the $\tau^+ \tau^-$ channel. A third quantity, called energy asymmetry, proposed by Cho, Misiak and Wyler [138], defined as

$$\mathcal{A} = \frac{N(E_{\ell^-} > E_{\ell^+}) - N(E_{\ell^+} > E_{\ell^-})}{N(E_{\ell^-} > E_{\ell^+}) + N(E_{\ell^+} > E_{\ell^-})}, \quad (212)$$

where $N(E_{\ell^-} > E_{\ell^+})$ denotes the number of lepton pairs where ℓ^+ is more energetic than ℓ^- in the B -rest frame, is, however, not an independent measure, as it is directly proportional to the FB asymmetry discussed above. The relation is [140]:

$$\int \mathcal{A}(\hat{s}) = \mathcal{B} \times A. \quad (213)$$

This is easy to notice if one writes the Mandelstam variable $u(\hat{s})$ in the dilepton c.m. and the B -hadron rest systems.

Next, we discuss the effects of LD contributions in the processes $B \rightarrow X_s \ell^+ \ell^-$. Note that the LD contributions due to the vector mesons such as J/ψ and ψ' , as well as the continuum $c\bar{c}$ contribution already discussed, appear as an effective $(\bar{s}_L \gamma_\mu b_L)(\bar{\ell} \gamma^\mu \ell)$ interaction term only, i.e. in the operator \mathcal{O}_9 . This implies that the LD-contributions should change C_9 effectively, C_7 as discussed earlier is dominated by the SD-contribution, and C_{10} has no LD-contribution. In accordance with this, the function $Y(\hat{s})$ is replaced by,

$$Y(\hat{s}) \rightarrow Y'(\hat{s}) \equiv Y(\hat{s}) + Y_{\text{res}}(\hat{s}), \quad (214)$$

where $Y_{\text{res}}(\hat{s})$ is given as [135],

$$Y_{\text{res}}(\hat{s}) = \frac{3}{\alpha^2} \kappa (3C_1 + C_2 + 3C_3 + C_4 + 3C_5 + C_6) \sum_{V_i=J/\psi, \psi', \dots} \frac{\pi \Gamma(V_i \rightarrow l^+ l^-) M_{V_i}}{M_{V_i}^2 - \hat{s} m_b^2 - i M_{V_i} \Gamma_{V_i}}, \quad (215)$$

where κ is a fudge factor, which appears due to the inadequacy of the factorization framework in describing data on $B \rightarrow J/\psi X_s$. Here we use $\kappa (3C_1 + C_2 + 3C_3 + C_4 + 3C_5 + C_6) = +0.88$ for the numerical calculation, which reproduces (in average) the measured branching ratios for $B \rightarrow J/\psi X_s$ and $B \rightarrow \psi' X_s$, after the contributions from the χ_c states have been subtracted. This is consistent with the treatment of LD-effects in [137] and [139], where further discussions and theoretical uncertainties on the LD-contributions can be seen. The long-distance effects lead to significant interference effects in the dilepton invariant mass distribution and the FB asymmetry in $B \rightarrow X_s \ell^+ \ell^-$ shown in Figs. 9 and 10, respectively. This can be used to test the SM, as the signs of the Wilson coefficients in general are model dependent.

The leading $(1/m_Q)$ power correction to the dilepton mass spectrum in $B \rightarrow X_s \ell^+ \ell^-$ has been worked out in [141] using heavy quark expansion. The correction was found to be positive and around 10% over a good part of the dilepton mass spectrum with the particular choice of the parameters λ_1 and λ_2 adopted in this paper. In the meanwhile, the estimate of the parameter λ_1 has changed (it has a negative value now) compared to what has been used in [141]. Apart from this, the analytic form of the power corrected result in [141] is also somewhat puzzling and remains to be verified as, on general grounds, one expects the heavy quark expansion to break down near the end-point of the dilepton mass spectrum, i.e., as $\hat{s} \rightarrow \hat{s}^{\text{max}}$, which is not suggested by the power-corrected spectrum reported in [141]. In the opinion of this author, the end-point spectrum requires integration over a range of dilepton masses (or smearing) to be calculable in the heavy quark expansion method. A detailed discussion of this point and a new derivation of power corrections to the dilepton mass spectrum and FB asymmetry will be presented in [140].

Taking into account the spread in the values of the input parameters, μ , Λ , m_t , and \mathcal{B}_{SL} discussed in the previous section in the context of $\mathcal{B}(B \rightarrow X_s + \gamma)$, we estimate the following branching ratios for the SD-piece only (i.e., from the intermediate top quark contribution only) [140]:

$$\begin{aligned} \mathcal{B}(B \rightarrow X_s e^+ e^-) &= (8.4 \pm 2.2) \times 10^{-6}, \\ \mathcal{B}(B \rightarrow X_s \mu^+ \mu^-) &= (5.7 \pm 1.2) \times 10^{-6}, \end{aligned}$$

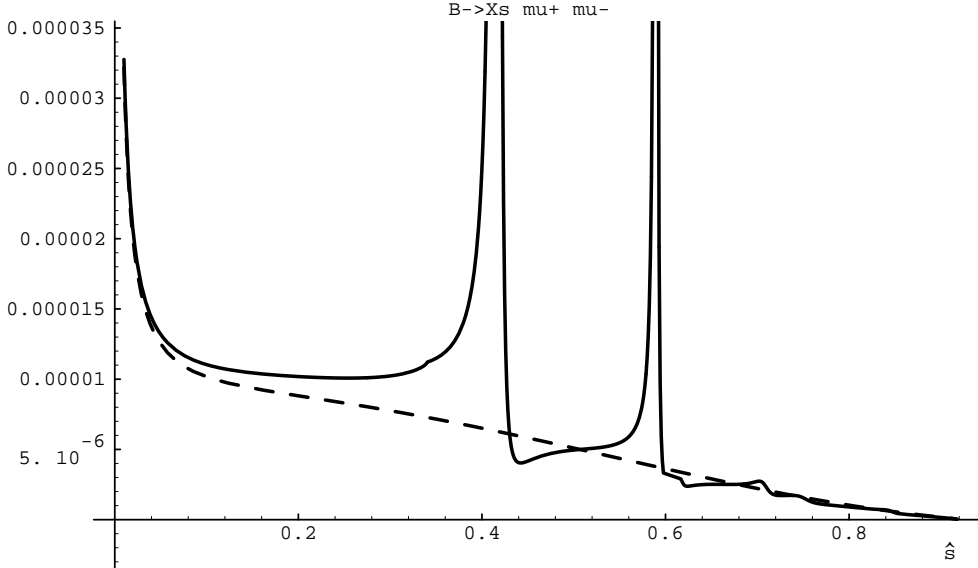


Figure 9: Dimuon invariant mass distribution in $B \rightarrow X_s \mu^+ \mu^-$ in the SM including next-to-leading order QCD correction. The dashed curve corresponds to the short-distance contribution only and the solid curve is the sum of the long-distance and short-distance contributions. (Figure taken from [140].)

$$\mathcal{B}(B \rightarrow X_s \tau^+ \tau^-) = (2.6 \pm 0.5) \times 10^{-7}, \quad (216)$$

where theoretical errors and the error on \mathcal{B}_{SL} have been added in quadrature. These estimates are consistent with the results presented in [131, 137]. The present experimental limit for the inclusive branching ratio in $B \rightarrow X_s \ell^+ \ell^-$ is actually still the one set by the UA1 collaboration some time ago [142], namely $\mathcal{B}(B \rightarrow X_s \mu^+ \mu^-) > 5.0 \times 10^{-5}$. As far as we know, there are no interesting limits on the other two modes, involving $X_s e^+ e^-$ and $X_s \tau^+ \tau^-$.

It is obvious from Fig. 9 that only in the dilepton mass region far away from the resonances is there a hope of extracting the Wilson coefficients governing the short-distance physics. The region below the J/ψ resonance is well suited for that purpose as the dilepton invariant mass distribution there is dominated by the SD-piece. Including the LD-contributions, following branching ratio has been estimated for the dilepton mass range $0.2 \leq \hat{s} \leq 0.36$ in [140]:

$$\mathcal{B}(B \rightarrow X_s \mu^+ \mu^-) = (1.3 \pm 0.3) \times 10^{-6}, \quad (217)$$

with $\mathcal{B}(B \rightarrow X_s e^+ e^-) \simeq \mathcal{B}(B \rightarrow X_s \mu^+ \mu^-)$. The FB-asymmetry is estimated to be in the range 10% - 27%, as can be seen in Fig. 10. These branching ratios and the FB asymmetry are expected to be measured within the next several years at BABAR, BELLE, CLEO, CDF, D0, and HERA-B. In the high invariant mass region, the short-distance contribution dominates. However, the rates are down by roughly an order of magnitude compared to the region below the J/ψ -mass. Estimates of the branching ratios are of $O(10^{-7})$, which should be accessible at the LHC.

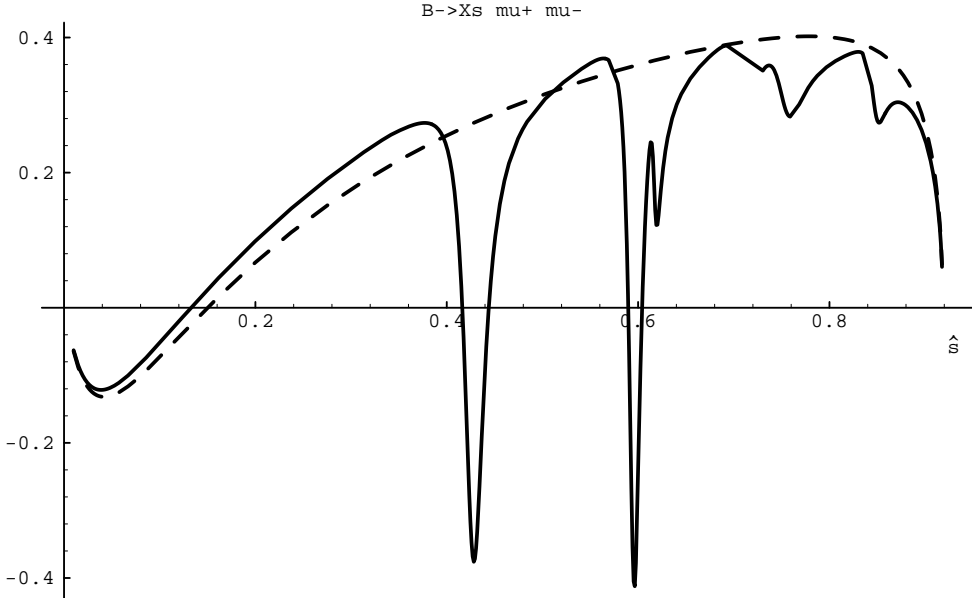


Figure 10: FB asymmetry for $B \rightarrow X_s \mu^+ \mu^-$ in the SM as a function of the dimuon invariant mass including the next-to-leading order QCD correction. The dashed curve corresponds to the short-distance contribution only and the solid curve is the sum of the long-distance and short-distance contributions. (Figure taken from [140].)

The experimental limits on the decay rates of the exclusive decays $B \rightarrow (K, K^*)\ell^+\ell^-$, being searched for by the CLEO and CDF collaborations [54, 110, 144], while arguably closer to the SM-based estimates, can only be interpreted in specific models of form factors, which hinders somewhat their transcription in terms of the information on the underlying Wilson coefficients. However, many of these form factors can be related to the known ones using ideas from heavy quark effective theory augmented with QCD sum rule estimates in studying the heavy to light form factors in B decays [145]. We will not take up such exclusive decays, important as they are, in these lectures and content ourselves with presenting the expected branching ratios for some of the experimentally interesting decay modes. Using the exclusive-to-inclusive ratios $R_{K\ell\ell} \equiv \Gamma(B \rightarrow K\ell^+\ell^-)/\Gamma(B \rightarrow X_s\ell^+\ell^-) = 0.07 \pm 0.02$ and $R_{K^*\ell\ell} \equiv \Gamma(B \rightarrow K^*\ell^+\ell^-)/\Gamma(B \rightarrow X_s\ell^+\ell^-) = 0.27 \pm 0.07$, which were estimated in [102], the results are presented in Table 2.

In conclusion, the semileptonic FCNC decays $B \rightarrow X_s\ell^+\ell^-$ (and also the exclusive decays) will provide very precise tests of the SM, as they will determine the signs and magnitudes of the three Wilson coefficients, C_7 , C_9^{eff} and C_{10} . This, perhaps, may also reveal physics beyond-the-SM if it is associated with not too high a scale. The MSSM model is a good case study where measurable deviations from the SM are anticipated and worked out [129, 138].

3.9 Summary and overview of rare B decays in the SM

The rare B decay mode $B \rightarrow X_s\nu\bar{\nu}$, and some of the exclusive channels associated with it, have comparatively larger branching ratios. The estimated inclusive branching ratio

in the SM is [102, 31, 146]:

$$\mathcal{B}(B \rightarrow X_s \nu \bar{\nu}) = (4.0 \pm 1.0) \times 10^{-5}, \quad (218)$$

where the main uncertainty in the rates is due to the top quark mass, as the top quark contribution completely dominates the decay rate, and a residual one from the semileptonic branching ratio \mathcal{B}_{SL} . The scale-dependence, which enters indirectly through the top quark mass, has been brought under control through the NLL corrections, calculated in [147]. The corresponding CKM-suppressed decay $B \rightarrow X_d \nu \bar{\nu}$ is related by the ratio of the CKM matrix element squared [102]:

$$\frac{\mathcal{B}(B \rightarrow X_d \nu \bar{\nu})}{\mathcal{B}(B \rightarrow X_s \nu \bar{\nu})} = \left[\frac{|V_{td}|}{|V_{ts}|} \right]^2. \quad (219)$$

Similar relations hold for the ratios of the exclusive decay rates, in which the r.h.s. depends additionally on the ratios of the form factors squared, which deviate from unity through $SU(3)$ -breaking terms, in close analogy with the exclusive radiative decays discussed earlier. These decays are particularly attractive probes of the short-distance physics, as the long-distance contributions are practically absent in such decays. Hence, relations such as the one in (219) provide, in principle, one of the best methods for the determination of the CKM matrix element ratio $|V_{td}|/|V_{ts}|$ [102]. From the practical point of view, however, these decay modes are rather difficult to measure, in particular at the hadron colliders and probably also at the B factories. The best chances are at the Z^0 -decays at LEP, and indeed the present best upper limit is based on the analysis of LEP data [146]. This derived limit [146]

$$\mathcal{B}(B \rightarrow X \nu \bar{\nu}) < 3.9 \times 10^{-4}, \quad (220)$$

will be hard to improve significantly in the foreseeable future. The estimated branching ratios in a number of inclusive and exclusive decay modes are given in Table 2, updating the estimates in [102].

Further down the entries in Table 2 are listed some two-body rare decays, such as $(B_s^0, B_d^0) \rightarrow \gamma\gamma$, studied in [150] - [154], where only the lowest order contributions are calculated, i.e., without any QCD corrections, and the decays $(B_s^0, B_d^0) \rightarrow \ell^+ \ell^-$, studied in the next-to-leading order QCD in [147]. Some of them, in particular, the decays $B_s^0 \rightarrow \mu^+ \mu^-$ and perhaps also the radiative decay $B_s^0 \rightarrow \gamma\gamma$, have a fighting chance to be measured at LHC. The estimated decay rates, which depend on the pseudoscalar coupling constant f_{B_s} (for B_s -decays) and f_{B_d} (for B_d -decays), together with the present experimental bounds are listed in Table 2. Since no QCD corrections have been included in the rate estimates of $(B_s, B_d) \rightarrow \gamma\gamma$, the branching ratios are somewhat uncertain. The constraints on beyond-the-SM physics that will eventually follow from these decays are qualitatively similar to the ones that (would) follow from the decays $B \rightarrow X_s + \gamma$ and $B \rightarrow X_s \ell^+ \ell^-$, which we have discussed at length earlier.

4 An Update of the CKM Matrix

In updating the CKM matrix elements, the Wolfenstein parametrization [14] has been used, which has been given earlier. The emphasis here is on those quantities which

constrain the CKM parameters, λ , A , ρ and η . However, for the sake of completeness we also quote the values for the other elements of the CKM matrix.

We recall that $|V_{us}|$ has been extracted with good accuracy from $K \rightarrow \pi e \nu$ and hyperon decays [3] to be

$$|V_{us}| = \lambda = 0.2205 \pm 0.0018 . \quad (221)$$

This agrees quite well with the determination of $V_{ud} \simeq 1 - \frac{1}{2}\lambda^2$ from β -decay,

$$|V_{ud}| = 0.9744 \pm 0.0010 . \quad (222)$$

The values of the matrix elements involving the charm quark row are: [3]:

$$|V_{cs}| = 1.01 \pm 0.18 ; \quad |V_{cd}| = 0.204 \pm 0.017 \quad (223)$$

The value of the third matrix element involving the charm quark V_{cb} is rather important for the CKM fits, as it determines the parameter A . This has been discussed earlier, yielding:

$$|V_{cb}| = 0.0388 \pm 0.0036 \implies A = 0.80 \pm 0.075 . \quad (224)$$

The other two CKM parameters ρ and η are constrained by the measurements of $|V_{ub}/V_{cb}|$, $|\epsilon|$ (the CP-violating parameter in the kaon system), x_d (B_d^0 - \overline{B}_d^0 mixing) and (in principle) ϵ'/ϵ ($\Delta S = 1$ CP-violation in the kaon system). The constraints from ϵ'/ϵ are not included, due to the various experimental and theoretical uncertainties surrounding it at present. For an up to date review of this topic, we refer to [31], which contains an exhaustive list of references to the original literature on this and other related topics.

The ratio $|V_{ub}/V_{cb}|$ is determined to be:

$$\left| \frac{V_{ub}}{V_{cb}} \right| = 0.08 \pm 0.02 \implies \sqrt{\rho^2 + \eta^2} = 0.36 \pm 0.08 . \quad (225)$$

The experimental value of $|\epsilon|$ is [3]

$$|\epsilon| = (2.26 \pm 0.02) \times 10^{-3} . \quad (226)$$

Theoretically, $|\epsilon|$ is essentially proportional to the imaginary part of the box diagram for K^0 - \overline{K}^0 mixing and is given by [155]

$$\begin{aligned} |\epsilon| = & \frac{G_F^2 f_K^2 M_K M_W^2}{6\sqrt{2}\pi^2 \Delta M_K} \hat{B}_K \left(A^2 \lambda^6 \eta \right) (y_c \{ \hat{\eta}_{ct} f_3(y_c, y_t) - \hat{\eta}_{cc} \} \\ & + \hat{\eta}_{tt} y_t f_2(y_t) A^2 \lambda^4 (1 - \rho)), \end{aligned} \quad (227)$$

where $y_i \equiv m_i^2/M_W^2$, and the functions f_2 and f_3 can be found in Ref. [120]. Here, the $\hat{\eta}_i$ are QCD correction factors, of which $\hat{\eta}_{cc}$ [156] and $\hat{\eta}_{tt}$ [157] were calculated some time ago to next-to-leading order, and $\hat{\eta}_{ct}$ was known only to leading order [158, 159]. Recently, this last renormalization constant was also calculated to next-to-leading order [160]. In the CKM fits published in [83], the following values for the renormalization-scale-invariant coefficients have been used: $\hat{\eta}_{cc} \simeq 1.32$, $\hat{\eta}_{tt} \simeq 0.57$, $\hat{\eta}_{ct} \simeq 0.47$, calculated for $\hat{m}_c = 1.3$ GeV and the NLO QCD parameter $\Lambda_{\overline{MS}} = 310$ MeV in Ref. [160].

The final parameter in the expression for $|\epsilon|$ is the renormalization-scale independent parameter \hat{B}_K , which represents our ignorance of the hadronic matrix element $\langle K^0 | (\bar{d}\gamma^\mu(1 - \gamma_5)s)^2 | \bar{K}^0 \rangle$. The evaluation of this matrix element has been the subject of much work. The earlier results are summarized in Ref. [161]. Some recent calculations of \hat{B}_K using the lattice QCD methods [33] and $1/N_c$ approach [165] are: $\hat{B}_K = 0.83 \pm 0.03$ [Sharpe [162]], $\hat{B}_K = 0.86 \pm 0.15$ [APE Collaboration [163]], $\hat{B}_K = 0.67 \pm 0.07$ [JLQCD Collaboration [164]], $\hat{B}_K = 0.78 \pm 0.11$ [Bernard and Soni [164]], and $\hat{B}_K = 0.70 \pm 0.10$ [Bijnens and Prades [165]].

We now turn to B_d^0 - \bar{B}_d^0 mixing. The present world average of $x_d \equiv \Delta M_d / \Gamma_d$, which is a measure of this mixing, is [167]

$$x_d = 0.71 \pm 0.04 , \quad (228)$$

which is based on time-integrated measurements which directly measure x_d , and on time-dependent measurements which measure the mass difference ΔM_d directly. This is then converted to x_d using the B_d^0 lifetime, which is known very precisely ($\tau(B_d) = 1.56 \pm 0.05$ ps) [69].

From a theoretical point of view it is better to use the mass difference ΔM_d , as it liberates one from the errors on the lifetime measurement. In fact, the present precision on ΔM_d , pioneered by time-dependent techniques at LEP, is quite competitive with the precision on x_d . The LEP average for ΔM_d has been combined with the one from CDF and that derived from time-integrated measurements yielding the present world average [167]

$$\Delta M_d = 0.457 \pm 0.019 \text{ (ps)}^{-1} . \quad (229)$$

The mass difference ΔM_d is calculated from the B_d^0 - \bar{B}_d^0 box diagram. Unlike the kaon system, where the contributions of both the c - and the t -quarks in the loop were important, this diagram is dominated by t -quark exchange:

$$\Delta M_d = \frac{G_F^2}{6\pi^2} M_W^2 M_B \left(f_{B_d}^2 B_{B_d} \right) \hat{\eta}_B y_t f_2(y_t) |V_{td}^* V_{tb}|^2 , \quad (230)$$

where, using Eq. (25), $|V_{td}^* V_{tb}|^2 = A^2 \lambda^6 \left[(1 - \rho)^2 + \eta^2 \right]$. Here, $\hat{\eta}_B$ is the QCD correction. In Ref. [157], this correction is analyzed including the effects of a heavy t -quark. It is found that $\hat{\eta}_B$ depends sensitively on the definition of the t -quark mass, and that, strictly speaking, only the product $\hat{\eta}_B(y_t) f_2(y_t)$ is free of this dependence. In the fits presented here we use the value $\hat{\eta}_B = 0.55$, calculated in the \overline{MS} scheme, following Ref. [157]. Consistency requires that the top quark mass be rescaled from its pole (mass) value to the value $\overline{m}_t(m_t(\text{pole}))$ in the \overline{MS} scheme, which is typically about 10 GeV smaller [62].

For the B system, the hadronic uncertainty is given by $f_{B_d}^2 B_{B_d}$, analogous to \hat{B}_K in the kaon system, except that in this case, also f_{B_d} is not measured. In the CKM fits [83], the following ranges for $f_{B_d}^2 B_{B_d}$ and \hat{B}_{B_d} , which are compatible with results from both lattice-QCD [32, 33, 34] and QCD sum rules [168], were used:

$$\begin{aligned} f_{B_d} &= 180 \pm 50 \text{ MeV} , \\ \hat{B}_{B_d} &= 1.0 \pm 0.2 . \end{aligned} \quad (231)$$

With this theoretical input, one can get an estimate of the CKM matrix element $|V_{td}|$. With ΔM_d known very precisely, and $\Delta m_t/m_t = \pm 6\%$ [8], the error on $|V_{td}|$ is dominated by theoretical error:

$$|V_{td}| = (0.92 \pm 0.02 \pm 0.10 \pm 0.28) \times 10^{-2} . \quad (232)$$

The three errors are from ΔM_d (expt), Δm_t and theory, respectively. Adding the errors in quadrature, this gives

$$|V_{td}| = (0.92 \pm 0.30) \times 10^{-2} , \quad (233)$$

which is better than the range $0.004 \leq |V_{td}| \leq 0.015$ following from unitarity [3].

To complete the estimates of all the nine CKM matrix elements, we list here the determination of $|V_{ts}|/|V_{cb}|$ from the inclusive branching ratio $\mathcal{B}(B \rightarrow X_s + \gamma)$, given in Eq. (166):

$$\frac{|V_{ts}|}{|V_{cb}|} = 0.85 \pm 0.22(\text{expt} + \text{th}), \quad (234)$$

where, like in $|V_{cb}|$, we have added the experimental and theoretical errors linearly. Combining it with $|V_{cb}| = 0.0388 \pm 0.0036$, gives

$$|V_{ts}| = 0.033 \pm 0.009(\text{expt} + \text{th}). \quad (235)$$

A determination of $|V_{tb}|$ can be derived from the CDF measurements Eq. (19). While compatible with the unitarity bound [3]

$$0.9988 \leq |V_{tb}| \leq 0.9995 , \quad (236)$$

the direct determination of $|V_{tb}|$ from CDF is far less accurate. The present knowledge of the nine CKM matrix elements is summarized in Table 3.

4.1 The present profile of the Unitarity Triangle

The entries in Table 3 provide a test of unitarity. Since, the value quoted for $|V_{tb}|$ is from unitarity, the other two constraints are:

$$\begin{aligned} |V_{ud}|^2 + |V_{us}|^2 + |V_{ub}|^2 &= 0.998 \pm 0.002 , \\ |V_{cd}|^2 + |V_{cs}|^2 + |V_{cb}|^2 &= 1.03 \pm 0.18 . \end{aligned} \quad (237)$$

This shows that unitarity is well satisfied. One could now ask the question, how well are the parameters ρ and η determined at present, which in turn determine the profile of the unitarity triangles. This is done by fitting the CKM parameters using the quantities we have discussed.

In order to find the allowed unitarity triangles, the computer program MINUIT was used to fit the CKM parameters A , ρ and η to the experimental values of $|V_{cb}|$, $|V_{ub}/V_{cb}|$, $|\epsilon|$ and x_d . Since λ is very well measured, it was fixed to its central value given above. Two types of fits can be attempted [83]:

- Fit 1: the “experimental fit.” Here, only the experimentally measured numbers are used as inputs to the fit with Gaussian errors; the coupling constants $f_{B_d}\sqrt{\hat{B}_{B_d}}$ and \hat{B}_K are given fixed values.

- Fit 2: the “combined fit.” Here, both the experimental and theoretical numbers are used as inputs assuming Gaussian errors for the theoretical quantities.

We first discuss the “experimental fit” (Fit 1). The goal here is to restrict the allowed range of the parameters (ρ, η) for given values of the coupling constants $f_{B_d}\sqrt{\hat{B}_{B_d}}$ and \hat{B}_K . For each value of \hat{B}_K and $f_{B_d}\sqrt{\hat{B}_{B_d}}$, the CKM parameters A , ρ and η are fit to the experimental numbers given earlier and the χ^2 is calculated. In the CKM fits performed in [83], specific values in the range 0.4 to 1.0 for \hat{B}_K were considered and it was shown that for $\hat{B}_K = 0.4$ a very poor fit to the data is obtained, so that such small values are quite disfavoured. The fits performed in the range $0.6 \leq \hat{B}_K \leq 1.0$, which adequately cover the more recent predictions given above, had a good quality.

In Fit 2 in [83], a central value plus an error to \hat{B}_K was assigned and two ranges for \hat{B}_K were considered:

$$\hat{B}_K = 0.8 \pm 0.2 , \quad (238)$$

which reflects the estimates of this quantity in lattice QCD, or

$$\hat{B}_K = 0.6 \pm 0.2 , \quad (239)$$

which overlaps with the values suggested by the earlier chiral perturbation theory estimates [166]. It was shown that there is not an enormous difference in the results for the two ranges. However, as now there seems to be a theoretical consensus emerging, with $\hat{B}_K \simeq 0.8$, we show the case where $f_{B_d}\sqrt{\hat{B}_{B_d}}$ is varied in the range 130 MeV to 230 MeV. The fits are presented as an allowed region in ρ - η space at 95% C.L. ($\chi^2 = \chi^2_{min} + 6.0$). The results are shown in Fig. 11. As we pass from Fig. 11(a) to Fig. 11(e), the unitarity triangles represented by these graphs become more and more obtuse. Even more striking than this, however, is the fact that the range of possibilities for these triangles is quite large. There are two things to be learned from this. First, our knowledge of the unitarity triangle is at present rather poor. Second, unless our knowledge of hadronic matrix elements improves considerably, measurements of $|\epsilon|$ and x_d , no matter how precise, will not help much in further constraining the unitarity triangle. This is why measurements of CP-violating rate asymmetries in the B system are so important [169, 16]. Being largely independent of theoretical uncertainties, they will allow us to accurately pin down the unitarity triangle. With this knowledge, we could deduce the correct values of \hat{B}_K and $f_{B_d}\sqrt{\hat{B}_{B_d}}$, and thus rule out or confirm different theoretical approaches to calculating these hadronic quantities.

Despite the large allowed region in the ρ - η plane, certain values of \hat{B}_K and $f_{B_d}\sqrt{\hat{B}_{B_d}}$ are disfavoured since they do not provide a good fit to the data. For example, fixing $\hat{B}_K = 0.8$, which is presently theoretically favoured, we can use the fitting program to provide the minimum χ^2 for various values of $f_{B_d}\sqrt{\hat{B}_{B_d}}$. The results are shown in Table 4, along with the best fit values of (ρ, η) . Since we have two variables $(\rho$ and $\eta)$, we use $\chi^2_{min} < 2.0$ as our “good fit” criterion, and we see that $f_{B_d}\sqrt{\hat{B}_{B_d}} < 130$ MeV and $f_{B_d}\sqrt{\hat{B}_{B_d}} > 240$ MeV give poor fits to the existing data.

We now discuss the “combined fit” (Fit 2). Since the coupling constants are not known and the best we have are estimates given in the range in Eq. (238), a reasonable profile of

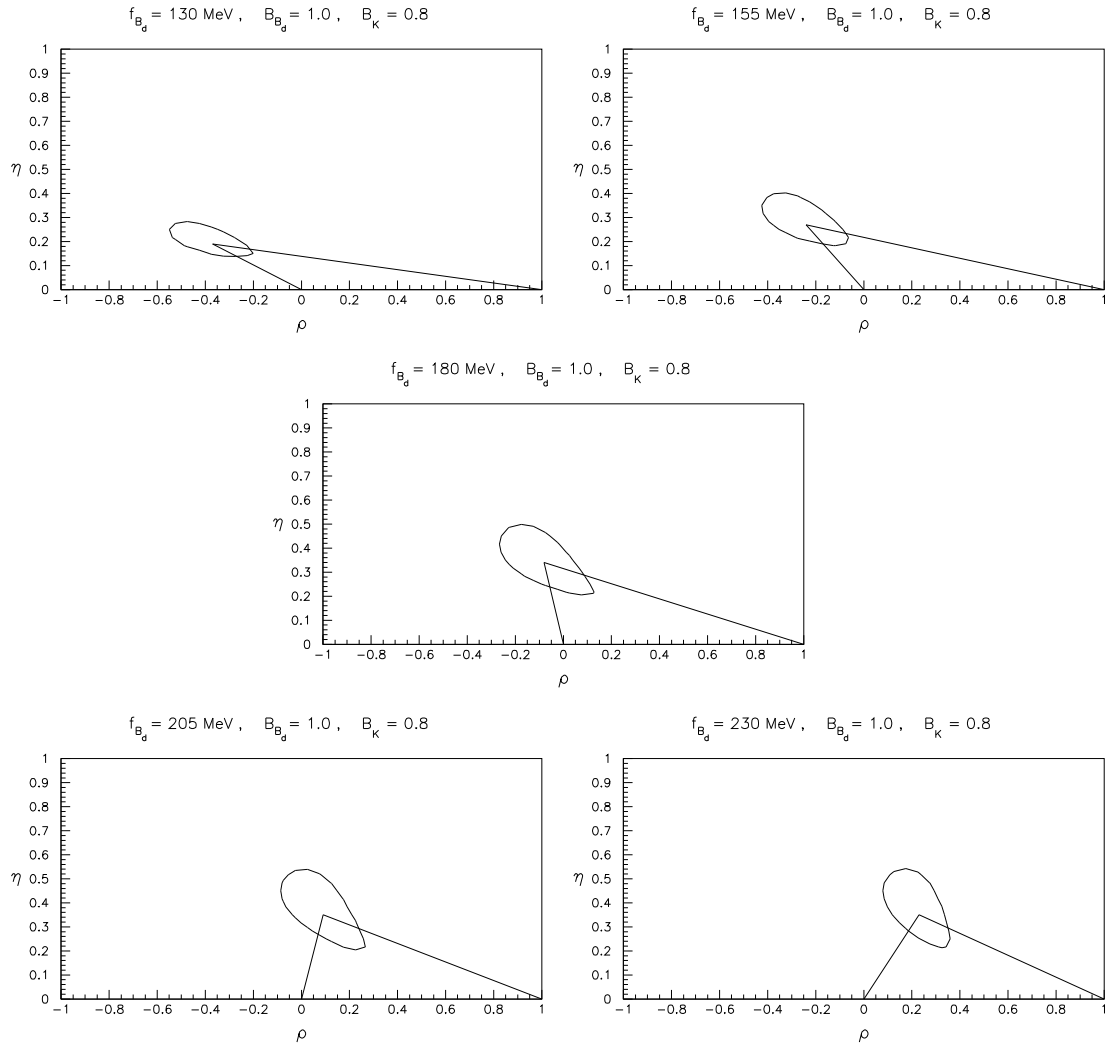


Figure 11: Allowed region in ρ - η space, from a fit to the experimental values given in the text. We have fixed $\hat{B}_K = 0.8$ and vary the coupling constant product $f_{B_d}\sqrt{\hat{B}_{B_d}}$ as indicated on the figures. The solid line represents the region with $\chi^2 = \chi^2_{min} + 6$ corresponding to the 95% C.L. region. The triangles show the best fit. (Figure taken from [83].)

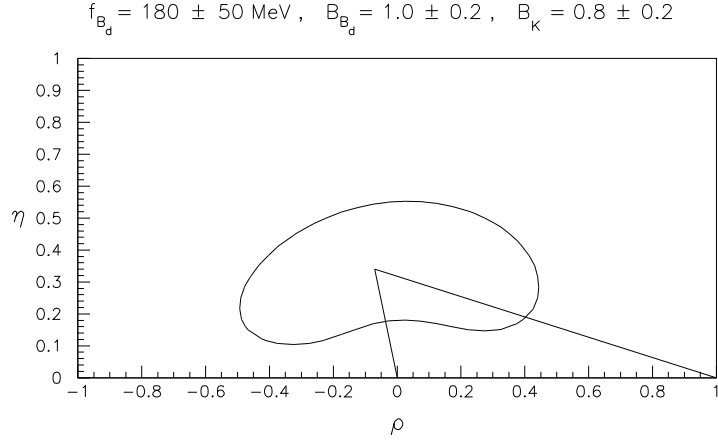


Figure 12: Allowed region in ρ - η space, from a simultaneous fit to both the experimental and theoretical quantities discussed in the text. The theoretical errors are treated as Gaussian for this fit. The solid line represents the region with $\chi^2 = \chi^2_{min} + 6$ corresponding to the 95% C.L. region. The triangle shows the best fit. (Figure taken from [83].)

the unitarity triangle at present can be obtained by letting the coupling constants vary in this range. The resulting CKM triangle region is shown in Fig. 12. As is clear from this figure, the allowed region is rather large at present. The preferred values obtained from the “combined fit” are

$$(\rho, \eta) = (-0.07, 0.34) \quad (\text{with } \chi^2 = 6.6 \times 10^{-2}) . \quad (240)$$

4.2 x_s and the Unitarity Triangle

Mixing in the B_s^0 - $\overline{B_s^0}$ system is quite similar to that in the B_d^0 - $\overline{B_d^0}$ system. The B_s^0 - $\overline{B_s^0}$ box diagram is again dominated by t -quark exchange, and the mass difference between the mass eigenstates ΔM_s is given by a formula analogous to that of Eq. (230):

$$\Delta M_s = \frac{G_F^2}{6\pi^2} M_W^2 M_{B_s} \left(f_{B_s}^2 B_{B_s} \right) \hat{\eta}_{B_s} y_t f_2(y_t) |V_{ts}^* V_{tb}|^2 . \quad (241)$$

Using the fact that $|V_{cb}| = |V_{ts}|$, it is clear that one of the sides of the unitarity triangle, $|V_{td}/\lambda V_{cb}|$, can be obtained from the ratio of ΔM_d and ΔM_s ,

$$\frac{\Delta M_s}{\Delta M_d} = \frac{\hat{\eta}_{B_s} M_{B_s} \left(f_{B_s}^2 B_{B_s} \right)}{\hat{\eta}_{B_d} M_{B_d} \left(f_{B_d}^2 B_{B_d} \right)} \left| \frac{V_{ts}}{V_{td}} \right|^2 . \quad (242)$$

All dependence on the t -quark mass drops out, leaving the square of the ratio of CKM matrix elements, multiplied by a factor which reflects $SU(3)_{\text{flavour}}$ breaking effects. The only real uncertainty in this factor is the ratio of hadronic matrix elements. Whether or not x_s can be used to help constrain the unitarity triangle will depend crucially on

the theoretical status of the ratio $f_{B_s}^2 B_{B_s} / f_{B_d}^2 B_{B_d}$. In what follows, we will take $\xi_s \equiv (f_{B_s} \sqrt{\hat{B}_{B_s}}) / (f_{B_d} \sqrt{\hat{B}_{B_d}}) = (1.16 \pm 0.1)$, consistent with both lattice-QCD [34, 32] and QCD sum rules [168]. (The SU(3)-breaking factor in $\Delta M_s / \Delta M_d$ is ξ_s^2 .)

The mass and lifetime of the B_s meson have now been measured at LEP and Tevatron and their present values are $M_{B_s} = 5370.0 \pm 2.0$ MeV and $\tau(B_s) = 1.55 \pm 0.10$ ps [69]. The QCD correction factor $\hat{\eta}_{B_s}$ is equal to its B_d counterpart, i.e. $\hat{\eta}_{B_s} = 0.55$. The main uncertainty in x_s (or, equivalently, ΔM_s) is now $f_{B_s}^2 B_{B_s}$. Using the determination of A given previously, $\tau_{B_s} = 1.55 \pm 0.10$ (ps) and $\overline{m_t} = 170 \pm 11$ GeV, we obtain

$$\begin{aligned} \Delta M_s &= (13.1 \pm 2.8) \frac{f_{B_s}^2 B_{B_s}}{(230 \text{ MeV})^2} \text{ (ps)}^{-1} , \\ x_s &= (20.3 \pm 4.5) \frac{f_{B_s}^2 B_{B_s}}{(230 \text{ MeV})^2} . \end{aligned} \quad (243)$$

The choice $f_{B_s} \sqrt{\hat{B}_{B_s}} = 230$ MeV corresponds to the central value given by the lattice-QCD estimates, and with this the CKM-fits discussed earlier give $x_s \simeq 20$ as the preferred value in the SM. Allowing the coefficient to vary by $\pm 2\sigma$, and taking the central value for $f_{B_s} \sqrt{\hat{B}_{B_s}}$, this gives

$$\begin{aligned} 11.4 &\leq x_s \leq 29.4 , \\ 7.5 \text{ (ps)}^{-1} &\leq \Delta M_s \leq 18.7 \text{ (ps)}^{-1} . \end{aligned} \quad (244)$$

It is difficult to ascribe a confidence level to this range due to the dependence on the unknown coupling constant factor. In particular, the upper limit is scaling as $[f_{B_s} \sqrt{\hat{B}_{B_s}} / (230 \text{ MeV})]^2$. All one can say is that the standard model predicts large values for x_s , most of which are above the present experimental limit $x_s > 8.8$ (equivalently $\Delta M_s > 6.1 \text{ (ps)}^{-1}$) [126, 167].

The ALEPH lower bound $\Delta M_s > 6.1 \text{ (ps)}^{-1}$ (95% C.L.) [126] and the present world average $\Delta M_d = (0.457 \pm 0.019) \text{ (ps)}^{-1}$ can be used to put a bound on the ratio $\Delta M_s / \Delta M_d$. The lower limit on ΔM_s is correlated with the value of f_s , the fraction of b quark fragmenting into B_s meson, as shown in the ALEPH analysis [126]. The value obtained from the measurement of the quantity $f_s BR(B_s \rightarrow D_s \ell \nu_\ell)$ is $f_s = (11.0 \pm 2.8)\%$. The time-integrated mixing ratios $\bar{\chi}$ and χ_d , assuming maximal mixing in the B_s - \overline{B}_s system $\chi_s = 0.5$, give $f_s = (9.9 \pm 1.9)\%$. The weighted average of these numbers is $f_s = (10.2 \pm 1.6)\%$ [167]. With $f_s = 10\%$, one gets $\Delta M_s > 5.6 \text{ (ps)}^{-1}$ at 95% C.L., yielding $\Delta M_s / \Delta M_d > 11.8$ at 95% C.L. Assuming, however, $f_s = 12\%$ gives $\Delta M_s > 6.1 \text{ (ps)}^{-1}$, yielding $\Delta M_s / \Delta M_d > 12.8$ at 95% C.L. We will use this latter number.

The 95% confidence limit on $\Delta M_s / \Delta M_d$ can be turned into a bound on the CKM parameter space (ρ, η) by choosing a value for the SU(3)-breaking parameter ξ_s^2 . We assume three representative values: $\xi_s^2 = 1.1, 1.35$ and 1.6 , and display the resulting constraints in Fig. 13. From this graph we see that the ALEPH bound marginally restricts the allowed ρ - η region for small values of ξ_s^2 , but does not provide any useful bounds for larger values.

Summarizing the discussion on x_s , we note that the lattice-QCD-inspired estimate $f_{B_s} \sqrt{\hat{B}_{B_s}} \simeq 230$ MeV and the CKM fit predict that x_s lies between 12 and 30, with a

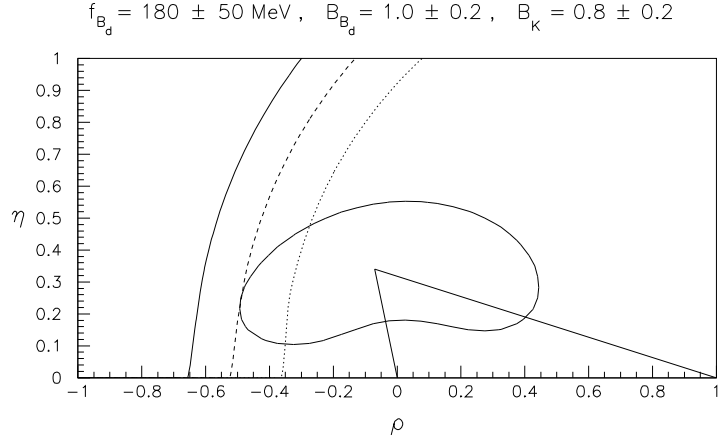


Figure 13: Further constraints in ρ - η space from the ALEPH bound on ΔM_s . The bounds are presented for 3 choices of the SU(3)-breaking parameter: $\xi_s^2 = 1.1$ (dotted line), 1.35 (dashed line) and 1.6 (solid line). In all cases, the region to the left of the curve is ruled out. (Figure taken from [83].)

central value around 20. The upper and lower bounds and the central value scale as $(f_{B_s} \sqrt{\hat{B}_{B_s}}/230 \text{ MeV})^2$. The present constraints from the lower bound on x_s on the CKM parameters are marginal but this would change with improved data. In particular, one expects to reach a sensitivity $x_s \simeq 15$ (or $\Delta M_s \simeq 10 \text{ ps}^{-1}$) at LEP combining all data and tagging techniques [167]. One expects comparable sensitivity at the SLC, where the beam polarization can be used advantageously, and at the HERA-B, CDF and D0 where the B_s mesons will be produced copiously. The entire range for x_s for the SM given in Eq. (244) will be accessible at the LHC. A measurement of x_s (equivalently ΔM_s) would be very helpful in further constraining the CKM parameter space.

5 CP Violation in the B System

This topic has been reviewed in [83], and since only marginal changes have taken place in the experimental situation and our present understanding of CP violation in the B system, we reproduce essentially this discussion here.

It is expected that the B system will exhibit large CP-violating effects, characterized by nonzero values of the angles α , β and γ in the unitarity triangle (Fig. 1) [169]. The most promising method to measure CP violation is to look for an asymmetry between $\Gamma(B^0 \rightarrow f)$ and $\Gamma(\overline{B^0} \rightarrow f)$, where f is a CP eigenstate. If only one weak amplitude contributes to the decay, the CKM phases can be extracted cleanly (i.e. with no hadronic uncertainties). Thus, $\sin 2\alpha$, $\sin 2\beta$ and $\sin 2\gamma$ can in principle be measured in $\overline{B_d} \rightarrow \pi^+ \pi^-$, $\overline{B_d} \rightarrow J/\psi K_S$ and $\overline{B_s} \rightarrow \rho K_S$, respectively.

Unfortunately, the situation is not that simple. In all of the above cases, in addition to the tree contribution, there is an additional amplitude due to penguin diagrams [170]. In general, this will introduce some hadronic uncertainty into an otherwise clean measure-

ment of the CKM phases. In the case of $\overleftrightarrow{B_d} \rightarrow J/\psi K_S$, the penguins do not cause any problems, since the weak phase of the penguin is the same as that of the tree contribution. Thus, the CP asymmetry in this decay still measures $\sin 2\beta$.

For $\overleftrightarrow{B_d} \rightarrow \pi^+ \pi^-$, however, although the penguin is expected to be small with respect to the tree diagram, it will still introduce a theoretical uncertainty into the extraction of α . Fortunately, this uncertainty can be removed by the use of isospin [171]. The key observation is that the $I = 2$ component of the $B \rightarrow \pi\pi$ amplitude is pure tree (i.e., it has no penguin contribution) and therefore has a well-defined CKM phase. By measuring the rates for $B^+ \rightarrow \pi^+ \pi^0$, $B^0 \rightarrow \pi^+ \pi^-$ and $B^0 \rightarrow \pi^0 \pi^0$, as well as their CP-conjugate counterparts, it is possible to isolate the $I = 2$ component and obtain α with no theoretical uncertainty. Thus, even in the presence of penguin diagrams, $\sin 2\alpha$ can in principle be extracted from the decays $B \rightarrow \pi\pi$. It must be admitted, however, that this isospin program is ambitious experimentally. If it cannot be carried out, the error induced on $\sin 2\alpha$ is of order $|P/T|$, where P (T) represents the penguin (tree) diagram. The ratio $|P/T|$ is difficult to estimate – it is dominated by hadronic physics. However, one ingredient is the ratio of the CKM elements of the two contributions: $|V_{tb}^* V_{td}/V_{ub}^* V_{ud}| \simeq |V_{td}/V_{ub}|$. From the fits in [83], the allowed range for the ratio of these CKM matrix elements is

$$1.2 \leq \left| \frac{V_{td}}{V_{ub}} \right| \leq 5.8 , \quad (245)$$

with the central value close to 3.

It is $\overleftrightarrow{B_s} \rightarrow \rho K_S$ which is most affected by penguins. In fact, the penguin contribution is probably larger in this process than the tree contribution. This decay is clearly not dominated by one weak (tree) amplitude, and thus cannot be used as a clean probe of the angle γ . Instead, two other methods have been devised, not involving CP-eigenstate final states. The CP asymmetry in the decay $\overleftrightarrow{B_s} \rightarrow D_s^\pm K^\mp$ can be used to extract $\sin^2 \gamma$ [172]. Similarly, the CP asymmetry in $B^\pm \rightarrow D_{CP}^0 K^\pm$ also measures $\sin^2 \gamma$ [173]. Here, D_{CP}^0 is a D^0 or $\overline{D^0}$ which is identified in a CP-eigenstate mode (e.g. $\pi^+ \pi^-$, $K^+ K^-$, ...).

These CP-violating asymmetries can be expressed straightforwardly in terms of the CKM parameters ρ and η . The 95% C.L. constraints on ρ and η found previously can be used to predict the ranges of $\sin 2\alpha$, $\sin 2\beta$ and $\sin^2 \gamma$ allowed in the standard model. The allowed ranges which correspond to each of the figures in Fig. 11, obtained from Fit 1, are found in Table 5. In this table we have assumed that the angle β is measured in $\overleftrightarrow{B_d} \rightarrow J/\psi K_S$, and have therefore included the extra minus sign due to the CP of the final state.

Since the CP asymmetries all depend on ρ and η , the ranges for $\sin 2\alpha$, $\sin 2\beta$ and $\sin^2 \gamma$ shown in Table 5 are correlated. That is, not all values in the ranges are allowed simultaneously. We illustrate this in Fig. 14, corresponding to the “experimental fit” (Fit 1), by showing the region in $\sin 2\alpha$ - $\sin 2\beta$ space allowed by the data, for various values of $f_{B_d} \sqrt{\hat{B}_{B_d}}$. Given a value for $f_{B_d} \sqrt{\hat{B}_{B_d}}$, the CP asymmetries are fairly constrained. The parameters used in the central figure in Fig. 14, namely $f_{B_d} \sqrt{\hat{B}_{B_d}} = 180$ MeV and $\hat{B}_K = 0.8$, are the best theoretical estimates at present. This figure and the third row in Table 5 then yield: $\sin 2\beta > 0.42$ and $\sin^2 \gamma > 0.68$. However, since there is still considerable uncertainty in the values of the coupling constants, a more reliable profile of

the CP asymmetries at present is given by the “combined fit” (Fit 2) of [83], where present theoretical and experimental values have been convoluted in their allowed ranges. The resulting correlation is shown in Fig. 15. From this figure one sees that the smallest value of $\sin 2\beta$ occurs in a small region of parameter space around $\sin 2\alpha \simeq 0.4\text{--}0.6$. Excluding this small tail, one expects the CP-asymmetry in $\overleftarrow{B_d} \rightarrow J/\Psi K_S$ to be at least 30%.

It may be difficult to extract γ using the techniques described above. First, since $\overleftarrow{B_s} \rightarrow D_s^\pm K^\mp$ involves the decay of B_s mesons, such measurements must be done at hadron colliders. At present, it is still debatable whether this will be possible. Second, the method of using $B^\pm \rightarrow D_{CP}^0 K^\pm$ to obtain γ requires measuring the rate for $B^+ \rightarrow D^0 K^+$. This latter process has an expected branching ratio of $\lesssim O(10^{-6})$, so this too will be hard.

Recently, a new method to measure γ was proposed [174]. Using a flavour SU(3) symmetry, along with the neglect of exchange- and annihilation-type diagrams, it was suggested that γ could be found by measuring rates for the decays $B^+ \rightarrow \pi^0 K^+$, $B^+ \rightarrow \pi^+ K^0$, $B^+ \rightarrow \pi^+ \pi^0$, and their charge-conjugate processes. The πK final states have both $I = 1/2$ and $I = 3/2$ components. The crucial ingredient is that the gluon-mediated penguin diagram contributes only to the $I = 1/2$ final state. Thus, a linear combination of the $B^+ \rightarrow \pi^0 K^+$ and $B^+ \rightarrow \pi^+ K^0$ amplitudes, corresponding to $I = 3/2$ in the πK system, can be related via flavour SU(3) to the purely $I = 2$ amplitude in $B^+ \rightarrow \pi^+ \pi^0$, permitting the construction of an amplitude triangle. The difference in the phase of the $B^+ \rightarrow \pi^+ \pi^0$ side and that of the corresponding triangle for B^- decays was found to be 2γ . SU(3) breaking can be taken into account by including a factor f_K/f_π in relating $B \rightarrow \pi\pi$ decays to the $B \rightarrow \pi K$ decays [175].

The key assumption is that the penguin is mediated by gluon exchange. However, there are also electroweak contributions to the penguins [176]. These electroweak penguins (EWP’s) are not constrained to be isosinglets. Thus, in the presence of EWP’s, there is no longer a triangle relation $B \rightarrow \pi K$ and $B \rightarrow \pi\pi$ amplitudes [177]. Indeed, electroweak penguins can, in principle, even invalidate the isospin analysis in $B \rightarrow \pi\pi$, since the $I = 2$ amplitude will include a contribution from EWP’s, and hence will no longer have a well-defined weak CKM phase. However, theoretical estimates [177, 178] show that electroweak penguins are expected to be relatively unimportant for $B \rightarrow \pi\pi$.

The question of the size of EWP’s has therefore become a rather interesting question, and a number of papers have recently appeared discussing this issue [179]. These include both theoretical predictions, as well as ways of isolating EWP’s experimentally. The general consensus is that EWP’s are large enough to invalidate the method of Ref. [174] for obtaining γ . However, two new methods making use of the flavour SU(3) symmetry, and which do not have any problems with electroweak penguins, have been suggested. Both are rather complicated, making use of the isospin quadrangle relation among $B \rightarrow \pi K$ decays, as well as $B^+ \rightarrow \pi^+ \pi^0$ plus an additional decay: $B_s \rightarrow \eta \pi^0$ in one case [178], $B^+ \rightarrow \eta K^+$ with $\eta = \eta_8$ in the other [180]. Although electroweak penguins do not cause problems, SU(3)-breaking effects which cannot be parametrized simply as a ratio of decay constants are likely to introduce errors of about 25% into both methods. It is clear that this is a subject of great interest at the moment, and work will no doubt continue. Recently, another quadrangle relation involving charged B decays $B^+ \rightarrow \eta K^+$ and $B^+ \rightarrow \eta' K^+$ along with the decays $B^+ \rightarrow \pi^+ K^0$ and $B^+ \rightarrow \pi^0 K^+$ has been proposed

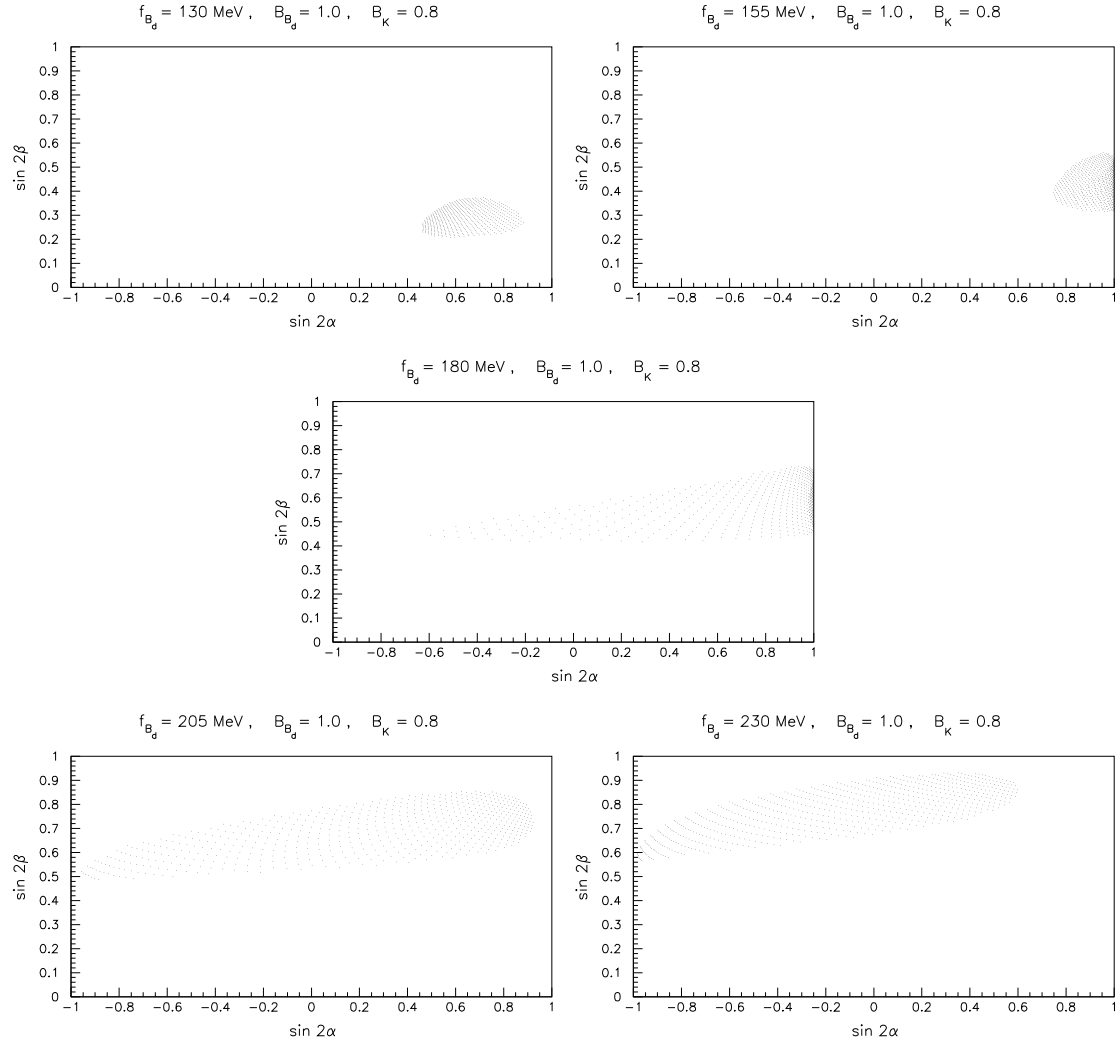


Figure 14: Allowed region of the CP asymmetries $\sin 2\alpha$ and $\sin 2\beta$ resulting from the “experimental fit” of the data for different values of the coupling constant $f_{B_d}\sqrt{\hat{B}_{B_d}}$ indicated on the figures a) – e). We fix $\hat{B}_K = 0.8$. (Figure taken from [83].)

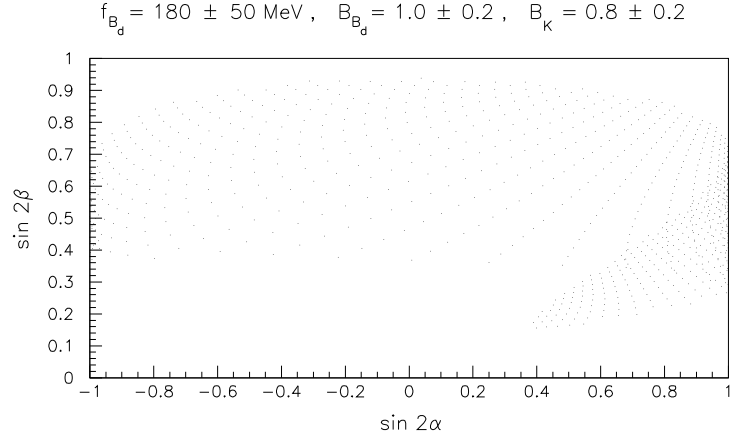


Figure 15: Allowed region of the CP asymmetries $\sin 2\alpha$ and $\sin 2\beta$ resulting from the “combined fit” of the data for the ranges for $f_{B_d}\sqrt{\hat{B}_{B_d}}$ and \hat{B}_K given in the text. (Figure taken from [83].)

to determine the weak phase γ [181].

5.1 Summary of the CKM fits and CP asymmetries in B Decays

We summarize the results of this section:

(i) We have presented an update of the CKM unitarity triangle using the theoretical and experimental improvements in the following quantities: $|V_{cb}|$, $|V_{ub}/V_{cb}|$, ΔM_d , $\tau(B_d)$, $\overline{m_t}$, $\hat{\eta}_{cc}$, $\hat{\eta}_{ct}$. The fits can be used to exclude extreme values of the pseudoscalar coupling constants, with the range $130 \text{ MeV} \leq f_{B_d}\sqrt{\hat{B}_{B_d}} \leq 270 \text{ MeV}$ still allowed for $\hat{B}_K = 1$. The lower limit of this range is quite \hat{B}_K -independent, but the upper limit is strongly correlated with the value chosen for \hat{B}_K . For example, for $\hat{B}_K = 0.8$ and 0.6 , $f_{B_d}\sqrt{\hat{B}_{B_d}} \leq 240$ and 210 MeV , respectively, is required for a good fit. The solutions for $\hat{B}_K = 0.8 \pm 0.2$ are slightly favoured by the data as compared to the lower values. These numbers are in very comfortable agreement with QCD-based estimates from sum rules and lattice techniques, and recently also with estimates from improved chiral perturbation theory. The statistical significance of the fit is, however, not good enough to determine the coupling constant more precisely. The fits in [83] show that $\hat{B}_K \leq 0.4$ is strongly disfavoured by the data, since the quality of fit for such values is very poor. This value of \hat{B}_K is now of very little theoretical interest, anyway.

(ii) The newest experimental and theoretical numbers restrict the allowed CKM unitarity triangle in the (ρ, η) -space somewhat more than before. However, the present uncertainties are still enormous – despite the new, more accurate experimental data, our knowledge of the unitarity triangle is still poor. This underscores the importance of measuring CP-violating rate asymmetries in the B system. Such asymmetries are largely independent of theoretical hadronic uncertainties, so that their measurement will allow us to accurately pin down the parameters of the CKM matrix. Furthermore, unless our

knowledge of the pseudoscalar coupling constants improves considerably, better measurements of such quantities as x_d will not help much in constraining the unitarity triangle. On this point, help may come from the experimental front. It may be possible to measure the parameter f_{B_d} , using isospin symmetry, via the charged-current decay $B_u^\pm \rightarrow \tau^\pm \nu_\tau$. With $|V_{ub}/V_{cb}| = 0.08 \pm 0.02$ and $f_{B_d} = 180 \pm 50$ MeV, one gets a branching ratio $BR(B_u^\pm \rightarrow \tau^\pm \nu_\tau) = (1.5\text{--}14.0) \times 10^{-5}$, with a central value of 5.2×10^{-5} . This lies in the range of the future LEP and asymmetric B -factory experiments, though at LEP the rate $Z \rightarrow B_c X \rightarrow \tau^\pm \nu_\tau X$ could be just as large as $Z \rightarrow B^\pm X \rightarrow \tau^\pm \nu_\tau X$. Along the same lines, the prospects for measuring (f_{B_d}, f_{B_s}) in the FCNC leptonic and photonic decays of B_d^0 and B_s^0 hadrons, $(B_d^0, B_s^0) \rightarrow \mu^+ \mu^-$, $(B_d^0, B_s^0) \rightarrow \gamma \gamma$ in future B physics facilities are not entirely dismal.

(iii) We have determined bounds on the ratio $|V_{td}/V_{ts}|$ from our fits. For $130 \text{ MeV} \leq f_{B_d} \sqrt{\hat{B}_{B_d}} \leq 270 \text{ MeV}$, i.e. in the entire allowed domain, at 95 % C.L. we find

$$0.13 \leq \left| \frac{V_{td}}{V_{ts}} \right| \leq 0.35 . \quad (246)$$

The upper bound from our analysis is more restrictive than the current experimental upper limit following from the CKM-suppressed radiative penguin decays $BR(B \rightarrow \omega + \gamma)$ and $BR(B \rightarrow \rho + \gamma)$, which at present yield at 90% C.L. [54]

$$\left| \frac{V_{td}}{V_{ts}} \right| \leq 0.64 - 0.75 , \quad (247)$$

depending on the model used for the SU(3)-breaking in the relevant form factors [121, 122]. Long-distance effects in the decay $B^\pm \rightarrow \rho^\pm + \gamma$ may introduce theoretical uncertainties comparable to those in the SU(3)-breaking part but the corresponding effects in the decays $B^0 \rightarrow (\rho^0, \omega) + \gamma$ are expected to be very small [124]. Furthermore, the upper bound is now as good as that obtained from unitarity, which gives $0.08 \leq |V_{td}/V_{ts}| \leq 0.36$, but the lower bound from our fit is more restrictive.

(iv) Using the measured value of m_t , we find

$$x_s = (20.3 \pm 4.5) \frac{f_{B_s}^2 B_{B_s}}{(230 \text{ MeV})^2} . \quad (248)$$

Taking $f_{B_s} \sqrt{\hat{B}_{B_s}} = 230$ (the central value of lattice-QCD estimates), and allowing the coefficient to vary by $\pm 2\sigma$, this gives

$$11.4 \leq x_s \leq 29.4 . \quad (249)$$

No reliable confidence level can be assigned to this range – all that one can conclude is that the SM predicts large values for x_s , most of which lie above the ALEPH 95% C.L. lower limit of $x_s > 8.8$.

(v) The ranges for the CP-violating rate asymmetries parametrized by $\sin 2\alpha$, $\sin 2\beta$ and $\sin^2 \gamma$ are determined at 95% C.L. to be

$$\begin{aligned} -1.0 &\leq \sin 2\alpha \leq 1.0 , \\ 0.21 &\leq \sin 2\beta \leq 0.93 , \\ 0.12 &\leq \sin^2 \gamma \leq 1.0 . \end{aligned} \quad (250)$$

(For $\sin 2\alpha < 0.4$, we find $\sin 2\beta \geq 0.3$.) Electroweak penguins may play a significant role in some methods of extracting γ . Their magnitude, relative to the tree contribution, is therefore of some importance. One factor in determining this relative size is the ratio of CKM matrix elements $|V_{td}/V_{ub}|$. We find

$$1.2 \leq \left| \frac{V_{td}}{V_{ub}} \right| \leq 5.8 . \quad (251)$$

6 Acknowledgements

I would like to thank Patricia Ball, Vladimir Braun, Gian Giudice, Marco Ciuchini, Christoph Greub, L. Handoko, Marek Jezabek, Boris Kayser, David London, Guido Martinelli, Tak Morozumi, Jon Rosner, Hubert Simma, Amarjit Soni and Arkady Vainshtein for helpful discussions. I also thank Vladimir Braun, Christoph Greub and Jon Rosner for reading the manuscript and for suggesting many improvements. The help of Patricia Ball for providing Figure 2 and Christoph Greub for providing Figures 3 and 4 is acknowledged. I am grateful to Gudrun Hiller, L. Handoko and Tak Morozumi for allowing me to include Figures 9 and 10 based on our joint paper [140] prior to its publication. Informative discussions on experimental issues with Roy Aleksan, Klaus Honscheid, Tatsuya Nakada, Henning Schröder, Tomasz Skwarnicki, Paris Sphicas and Ed Thorndike are also gratefully acknowledged. Finally, I would like to thank the organizers of the Nathiagali summer college, in particular its patron, Dr. Ishfaq Ahmed, the Co-Director of the college, Professor Riazuddin, and its scientific secretary, Dr. K.A. Shoaib, for their warm hospitality, scientific coordination and a great stay in the Murree hill tracts. These lectures are dedicated to Professor Abdus Salam on his 70th birthday.

References

- [1] S.L. Glashow, Nucl. Phys. **22** (1961) 579; S. Weinberg, Phys. Rev. Lett. **19** (1967) 1264; A. Salam, in *Elementary Particle Theory*, ed. N. Svartholm (Almqvist and Wiksell, Stockholm) (1968).
- [2] See, for example, L.B. Okun, Leptons and Quarks (Elsevier Science Publishers B.V., Amsterdam) (1984).
- [3] L. Montanet et al. (Particle Data Group), Phys. Rev. **D50** (1994) 1173.
- [4] The LEP Collaborations ALEPH, DELPHI, L3, OPAL and the LEP Electroweak Group, preprint CERN-PPE/95-172 (1995).
- [5] F. Abe et al. (CDF Collaboration), Phys. Rev. Lett. **74** (1995) 2626; S. Abachi et al. (D0 Collaboration), Phys. Rev. Lett. **74** (1995) 2632.
- [6] P. Bamert et al., preprint McGill-96/04; UdeM-GPP-TH-96-34; WIS-96/09 (1996) [hep-ph/9602438].
- [7] Working Group Report on the Determination of the Mass of the W Boson, Conveners: Z. Kunszt and W.J. Stirling, preprint hep-ph/9602352, to appear in: Physics at LEP2, Vol. 1 (eds. G. Altarelli, T. Sjostrand and F. Zwirner) (1996).
- [8] Th. Müller, Plenar Vortrag auf der Frühjahrstagung 1996 der deutschen Physikalischen Gesellschaft - Sektion Teilchenphysik, Hamburg, FRG, März 18-21, 1996.
- [9] A.L. Kagan, Phys. Rev. **D51** (1995) 6196; L. Roszkowski and M. Shifman, Phys. Rev. **D53** (1996) 404.
- [10] M. Kobayashi and K. Maskawa, Prog. Theor. Phys. **49** (1973) 652.
- [11] N. Cabibbo, Phys. Rev. Lett. **10** (1963) 531.
- [12] S.L. Glashow, J. Iliopoulos and L. Maiani, Phys. Rev. **D2** (1970) 1285.
- [13] F. Abe et al. (CDF Collaboration), FERMILAB-CONF-95-237-E (1995).
- [14] L. Wolfenstein, Phys. Rev. Lett. **51** (1983) 1945.
- [15] A.J. Buras and G. Buchalla, Phys. Lett. **B336** (1994) 263.
- [16] R. Aleksan, B. Kayser and D. London, Phys. Rev. Lett. **73** (1994) 18.
- [17] C. Jarlskog, Phys. Rev. Lett. **55** (1985) 1039; Z. Phys. **C29** (1985) 491; and in *CP Violation*, ed. C. Jarlskog (World Scientific, Singapore) (1989) 3.

- [18] V.A. Rubakov and M.E. Shaposhnikov, preprint CERN-TH/96-13; INR-913/96 [hep-ph/9603208]; to appear in Andrei Sakharov's 75th anniversary memorial volume, *Ups. Fiz. Nauk*, vol. 166, No. 5, 1996).
- [19] N. Cabibbo and L. Maiani, *Phys. Lett.* **B79** (1978) 109.
- [20] M. Suzuki, *Nucl. Phys.* **B145** (1978) 420.
- [21] A. Ali and E. Pietarinen, *Nucl. Phys.* **B154** (1979) 519.
- [22] G. Altarelli et al., *Nucl. Phys.* **B208** (1982) 365.
- [23] Q. Hokim and X.Y. Pham, *Phys. Lett.* **B122** (1983) 297.
- [24] A. Falk et al., *Phys. Lett.* **B 326** (1994) 145; A. Czarnecki, M. Jezabek, and J.H. Kühn, *Phys. Lett.* **B 346** (1995) 335.
- [25] M. Jezabek and J.H. Kühn, *Nucl. Phys.* **B320** (1989) 20.
- [26] R.E. Behrends, R.J. Finkelstein and A. Sirlin, *Phys. Rev.* **101** (1956) 866; S.M. Berman, *Phys. Rev.* **112** (1958) 267; T. Kinoshita and A. Sirlin, *Phys. Rev.* **113** (1959) 1652.
- [27] G. Altarelli and L. Maiani, *Phys. Lett.* **B52** (1974) 351; M.K. Gaillard and B.W. Lee, *Phys. Rev. Lett.* **33** (1974) 108.
- [28] A. I. Vainshtein, V.I. Zakharov and M.A. Shifman, *JETP* **45** (1977) 670.
- [29] G. Altarelli et al., *Phys. Lett.* **B99** (1981) 141; *Nucl. Phys.* **B187** (1981) 461.
- [30] A.J. Buras and P.H. Weisz, *Nucl. Phys.* **B333** (1990) 66.
- [31] G. Buchalla, A.J. Buras, and M.E. Lautenbacher, MPI-Ph/95-104; TUM-T31-100/95; FERMILAB-PUB-95/305-T; SLAC-PUB 7009; [hep-ph/9512380].
- [32] C. Michael, preprint [hep-ph/9510203], to appear in: *Proc. of the 17th Int. Symp. on Lepton and Photon Interactions*, Beijing, P.R. China, August 1995.
- [33] A. Soni, preprint [hep-lat/9510036] (1995).
- [34] J. Shigemitsu, in: *Proc. of the XXVII Int. Conf. on High Energy Physics*, Glasgow, Scotland, July 1994, edited by P.J. Bussey and I.G. Knowles (IOP Publications Ltd., Bristol, 1995) 135.
- [35] M. Shifman, A. Vainshtein and V.I. Zakharov, *Nucl. Phys.* **B147** (1979) 385, 448.
- [36] V.M. Braun, preprint NORDITA-95-69-P (1995) [hep-ph/9510404], to appear in: *Proc. of the Int. Europhys. Conf. on High Energy Physics*, Brussels, Belgium, Jul 27-31, 1995.

- [37] H.D. Politzer and M. Wise, Phys. Lett. **B206** (1988) 681; *ibid.* **B208** (1988) 504; M. Voloshin and M. Shifman, Sov. J. Nucl. Phys. **45** (1987) 292; *ibid.* **47** (1988) 511; E. Eichten and B. Hill, Phys. Lett. **B234** (1990) 511; H. Georgi, Phys. Lett. **B240** (1990) 447; B. Grinstein, Nucl. Phys. **B339** (1990) 253.
- [38] N. Isgur and M. Wise, Phys. Lett. **B232** (1989) 113; *ibid.* **B237** (1990) 527.
- [39] J. Chay, H. Georgi and B. Grinstein, Phys. Lett. **B247** (1990) 399.
- [40] I. Bigi, N. Uraltsev and A. Vainshtein, Phys. Lett. **B293** (1992) 430; [E: **B297** (1993) 477]; B. Blok and M. Shifman, Nucl. Phys. **B399** (1993) 441, *ibid.* 459; I. Bigi et al., Phys. Rev. Lett. **71** (1993) 496 and in: Proc. of the Annual Meeting of the Division of Particles and Fields of the APS, Batavia, Illinois, 1992, edited by C. Albright et al. (World Scientific, Singapore), 610.
- [41] A.V. Manohar and M.B. Wise, Phys. Rev. **D49** (1994) 1310.
- [42] B. Blok et al., Phys. Rev. **D49** (1994) 3356 [E: **D50** (1994), 3572].
- [43] I. Bigi et al., in: B Decays, edited by S. Stone, Second Edition (World Scientific, Singapore, 1994) 132; I. Bigi, preprint UND-HEP-95-BIG02 (1995) [hep-ph/9508408].
- [44] H. Georgi, in Proceedings of TASI 1991, Boulder, Colorado, 1991, edited by R.K. Ellis, C.T. Hill and J.D. Lykken (World Scientific, Singapore, 1992) p. 589.
- [45] M. Neubert, Phys. Rep. **245** (1994) 259.
- [46] N. Isgur and M.B. Wise, in: B Decays, edited by S. Stone, Second Edition (World Scientific, Singapore, 1994) 231.
- [47] M. Shifman, preprint TPI-MINN-95/15-T, [hep-ph/9505289]; to appear in: Proc. of the V Int. Symp. on Particles, Strings and Cosmology - PASCOS-, Johns Hopkins University, Baltimore, USA, March 22 - 25, 1995.
- [48] A. Vainshtein, preprint TPI-MINN-95/34-T [hep-ph/9512419]; to appear in Proc. of the Int. Europhys. Conf. on High Energy Physics, Brussels, Belgium, Jul 27-31, 1995
- [49] M. Neubert, preprint CERN-TH/95-307 (1995) [hep-ph/9511409], to appear in Proc. of the 17th Int. Symp. on Lepton and Photon Interactions, Beijing, P.R. China, August 1995; CERN-TH/96-55 [hep-ph/9604412].
- [50] For an exhaustive discussion of relativistic kinematics, see the classic book by E. Byckling and K. Kajantie: Particle Kinematics (John Wiley & Sons, New York) (1972).

- [51] E. Bagan, P. Ball, V.M. Braun, and P. Gosdzinsky, Nucl. Phys. **B432** (1994) 3.
- [52] E. Bagan, P. Ball, V.M. Braun, and P. Gosdzinsky, Phys. Lett. **B342** (1995) 362 [E: to appear in Phys. Lett. B].
- [53] E. Bagan, P. Ball, B. Fiol, and P. Gosdzinsky, Phys. Lett. **B351** (1995) 546.
- [54] T. Skwarnicki, preprint [hep-ph/9512395], to appear in: Proc. of the 17th Int. Symp. on Lepton Photon Interactions, Beijing, P.R. China, August 1995.
- [55] S. Bertolini, F. Borzumati, A. Masiero, and G. Ridolfi, Nucl. Phys. **B353** (1991) 591.
- [56] M. Ciuchini, E. Gabrielli, and G.F. Giudice, preprint CERN-TH-96/73 [hep-ph/9604438].
- [57] N.G. Deshpande and X.-G. He, Phys. Lett. **B336** (1994) 471; and in Proc. of the XXVII Int. Conf. on High Energy Physics, Glasgow, Scotland, July 1994, edited by P.J. Bussey and I.G. Knowles (IOP Publications Ltd., Bristol, 1995) 1311.
- [58] P. Ball and V.M. Braun, Phys. Rev. **D49** (1994) 2472; V. Eletsky and E. Shuryak, Phys. Lett. **B276** (1992) 191; M. Neubert, Phys. Lett. **B322** (1994) 419.
- [59] P. Ball and V.M. Braun in [58].
- [60] A. Ali and C. Greub, Phys. Lett. **B361** (1995) 146.
- [61] M. Gremm, A. Kapustin, Z. Ligeti, and M.B. Wise, preprint CALT-68-2043; [hep-ph/9603314]. See also, D.S. Hwang, C.S. Kim, and W. Namgung, preprint KEK-TH-473 (1996) [hep-ph/9604225].
- [62] N. Gray, D.J. Broadhurst, W. Grafe, and K. Schilcher, Z. Phys. **C48** (1990) 673.
- [63] H. Leutwyler, preprint CERN-TH/96-25 [hep-ph/9602255].
- [64] M. Neubert and C.T. Sachrajda, preprint CERN-TH/96-19; SHEP 96-03 [hep-ph/9603202].
- [65] G. Altarelli, G. Martinelli, S. Petrarca, and F. Rapuano, preprint CERN-TH/96-77 (1996) [hep-ph/9604202].
- [66] M. Luke, M. Savage, and M.B. Wise, Phys. Lett. **B343** (1995) 329.
- [67] P. Ball, M. Beneke, and V.M. Braun, Phys. Rev. **D52** (1995) 3929.
- [68] S. Brodsky, G.P. Lepage, and P.B. Mackenzie, **Phys. Rev. D28** (1983) 228.
- [69] I.J. Kroll, preprint FERMILAB-CONF-96-032 [hep-ph/9602005], to appear: in Proc. of the 17th Int. Symp. on Lepton and Photon Interactions, Beijing, P.R. China, August 1995.

- [70] G. Apollinari (CDF Collaboration), presented at the Aspen Winter Conference on Particle Physics, Aspen, Colorado, January 1966 [URL: <http://www-cdf.fnal.gov/physics/new/bottom/cdf3395/>].
- [71] N.G. Uraltsev, preprint CERN-TH-96-40 (1996) [hep-ph/9602324].
- [72] J. Rosner, preprint CERN-TH-96/24; EFI-96-03 [hep-ph/9602265].
- [73] B. Guberina et al., Phys. Lett. **B89** (1979) 811.
- [74] P. Abreu et al. (DELPHI Collaboration), preprint DELPHI 95-107 PHYS 542 (1995); to appear in Proc. of the Int. Europhys. Conf. on High Energy Physics, Brussels, Belgium, Jul 27-31, 1995.
- [75] P. Colangelo and F. De Fazio, preprint BARI-TH/96-230 [hep-ph/9604425].
- [76] M.E. Luke, Phys. Lett. **B252** (1990) 447.
- [77] C.G. Boyd and D.E. Brahm, Phys. Lett. **B257** (1991) 393.
- [78] M. Neubert and V. Rieckert, Nucl. Phys. **B382** (1992) 97; M. Neubert, Phys. Lett. **B264** (1991) 455, Phys. Rev. **D46** (1992) 2212.
- [79] M.B. Voloshin and M.A. Shifman, Sov. J. Nucl. Phys. **45** (1987) 292.
- [80] M. Neubert, preprint CERN-TH/95-107 [hep-ph/9505238], to appear in Proc. of 30th Rencontres de Moriond: Electroweak Interactions and Unified Theories, Meribel les Allues, March 11 - 18, 1995.
- [81] A. Czarnecki, Phys. Rev. Lett. **76** (1996) 4124.
- [82] Sheldon Stone (private communication).
- [83] A. Ali and D. London, preprint DESY 95-148, UdeM-GPP-TH-95-32 [hep-ph/9508272], to appear in Proc. of the 6th Int. Symp. on Heavy Flavour Physics, Pisa, June 6 -9, 1995.
- [84] The impact of the ARGUS results on elementary particle physics is summarized recently in H. Albrecht et al. (ARGUS Collaboration), preprint DESY 96-015 (1996), which contains references to the original literature.
- [85] C.G. Boyd, B. Grinstein and R.F. Lebed, Phys. Lett. **B353** (1995) 306; Nucl. Phys. **B461** (1996) 493.
- [86] J. Bartelt et al. (CLEO Collaboration), Phys. Rev. Lett. **64** (1990) 16.
- [87] E. Thorndike, in Proc. of the Int. Europhys. Conf. on High Energy Physics, Brussels, Belgium, Jul 27-31, 1995; R. Ammar et al. (CLEO Collaboration), contributed paper to this conference (EPS-0165) (1995).
- [88] N. Isgur, D. Scora, B. Grinstein, and M. Wise, Phys. Rev. **D39** (1989) 799.

[89] P. Ball and V.M. Braun, preprint CERN-TH/96-12, NORDITA-96-10-P [hep-ph/9602323], and private communication.

[90] M.S. Alam et al. (CLEO Collaboration), Phys. Rev. Lett. **74** (1995) 2885.

[91] R. Ammar et al. (CLEO Collaboration), Phys. Rev. Lett. **71** (1993) 674.

[92] T. Inami and C.S. Lim, Prog. Theor. Phys. **65** (1981) 297.

[93] S. Bertolini, F. Borzumati and A. Masiero, Phys. Rev. Lett. **59** (1987) 180; R. Grigjanis et al., Phys. Lett. **B213** (1988) 355; B. Grinstein, R. Springer, and M.B. Wise, Phys. Lett. **202** (1988) 138; Nucl. Phys. **B339** (1990) 269; G. Cella et al., Phys. Lett. **B248** (1990) 181.

[94] M. Ciuchini et al., Phys. Lett. **B316** (1993) 127; Nucl. Phys. **B415** (1994) 403; G. Cella et al., Phys. Lett. **B325** (1994) 227; M. Misiak, Nucl. Phys. **B393** (1993) 23; [E. **B439** (1995) 461].

[95] A. Ali and C. Greub, Z. Phys. **C49** (1991) 431; Phys. Lett. **B259** (1991) 182.

[96] A. Ali and C. Greub, Phys. Lett. **B287** (1992) 191.

[97] A. Ali and C. Greub, Z. Phys. **C60** (1993) 433.

[98] N. Pott, preprint TUM-T31-93/95 [hep-ph/9512252].

[99] K. Adel and Y.-p. Yao, Phys. Rev. **D49** (1994) 4945.

[100] C. Greub, T. Hurth and D. Wyler, preprints SLAC-PUB-96-7113, ZU-TH/2/1996 [hep-ph/9602281] and SLAC-PUB-96-7144 [hep-ph-9603404].

[101] A.J. Buras, M. Misiak, M. Münz, and S. Pokorski, Nucl. Phys. **B424** (1994) 374.

[102] A. Ali, C. Greub and T. Mannel, DESY Report 93-016 (1993), and in B-Physics Working Group Report, ECFA Workshop on a European B-Meson Factory, ECFA 93/151, DESY 93-053 (1993), edited by R. Aleksan and A. Ali.

[103] M. Ciuchini et al., Phys. Lett. **B334** (1994) 137.

[104] D. Atwood, B. Blok, and A. Soni, preprint TECHNION-PH-94-11 (1994) [hep-ph-9408373]; H.-Y. Cheng, preprint IP-ASTP-23-94 [hep-ph-9411330] (1994); J.M. Soares, Phys. Rev. **D53** (1996) 241; J. Milana, Phys. Rev. **D53** (1996) 1403; G. Eilam, A. Ioannissian, and R.R. Mendel, preprint TECHNION-PH-95-4 [hep-ph-9505222].

[105] Cheng in [104].

[106] N.G. Deshpande, X.-G. He, and J. Trampetic, Phys. Lett. **B367** (1996) 362.

- [107] E. Golowich and S. Pakvasa, Phys. Rev. **D51**, 1215 (1995).
- [108] G. Ricciardi, Phys. Lett. **B355** (1995) 313.
- [109] M. Bauer, B. Stech, and M. Wirbel, Z. Phys. **C34** (1987) 103.
- [110] T.E. Browder and K. Honscheid, Prog. Part. Nucl. Phys. **35** (1995) 81.
- [111] A. Ali and C. Greub, to be published.
- [112] G. Korchemsky and G. Sterman, Phys. Lett. **B340** (1994) 96.
- [113] R.D. Dikeman, M. Shifman, and R.G. Uraltsev, Int. J. Mod. Phys. **A11** (1996) 571.
- [114] V. Sudakov, Sov. Phys. JETP **3** (1956) 65 ;
G. Altarelli, Phys. Rep. **81** (1982) 1.
- [115] A. Kapustin, Z. Ligeti and H.D. Politzer, Phys. Lett. **B357** (1995) 653.
- [116] M. Neubert, Phys. Rev. **D49** (1994) 4623.
- [117] I. Bigi et al., Phys. Rev. Lett. **71**, (1993) 496; Int. J. Mod. Phys. **A9**, 2467 (1994).
- [118] R. Jaffe and L. Randall, Nucl. Phys. **B412** (1994) 79.
- [119] E. Bagan, P. Ball, V.M. Braun, and H.G. Dosch, Phys. Lett. **B278**, 457 (1992).
- [120] A. Ali and D. London, Z. Phys. **C65** (1995) 431.
- [121] A. Ali, V.M. Braun and H. Simma, Z. Phys. **C63** (1994) 437.
- [122] P. Ball, TU-München Report TUM-T31-43/93 (1993);
P. Colangelo et al., Phys. Lett. **B317** (1993) 183;
S. Narison, Phys. Lett. **B327** (1994) 354;
J. M. Soares, Phys. Rev. **D49** (1994) 283.
- [123] A. Khodzhamirian, G. Stoll, and D. Wyler, Phys. Lett. **B358** (1995) 129.
- [124] A. Ali and V.M. Braun, Phys. Lett. **B359** (1995) 223.
- [125] I.I. Balitsky, V.M. Braun, and A.V. Kolesnichenko, Nucl. Phys. **312** (1989) 509.
- [126] D. Buskulic et al. (ALEPH Collaboration), Phys. Lett. **B356** (1995) 409.
- [127] J. Hewett, Phys. Rev. Lett. **70** (1993) 1045, SLAC-PUB-6521 (1994) [hep-ph/9406302];
V. Barger, M.S. Berger, and R.J.N. Phillips, Phys. Rev. Lett. **70** (1993) 1368;
T. Hayashi, M. Matsuda, and M. Tanimoto, Prog. Theor. Phys. **89** (1993) 1047;
T.G. Rizzo, Phys. Rev. **D50** (1994) 3303.

[128] R. Barbieri and G.F. Giudice, Phys. Lett. **B309** (1993) 86;
 N. Oshimo, Nucl. Phys. **B404** (1993) 20;
 R. Garisto and J.N. Ng, Phys. Lett. **B315** (1993) 372;
 M.A. Diaz, Phys. Lett. **B322** (1994) 207;
 F. Borzumati, Z. Phys. **C63** (1994) 291;
 R. Nath and R. Arnowitt, Phys. Lett. **B336** (1994) 395;
 S. Bertolini and F. Vissani, Z. Phys. **C67** (1995) 513;
 J. Lopez et al., Phys. Rev. **D51** (1995) 147;
 F. Borzumati, M. Drees, and M.M. Nojiri, Phys. Rev. **D51** (1995) 341.

[129] A. Ali, G. F. Giudice and T. Mannel, Z. Phys. **C67** (1995) 417.

[130] M. Misiak in ref. [94].

[131] A.J. Buras and M. Münz, Phys. Rev. **D52** (1995) 186.

[132] C. S. Lim, T. Morozumi and A. I. Sanda, Phys. Lett. **218** (1989) 343;
 N. G. Deshpande, J. Trampetic and K. Panose, Phys. Rev. **D39** (1989) 1461;
 P. J. O'Donnell and H. K. K. Tung, Phys. Rev. **D43** (1991) R2067.
 N. Paver and Riazuddin, Phys. Rev. **D45** (1992) 978.

[133] A. F. Falk, M. Luke and M. J. Savage, Phys. Rev. **D49** (1994) 3367.

[134] K. Fujikawa and A. Yamada, Phys. Rev. **D49** (1994) 5890;
 P. Cho and M. Misiak, Phys. Rev. **D49** (1994) 5894.

[135] A. Ali, T. Mannel and T. Morozumi, Phys. Lett. **B273** (1991) 505.

[136] J. Hewett, Phys. Rev. **D53** (1996) 4964.

[137] F. Krüger and L.M. Sehgal, preprint PITHA 96/4 [hep-ph/9603237].

[138] P. Cho, M. Misiak, and D. Wyler, preprint ZU-TH 24/95, CALT-68-2028 [hep-ph/9601360].

[139] Z. Ligeti and M.B. Wise, Phys. Rev. **D53** (1996) 4937.

[140] A. Ali, G. Hiller, L.T. Handoko, and T. Morozumi, (to be published).

[141] A.F. Falk, M. Luke, and M.J. Savage, Phys. Rev. **D49** (1994) 3367.

[142] C. Albajar et al. (UA1), Phys. Lett. **B262** (1991) 163.

[143] CDF Collaboration, Fermilab Conf. 95/201-E(1995).

[144] P. Sphicas (CDF), private communication.

- [145] A. Ali and T. Mannel, Phys. Lett. **B264** (1991) 447 [E. **B274** (1992) 526];
 A. Ali, C. Greub and T. Mannel, in [102];
 G. Bailie, Z. Phys. **C61** (1994) 667;
 P. Colangelo et al., Phys. Rev. **D53** (1996) 3672;
 Z. Ligeti and M.B. Wise, in [139];
 W. Roberts, preprint CEBAF-TH-95-20 (1995), [hep-ph/9512253].
- [146] Y. Grossman, Z. Ligeti, and E. Nardi, preprint WIS-95-49-PH (1995) [hep-ph/9510378].
- [147] G. Buchalla, and A.J. Buras, Nucl. Phys. **B400** (1993) 225.
- [148] CDF Collaboration, Fermilab Conf. 95/201-E(1995).
- [149] L3 Collaboration, contributed paper to the EPS Conference, (EPS-0093-2) Brussels, 1995.
- [150] G.-L. Lin, J. Liu, and Y.-P. Yao, Phys. Rev. **D42** (1990) 2314.
- [151] H. Simma and D. Wyler, Nucl. Phys. **B344** (1990) 283.
- [152] S. Herrlich and J. Kalinowski, Nucl. Phys. **381** (1992) 501.
- [153] T.M. Aliev and G. Turan, Phys. Rev. **D48** (1993) 1176.
- [154] G.G. Devidze, G.R. Jibuti, and A.G. Liparteliani, preprint HEP Institute, Univ. of Tbilisi (revised version) (1995).
- [155] A.J. Buras, W. Slominski, and H. Steger, Nucl. Phys. **B238** (1984) 529; *ibid.* **B245** (1984) 369.
- [156] S. Herrlich and U. Nierste, Nucl. Phys. **B419** (1994) 292.
- [157] A.J. Buras, M. Jamin and P.H. Weisz, Nucl. Phys. **B347** (1990) 491.
- [158] See, for example, A.J. Buras and M.K. Harlander, in *Heavy Flavours*, edited by A.J. Buras and M. Lindner, Advanced Series on Directions in High Energy Physics (World Scientific, Singapore, 1992), Vol. 10.
- [159] J. Flynn, Mod. Phys. Lett. **A5** (1990) 877.
- [160] S. Herrlich and U. Nierste, Phys. Rev. **D52** (1995) 6505.
- [161] A. Ali and D. London, J. Phys. G: Nucl. Part. Phys. **19** (1993) 1069.
- [162] S. Sharpe, Nucl. Phys. B(Proc. Suppl.) **34** (1994) 403.
- [163] M. Crisafulli et al. (APE Collaboration), Phys. Lett. **B369** (1996) 325.
- [164] S. Aoki et al. (JLQCD Collaboration), preprint UTHEP-322 (1995) [hep-lat/9510012]. The numbers cited for B_K from the JLQCD collaboration as well as from the work of Soni and Bernard are quoted by Soni in his review [33].

- [165] J. Bijnens and J. Prades, Nucl. Phys. **B444** (1995) 523.
- [166] A. Pich and J. Prades, Phys. Lett. **B346** (1995) 342, and references cited therein.
- [167] Sau Lan Wu, preprint WISC-EX-96-343 [hep-ex/9602003], to appear in Proc. of the 17th Int. Symp. on Lepton and Photon Interactions, Beijing, P.R. China, August 1995.
- [168] S. Narison, Phys. Lett. **B322** (1994) 247;
S. Narison and A. Pivovarov, *ibid* **B327** (1994) 341.
- [169] For reviews, see, for example, Y. Nir and H.R. Quinn, in *B Decays*, edited by S. Stone (World Scientific, Singapore, 1992) 362; I. Dunietz, *ibid* 393.
- [170] D. London and R. Peccei, Phys. Lett. **B223** (1989) 257;
B. Grinstein, Phys. Lett. **B229** (1989) 280;
M. Gronau, Phys. Rev. Lett. **63** (1989) 1451, Phys. Lett. **B300** (1993) 163.
- [171] M. Gronau and D. London, Phys. Rev. Lett. **65** (1990) 3381.
- [172] R. Aleksan, I. Dunietz, and B. Kayser, Z. Phys. **C54** (1992) 653.
- [173] M. Gronau and D. Wyler, Phys. Lett. **B265** (1991) 172. See also M. Gronau and D. London, Phys. Lett. **B253** (1991) 483;
I. Dunietz, Phys. Lett. **B270** (1991) 75.
- [174] M. Gronau, J.L. Rosner, and D. London, Phys. Rev. Lett. **73** (1994) 21. See also O.F. Hernández, D. London, M. Gronau and J.L. Rosner, Phys. Lett. **B333** (1994) 500, M. Gronau, D. London, O.F. Hernández, and J.L. Rosner, Phys. Rev. **D50** (1994) 4529;
A.J. Buras and R. Fleischer, Phys. Lett. **B341** (1995) 379.
- [175] M. Gronau, D. London, O.F. Hernández, and J.L. Rosner, preprint TECHNION-
PH-95-10 (1995) [hep-ph/9504326].
- [176] R. Fleischer, Z. Phys. **C62** (1994) 81, Phys. Lett. **B321** (1994) 259; 332.
- [177] N.G. Deshpande and X.-G. He, Phys. Rev. Lett. **74** (1995) 26.
- [178] M. Gronau, D. London, O.F. Hernández, and J.L. Rosner, preprint TECHNION-
PH-95-11 (1995) [hep-ph/9504327].
- [179] R. Fleischer, Phys. Lett. **B332** (1994) 419;
N.G. Deshpande and X.-G. He, Phys. Lett. **B345** (1995) 547;
G. Kramer and W.F. Palmer, Phys. Rev. **D52** (1995) 6411;
A.J. Buras and R. Fleischer, **B365** (1996) 390.
- [180] N.G. Deshpande and X.-G. He, Phys. Rev. Lett. **75** (1995) 3064.
- [181] M. Gronau and J.L. Rosner, Phys. Rev. **D53** (1996) 2516.

Decay Modes	$\mathcal{B}(\text{SM})$	Measurements and Upper Limits (90% C.L.)
$(B_d, B_u) \rightarrow X_s \gamma$	$(3.2 \pm 0.58) \times 10^{-4}$	$(2.32 \pm 0.67) \times 10^{-4}$ CLEO [90]
$(B_d, B_u) \rightarrow K^* \gamma$	$(4.0 \pm 2.0) \times 10^{-5}$	$(4.5 \pm 1.5 \pm 0.9) \times 10^{-5}$ CLEO [91]
$(B_d, B_u) \rightarrow X_d \gamma$	$(1.0 \pm 0.8) \times 10^{-5}$	—
$B_u \rightarrow \rho^\pm + \gamma$	$(1.9 \pm 1.6) \times 10^{-6}$	$< 2.0 \times 10^{-5}$ CLEO [110]
$B_d \rightarrow \rho^0 + \gamma$	$(0.85 \pm 0.65) \times 10^{-6}$	$< 2.4 \times 10^{-5}$ CLEO [110]
$B_d \rightarrow \omega + \gamma$	$(0.85 \pm 0.65) \times 10^{-6}$	$< 1.05 \times 10^{-5}$ CLEO [110]
$(B_d, B_u) \rightarrow X_s e^+ e^-$	$(8.4 \pm 2.2) \times 10^{-6}$	—
$(B_d, B_u) \rightarrow X_d e^+ e^-$	$(4.9 \pm 4.3) \times 10^{-7}$	—
$(B_d, B_u) \rightarrow X_s \mu^+ \mu^-$	$(5.7 \pm 1.3) \times 10^{-6}$	$< 5.0 \times 10^{-5}$ UA1 [142]
$(B_d, B_u) \rightarrow X_d \mu^+ \mu^-$	$(3.3 \pm 2.8) \times 10^{-7}$	—
$(B_d, B_u) \rightarrow X_s \tau^+ \tau^-$	$(2.6 \pm 0.5) \times 10^{-7}$	—
$(B_d, B_u) \rightarrow X_d \tau^+ \tau^-$	$(1.5 \pm 1.3) \times 10^{-8}$	—
$(B_d, B_u) \rightarrow K e^+ e^-$	$(5.9 \pm 2.3) \times 10^{-7}$	$< 1.2 \times 10^{-5}$ CLEO [54]
$(B_d, B_u) \rightarrow K \mu^+ \mu^-$	$(4.0 \pm 1.5) \times 10^{-7}$	$< 0.9 \times 10^{-5}$ CLEO [54]
$(B_d, B_u) \rightarrow K^* e^+ e^-$	$(2.3 \pm 0.9) \times 10^{-6}$	$< 1.6 \times 10^{-5}$ CLEO [54]
$(B_d, B_u) \rightarrow K^* \mu^+ \mu^-$	$(1.5 \pm 0.6) \times 10^{-6}$	$< 2.5 \times 10^{-5}$ CDF [148]
$(B_d, B_u) \rightarrow X_s \nu \bar{\nu}$	$(4.0 \pm 1.0) \times 10^{-5}$	$< 3.9 \times 10^{-4}$ [146]
$(B_d, B_u) \rightarrow X_d \nu \bar{\nu}$	$(2.3 \pm 2.0) \times 10^{-6}$	—
$(B_d, B_u) \rightarrow K \nu \bar{\nu}$	$(3.2 \pm 1.6) \times 10^{-6}$	—
$(B_d, B_u) \rightarrow K^* \nu \bar{\nu}$	$(1.1 \pm 0.55) \times 10^{-5}$	—
$B_s \rightarrow \gamma \gamma$	$(3.0 \pm 1.0) \times 10^{-7}$	$< 1.1 \times 10^{-4}$ L3 [149]
$B_d \rightarrow \gamma \gamma$	$(1.2 \pm 1.1) \times 10^{-8}$	$< 3.8 \times 10^{-5}$ L3 [149]
$B_s \rightarrow \tau^+ \tau^-$	$(7.4 \pm 2.1) \times 10^{-7}$	—
$B_d \rightarrow \tau^+ \tau^-$	$(3.1 \pm 2.9) \times 10^{-8}$	—
$B_s \rightarrow \mu^+ \mu^-$	$(3.5 \pm 1.0) \times 10^{-9}$	$< 8.4 \times 10^{-6}$ CDF [148]
$B_d \rightarrow \mu^+ \mu^-$	$(1.5 \pm 1.4) \times 10^{-10}$	$< 1.6 \times 10^{-6}$ CDF [148]
$B_s \rightarrow e^+ e^-$	$(8.0 \pm 3.5) \times 10^{-14}$	—
$B_d \rightarrow e^+ e^-$	$(3.4 \pm 3.1) \times 10^{-15}$	—

Table 2: Estimates of the branching fractions for FCNC B -decays in the standard model taking into account the uncertainties in the input parameters as discussed in the text. The entries in the second column correspond to the short-distance contributions only except for the radiative decays $B_u \rightarrow \rho^\pm + \gamma$ and $B_d \rightarrow (\rho^0, \omega) + \gamma$, where long-distance effects have also been included. For the two-body branching ratios, we have used $f_{B_d} = 200$ MeV and $f_{B_s}/f_{B_d} = 1.16$. The CKM matrix element ratio is taken as $|V_{td}|/|V_{ts}| = 0.24 \pm 0.11$, as determined from the present fits, and this error is folded in quadrature with the other errors in estimating the relevant branching fractions. Experimental measurements and upper limits are also listed. Note that the limit quoted from [146] is an indirect one.

$ V_{ij} $	Present Value
$ V_{ud} $	0.9744 ± 0.0010 [3]
$ V_{us} $	0.2205 ± 0.0011 [3]
$ V_{ub} $	$(3.1 \pm 0.8) \times 10^{-3}$ [3]
$ V_{cd} $	0.204 ± 0.017 [3]
$ V_{cs} $	1.01 ± 0.18 [3]
$ V_{cb} $	0.0388 ± 0.0036 [83]
$ V_{td} $	$(9.2 \pm 3.0) \times 10^{-3}$
$ V_{ts} $	0.033 ± 0.009
$ V_{tb} $	0.9991 ± 0.0004 [3]

Table 3: Present values of the CKM matrix elements $|V_{ij}|$. Note that the value of $|V_{tb}|$ follows from unitarity. All others are measured in decays discussed in the text and in the PDG review [3], from which references to the original literature can be traced.

$f_{B_d} \sqrt{\hat{B}_{B_d}}$ (MeV)	(ρ, η)	χ^2_{min}
120	(-0.42, 0.16)	3.04
130	(-0.37, 0.19)	1.32
140	(-0.32, 0.23)	0.43
150	(-0.27, 0.26)	0.07
160	(-0.22, 0.29)	1.4×10^{-3}
170	(-0.15, 0.32)	0.05
180	(-0.08, 0.34)	0.09
190	(-0.01, 0.35)	0.06
200	(0.06, 0.35)	0.01
210	(0.13, 0.35)	0.02
220	(0.18, 0.35)	0.2
230	(0.23, 0.35)	0.61
240	(0.28, 0.35)	1.29
250	(0.32, 0.35)	2.22

Table 4: The “best values” of the CKM parameters (ρ, η) as a function of the coupling constant $f_{B_d} \sqrt{\hat{B}_{B_d}}$, obtained by a minimum χ^2 fit to the experimental data, including the renormalized value of $m_t = 170 \pm 11$ GeV. We fix $\hat{B}_K = 0.8$. The resulting minimum χ^2 values from the MINUIT fits are also given. (Table taken from [83].)

$f_{B_d}\sqrt{\hat{B}_{B_d}}$ (MeV)	$\sin 2\alpha$	$\sin 2\beta$	$\sin^2 \gamma$
130	0.46 – 0.88	0.21 – 0.37	0.12 – 0.39
155	0.75 – 1.0	0.31 – 0.56	0.34 – 0.92
180	–0.59 – 1.0	0.42 – 0.73	0.68 – 1.0
205	–0.96 – 0.92	0.49 – 0.86	0.37 – 1.0
230	–0.98 – 0.6	0.57 – 0.93	0.28 – 0.97

Table 5: The allowed ranges for the CP asymmetries $\sin 2\alpha$, $\sin 2\beta$ and $\sin^2 \gamma$, corresponding to the constraints on ρ and η shown in Fig. 11. Values of the coupling constant $f_{B_d}\sqrt{\hat{B}_{B_d}}$ are stated. We fix $\hat{B}_K = 0.8$. The range for $\sin 2\beta$ includes an additional minus sign due to the CP of the final state $J/\Psi K_S$. (Table taken from [83].)